THE STRATIGRAPHY AND GEOCHRONOLOGY OF EMERGENT FOSSIL REEF DEPOSITS OF WESTERN AUSTRALIA

Thesis submitted by

Michael John O'LEARY B.Sc. (Hons) *Qld*

In May 2007

For the degree of Doctor of Philosophy

In the School of Earth Sciences

James Cook University

STATEMENT OF ACCESS

I, the undersigned, author of this work, understand that James Cook University will make this thesis available for use within the University Library and, via the Australian Digital Theses network, for use elsewhere.

I understand that, as an unpublished work, a thesis has significant protection under Copyright Act and;

I do not wish to place any further restriction on access to this work, with the exception of the following:

All users consulting this thesis are required to sign the following statement:

"In consulting this thesis I agree not to copy or closely paraphrase it in whole or in part without the written consent of the author, and to make proper written acknowledgement for any assistance which I have obtained from it"

07-05-2007

Michael O'Leary

2007

STATEMENT OF SOURCES

DECLARATION

I declare that this thesis is my own work and has not been submitted in any other form for another degree or diploma at any university or other institution of tertiary education. Information derived from the published or unpublished work of others has been acknowledged in the text and a list of references is given.

07-05-2007

Michael O'Leary

2006

ABSTRACT

Corals provide the most widely used sea-level archive. Many coral species survive only in shallow water, therefore fossil corals emergent or submergent relative to present reefs, along stable coastlines, suggest variations in past sea level. Along the coastal margin of Western Australia (WA) an extensive series of marine isotope stage (MIS) 5e reefs outcrop at 3 ± 1 m above sea level. The consistency of reef elevation along thousands of km of WA coastline demonstrates the tectonic stability of this trailing intraplate continental margin. There is also evidence of erosional terraces or incipient reef development at elevations above this +3 m sea-level benchmark. Some workers reasoned that the higher elevation of these marine units is an artefact of localized tectonism or warping. This rationale fails to address: 1) intertidal deposits at multiple elevations in close proximity; 2) the distinct geomorphological difference between the lower and upper marine units; and 3) the similarity in elevation between WA emergent marine deposits and those found on stable carbonate platforms of The Bahamas and Bermuda. With accurate and precise dating of these emergent reef deposits it may be possible to characterise the nature of sea level during MIS 5e.

Coral skeletons are constructed of chemically unstable aragonite. Older coral material is generally more diagenetically altered, often suffering the addition or loss of uranium or thorium, which leads to inaccurate U-series age calculations. Coral diagenesis is generally determined by changes in carbonate mineralogy, but a more subtle form of geochemical alteration may affect the uranium-thorium age of corals that appear mineralogically pristine.

In an attempt to extract meaningful ages from corals that have undergone isotopic exchange, modeled alpha-recoil processes were used to calculate open-system ages. These open-system ages are based on the assumption that alpha-recoil mobilisation is the only diagenetic process operating within the coral/reef unit. Independent age controls including: 1) the known duration of MIS 5e; 2) stratigraphic superposition; and 3) age equivalence within individual corals, were used to test the reliability and accuracy of uncorrected and open-system corrected coral ages. Despite claims to the contrary, this study found open-system corrections to fail the above prescribed age tests, such that open-system corrections did not reflect the corals true age.

Investigations into the nature of MIS 5e sea levels were focused on two contrasting locations, Cape Cuvier, a high-energy coastal site, and Shark Bay, a low

energy marine embayment. Both sites point to an extended period of widespread coral reef development at +2 to +4 m elevation with incipient reef and erosional terraces at between +6 and +10 m. The incipient nature of the upper coralgal rim and the fact that the lower terrace was not able to utilize the newly available accommodation space points to a brief but rapid sea level excursion to this new elevation. High-precision U-series dating returned coral ages that were inconsistent with the stratigraphic interpretation of the site and other known MIS 5e sea level curves.

In an attempt to fill in the temporal and spatial gaps left by coral dating, the U-series method was applied to crustose coralline algae (CCA). This study shows that living CCA capture a modern seawater equivalent $\delta^{234}U$ value of 147.02 ± 1.5 ‰, and initial uranium concentrations of 0.2 ± 0.07 ppm. These initial chemistries allow for the examination of uranium and thorium isotopic evolution over geological timescales, however uranium uptake and detrital ^{232}Th contamination limit the usage of this material in U-series dating.

Although we are confident of our interpretation of the sea-level history in WA during MIS 5e, we offer the following considerations: 1) field observations and relationships remain the most reliable means of determining the succession of events in the case of MIS 5e; 2) despite increased measuring precision of "high tech" dating methods, there is not necessarily a concomitant increase in the accuracy of the ages; and, 3) open-system corrections are not a reliable tool for determining a coral's true age.

STATEMENT OF THE CONTRIBUTION BY OTHERS

This thesis has benefited greatly from the contribution by others to the formulation of ideas, the development of research approaches, and the interpretation and critical review of the data. Paul Hearty and Malcolm McCulloch were instrumental in providing the impetus to investigate the nature of sea level and climate during the peak of the last interglacial as recorded in emergent reef deposits along the West Australian coastline. Many of the fundamental questions that have been addressed in this thesis stemmed from previous work undertaken by these individuals and hypotheses that were generated from the same. Paul Hearty and Malcolm McCulloch acquired the initial Australian Research Council funding which funded this research and my Ph.D. stipend. A James Cook University graduate research scheme grant (MRG) provided extra funding for fieldwork in Western Australia. Both of these individuals have also contributed much to the acquisition and interpretation of the data generated herein, and in the presentation of results. However, both recognise This Author's role as chief investigator in these studies, and as having acquired the majority of the data, formulating the bulk of the interpretations, preparing of drafts, and refining of the manuscripts.

STATEMENT OF CONTENT

The body of this thesis is presented as four separate, self-contained works, which will be submitted to scientific journals of international significance, in a similar format. Due to the completeness of each section a small amount of repetition has been unavoidable. This particularly the case with the methods section, which describes the analytical techniques used in U-series dating of corals. There has also been some overlap in data interpretation.

ACKNOWLEDGEMENTS

The Author would like to acknowledge the contributions of the following individuals and groups towards the work presented herein.

The Canberra crew: A big thanks to Malcolm McCulloch at the RSES, Australian National University for providing support, technical skills and considerable runtime to analyse my corals, Graham Mortimer for his patience and shared office space as well as Bridget, Lois, Eva, Carles. To Pete, and Sarah for providing accommodation and Damian for providing accommodation and homebrew.

The West Australian crew: To all those people who helped me out with field work, a special thanks to CALM in Exmouth and Denham for access to sites and permission to collect corals within National Parks. To Dampier Salt Ltd for access onto their mine lease and finally to Dave Bauer of Arid Landscapes whose logistical support was greatly appreciated.

The Sydney crew: To Tick, Sav and Dom, although you place was a bit like a transit lounge for me thanks for being so accommodating, the bed was always soft and the beer always cold.

The Townsville crew: So many people I would like to thank for their help, friendship and support. First to my best mates Jo Jo, Belinda and Andy; friends and flat mates, de Jersey, Katie, Dave, Aileen, and Ellie; as well as Toni and Kirsten; and Thomas for his constant distractions and wild adventures. Shelley and little Kai my newest (literally) best friend

The Family: To my Mum and Dad you both instilled qualities in me that I am proud and for that I thankyou, to my sister Lisa who is embarking on her own adventure and the rest of the Previtera clan.

Academic supervisors official and unofficial: Thanks again must go to Malcolm McCulloch, Jody Webster and Peter Ridd. But most thanks must go to Paul Hearty, friend and mentor, for all your support, guidance, encouragement and patience.

Finally I'd like to thank Caro, although you appeared late in the game, you turned out to be a match winner for me in more ways than one.

TABLE OF CONTENTS

SECTION A

COMPARISON OF UNCORRECTED AND OPEN-SYSTEM CORRECTED U-SERIES CORAL AGES FROM FOSSIL CORAL REEFS, WESTERN AUSTRALIA

SECTION B

MORPHOSTRATIGRAPHY AND GEOCHRONOLOGY OF A FOSSIL FRINGING REEF: CAPE CUVIER, WESTERN AUSTRALIA

SECTION C

CORAL REEF AND STROMATOLITE DEVELOPMENT IN SHARK BAY DURING RECENT AND LAST INTERGLACIAL SEA-LEVEL HIGH-STANDS

SECTION D

URANIUM-SERIES DATING OF CRUSTOSE CORALLINE ALGAE (CORALLINACEAE)

LIST OF FIGURES AND TABLES

Section A

Section B

Section C

Section D

INTRODUCTION

Western Australia (WA) figures prominently in the traditional literature on Quaternary sea level, largely as a result of Fairbridge (1948; 1950; 1954; 1961), Teichert (1947; 1950), and Logan *et al.* (1970). In the context of the 'stable coast' paradigm WA holds a strong attraction. Its position as an intraplate continental margin, in the far field of former ice sheets, minimizes the potential for vertical displacement as a result of glacio-isostatic or tectonic processes. This is exemplified in the near constant +3 ± 1 m elevations of well-developed fossil reef deposits and erosional terraces exposed along 2500 km of WA coastline (Stirling et al., 1998) from Cape Leeuwin in the south (34.4° S) to Vlamingh Head in the northwest (21.8° S). These reef and terrace features are common to many stable coastlines around the world (Hearty *et al.*, in review (a))

Based on field studies and gemorphological interpretations, Fairbridge, Teichert and Logan correctly identified these emergent coral reef units as belonging to Late Pleistocene sea-level highstands. Subsequent radiometric (α-spectrometry) coral ages from Fairbridge Bluff, Rottnest Island and Boundary Beach, Red Bluff (Veeh, 1966) returned somewhat imprecise ages of 100 ± 20 and 120 ± 40 ka, but did confirm that reef units belonged to the broad last interglacial cycle known as marine isotope stage (MIS) 5 (~74-135 ka). Veeh *et al.* (1976) further refined the interval of reef development to the peak of the last interglacial, marine isotope stage (MIS) 5e, via α-spectrometry of corals from an emergent fringing reef complex at Cape Cuvier.

Despite the ubiquitous nature of the +3 ± 1 m terrace along the WA coastline, geomorphological investigations (Denman and Van de Graaff, 1977; Veeh *et al.*, 1979 and Van de Graaff *et al.*, 1979) from the Lake Macleod and Cape Range areas identified incipient reef and erosional terraces up to 6 m higher than the archetypal +3 ± 1 m benchmark. There appears to be a contradiction when invoking a warping or uplift

scenario for these higher marine units against a stable coast paradigm, and lacking accurate dating methods, the true nature of these upper marine deposits could not be assessed with confidence.

Since the introduction of high-precision thermal ionisation (TIMS) and multi-collector inductively coupled plasma mass spectrometric (MC ICPMS) dating techniques, over 100 coral dates have been published from WA (Zhu *et al.*, 1993; Collins *et al.*, 1993a; Stirling *et al.*, 1995; Eisenhauer *et al.*, 1996; Stirling *et al.*, 1998; Collins *et al.*, 2003). Despite this, the exact timing, duration and behaviour of sea level during MIS 5e in WA remain controversial. Not only do estimates for the timing of onset and termination of the last interglacial vary widely between localities, the details of sea-level fluctuations within this interval also remain uncertain. For example Stirling *et al.* (1995; 1998) reported a single phase of constant high sea-level for WA between 128 ± 1 and 116 ± 1 ka, while studies by Chen *et al.* (1991) from Bahamas, and Muhs *et al.* (2002) from Hawaii place the initiation and termination of MIS 5e at 132 and 114 ka, respectively. Furthermore, studies from the Bahamas (Neumann and Hearty, 1996), Bermuda (Hearty, 2002), Hawaii (Sherman *et al.*, 1993; Hearty *et al.*, 2000), and the Mediterranean (Hearty *et al.*, 1986; Riccio *et al.*, 2001) report multiple sea-level oscillations during MIS 5e. These studies describe MIS 5e sea level as a series of intervals of transition and stability. First a relatively stable early 5e at +2.5 ± 1 m, second, a short regression of a few meters, third, another brief rise to +3-4 m. The termination of MIS 5e was marked by abrupt shifts of sea level between +6 and +9 m that formed multiple notches and narrow benches.

Much of the uncertainty surrounding the timing and absolute elevations of sea-level events is the result of both poor stratigraphic interpretation and inaccurate uranium-series (U-series) age calculations. Furthermore, coral reefs are less than ideal monitors of sea-level change; rather, they might be preferred as monitors of sea-level stability as their response time and depositional tempo may be measured in hundreds or thousands of

years (Hearty *et al.* (in review (b)). Given the possibility that sea-level shifts of several metres may take as little as tens to hundreds of years to occur (Blanchon and Shaw, 1995; Neumann and Hearty, 1996), reefs are a less than optimal geological media for monitoring such sea-level changes. Their response may be slow, or nonexistant.

In paleo-sea-level reconstructions the first presumption is that a measured sea-level datum has not been affected by vertical displacement and so represents eustatic sea level. If vertical displacement is suspected, knowledge of uplift rate over time will be required. This is usually resolved by correlating the uplifted sea-level benchmark with a contemporaneous benchmark from regions that have not experienced tectonic uplift.

The second presumption is that a measured U-series age represents a coral's true age. The primary criterion in determining the reliability of coral U-series ages has been to back calculate measured $\delta^{234}U$ activity ratios (Edwards *et al.*, 1987a; Chen *et al.*, 1991; Stirling *et al.*, 1995) that should correspond to modern seawater $^{234}U/^{238}U$ activity of 146.6 ± 2.5‰ (Robinson *et al* 2004). However, it is more often the case that fossil corals exhibit higher initial $\delta^{234}U$ ($\delta^{234}U_{initial}$) values than living corals (Bender *et al.*, 1979; Bard *et al.*, 1992; Gallup *et al.*, 1994; Stirling *et al.*, 1995; 2001) usually the result of open-system isotopic exchange processes. There are a number of potential mechanisms that may contribute to open-system behaviour in corals including dissolution and precipitation reactions (Bar-Matthews *et al.*, 1993), decay dependent alpha-recoil mobilization (Fruijtier *et al.*, 2000; Henderson *et al.*, 2001) and solid state diffusion (Cherniak, 1997). While uranium solid-state diffusion is expected to be negligible on a 10^4-10^5 year timescale and not an important process (Robinson *et al.*, 2006) in this case, other mechanisms related to mineralisation (Bar-Matthews *et al.*, 1993) and alpha-recoil processes (Thompson *et al.*, 2003) are known to produce the range of isotopic anomalies commonly observed in corals.

While it is possible to screen corals for diagenetic anomalies using general petrographic and geochemical parameters, the effects of alpha-recoil isotopic exchange can lead to age uncertainties in even the most pristine coral samples. This isotopic error may be more statistically significant than measured analytical error. As a result of these age uncertainties, there have been several attempts to correct for isotopic anomalies observed in corals using open-system models of Thompson *et al.* (2003), Villament and Feuillet (2003) and Scholz *et al.* (2004). However, it is understood that these open-system corrections can introduce their own age uncertainties (Robinson *et al.*, 2006).

The desire to understand the true nature of sea level in WA during the penultimate interglacial, and its relation to other globally important sites, has motivated the work presented in this dissertation. However, in the attempt to resolve these outstanding sea-level issues, we must first address the following questions: 1) Does the measured sea-level datum represent a eustatic sea-level elevation? 2) How reliable are the measured U-series coral dates? 3) Do open-system age corrections represent a coral's true age?

I attempted to resolve some of these questions through: 1) detailed geologic and morphologic investigations using the same techniques successfully employed by early workers (Teichert, Fairbridge and Logan); 2) examination of the degree of uranium and thorium isotopic shift from a closed-system seawater evolution curve; and 3) comparison of U-series age with independent age controls including stratigraphic superposition and age equivalence within individual corals.

The initial aim of Section A is to select corals, based on geochemical and age control protocols, whose uncorrected and corrected U-series ages come closest to representing the corals true age. This screened age data are then applied to two geographically different locations at Cape Cuvier (Section B) and Shark Bay (Section C). Detailed stratigraphic and geomorphic analyses are combined with U-series coral age data

in an attempt to resolve paleosea-level and tectonic issues at both these localities. This study also recognises some of the geographical and ecological limitations in utilizing corals as a dating medium. Thus, in the final section (D), the potential utility of U-series dating of crustose coralline algae is explored.

It is evident from previous publications from stable carbonate platforms (Neumann and Hearty, 1996; Hearty and Neumann 2001; Hearty 2002) that sea-level events may be brief and oscillatory, leaving little geological evidence, and making them very difficult do date. The brief duration of the stillstand results in notches, rubble benches, or incipient coral reef development. These thin and patchy incipient reefs are generally more prone to burial, erosion or diagenesis, thus rarely offering any datable material. At the outset of this study, it was hoped that the dual use of detailed stratigraphic analysis and high-precision U-series dating would offer the best opportunity to resolve the outstanding questions of Quaternary sea levels. This overall objective will be evaluated in the following Sections.

REFERENCES

Bar-Matthews, M., Wasserburg, G.J., Chen J.H., 1993. Diagenesis of fossil coral skeletons—correlation between trace-elements, textures, and U-234/U-238. Geochimica et Cosmochimica Acta 57, 257-276.

Bard, E., Fairbanks, R.G., Hamelin, B., 1992. How accurate are the U/Th ages obtained by mass spectrometry on coral terraces, in: G.J. Kukla, E. Went (Eds.), Start of a Glacial, NATO ASI Series 13, Springer, Berlin, pp. 15-21.

Blanchon, P., Shaw, J., 1995. Reef drowning during the last deglaciation: Evidence for catastrophic sea-level rise and ice-sheet collapse. Geology 23(1), 4-8.

Bender, M.L., Fairbanks, R.G., Taylor, F.W., Matthews, R.K., Goddard, J.G., Broecker, W.S., 1979. Uranium-series dating of Pleistocene reef tracts of Barbados, West Indies. Geological Society of America Bulletin 90, 577-594.

Cherniak, D.J., 1997. An experimental study of strontium and lead diffusion in calcite, and implications for the carbonate diagenesis and metamorphism. Geochimica et Cosmochimica Acta 61, 4173-4179.

Chen J.H., Curran H.A., White, B., Wasserburg, G.J., 1991. Precise chronology of the Last Interglacial period: 234U230Th data from fossil coral reefs in the Bahamas. Geological Society of America Bulletin 103, 82-97.

Collins, L.B., Zhu, Z.R., Wyrwoll, K.H., Hatcher, B.G., Playford, P.E., Chen, J.H., Eisenhauer, A., Wasserburg, G.J., 1993a. Late Quaternary evolution of coral reefs on a cool-water carbonate margin: the Abrolhos carbonate platforms, Southwest Australia. Marine Geology 110, 203 – 212.

Denman, P.D., van de Graaff, W.J.E., 1977. Emergent Quaternary marine deposits in the Lake MacLeod area, Western Australia. Western Australia Geological Survey Annual Report, 1976, 32-36.

Edwards, R.L., Chen, J.H., Wasserburg, G.J., 1987a. ^{238}U, ^{234}U, ^{230}Th, ^{232}Th systematics and the precise measurement of time over the past 500,000 years. Earth and Planetary Science Letters 81, 175-192.

Eisenhauer, A., Zhu, Z.R., Collins, L.B., Wyrwoll, K.H., Eichstatter, R., 1996. The Last Interglacial sea level change: new evidence from the Abrolhos Islands, West Australia. Geol. Rundsch. 85, 606-614.

Fairbridge, R.W., 1948. Notes on the geomorphology of the Pelsart Group of the Houtman's Abrolhos Islands. Journal of the Royal Society of Western Australia 33, 1-36.

Fairbridge, R.W., 1950. The geology and geomorphology of Point Peron, Western Australia. Journal of the Royal Society of Western Australia 34, 35-72.

Fairbridge, R.W., 1954. Quaternary eustatic data for Western Australia and adjacent states. Proceedings' of the Pan Indian Ocean Science Congress, Perth, Western

Australia, 64-84.

Fairbridge, R.W., 1961. Eustatic changes in sea level. Physics and Chemistry of the Earth 4, 99-187.

Fruijtier, C., Elliot, T., Schlager, W., 2000. Mass-spectrometric $^{234}U/^{230}Th$ ages from the Key Largo Formation, Florida Keys, United States: Constraints on diagenetic age disturbance. GSA Bulletin 112, 267-277.

Gallup, C.D., Edwards, R.L., Johnson, R.G., 1994. The Timing of high sea levels over the past 200,000 years. Science 263, 796-800.

Hearty, P.J., 1987. New data on the Pleistocene of Mallorca. Quaternary Science Reviews 6, 245-257.

Hearty, P.J., 1998. The geology of Eleuthera Island, Bahamas: a Rosetta Stone of Quaternary stratigraphy and sea-level history. Quaternary Science Reviews 17, 333-355.

Hearty, P.J., Kaufman, D.S., Olson, S.L., and James, H.F., 2000. Stratigraphy and whole-rock amino acid geochronology of key Holocene and Last Interglacial carbonate deposits in the Hawaiian Islands. Pacific Science 54(4), 423-442.

Hearty, P.J., and Neumann, A.C., 2001. Rapid sea-level and climate change at the close of the Last Interglaciation (MIS 5e): Evidence from the Bahama Islands. Quaternary Science Reviews 20, 1881-1895.

Hearty, P.J., 2002. A revision of the late Pleistocene stratigraphy of Bermuda. Sedimentary Geology 153 (1-2), 1-21.

Hearty, P.J., Neumann, A.C., Hollin, J.T., O'Leary M.J., McCulloch M.T., in review (a). Sea level oscillations during the last interglaciation (sensu stricto MIS 5e). Quaternary Science Reviews.

Hearty, P.J., Neumann, A.C., O'Leary M.J., in review (b). Comment on "Record of MIS 5 sea-level highstands based on U/Th dated coral terraces of Haiti" (B. Dumas, C.T. Hoang, and J. Raffy, 2006, Quaternary International, v. 145-146, p. 106-118). Quaternary International.

Henderson, G.M., Slowey, N.C., Fleisher, M.Q., 2001. U-Th dating of carbonate platform and slope sediments. Geochemica et Cosmochemica Acta 65, 2757-2770.

Logan, B.W., Read, J.F., Davis, G.R., 1970. History of carbonate sedimentation, Quaternary Epoch, Shark Bay, Western Australia. American Association of Petroleum Geologists Memoirs 13, 38 – 84.

Muhs, D.R., Simmons, K.R., Steinke, B., 2002. Timing and warmth of the Last Interglacial period: new U/Th evidence from Hawaii and Bermuda and a new fossil compilation for North America. Quaternary Sciences Reviews 21, 1355-1383.

Neumann, A.C., Hearty, P.J., 1996. Rapid sea-level changes at the close of the last interglacial (stage 5e) recorded in Bahamian Island geology. Geology 24, 775-778.

Riccio, A., Riggio, F., Romano, P., 2001. Sea level fluctuations during Oxygen Isotope Stage 5: new data from fossil shorelines in the Sorrento Peninsula (Southern Italy). Zeitschrift fur Geomorphologie N.F. 45(1), 121-137.

Robinson, L.F., Belshaw, N. S., Henderson ,G.M., 2004. U and Th concentrations and isotope ratios in modern carbonates and waters from the Bahamas. Geochimica et Cosmochimica Acta 68, 1777–1789.

Robinson, L.F., Adkins, J.F., Fernandez, D.P., Burnett D.S., Wang, S-L., Gagnon, A.C., Krakauer, N., 2006. Primary U-distribution in scleractinian corals and its implications for U-series dating. Geochemistry Geophysics Geosystems 7 (5), 1-20.

Sherman, C.E., Glenn, C.R., Jones, A.T., Burnett, W.C., Schwarcz, H.P., 1993. New evidence for two highstands of the sea during the last interglacial, oxygen isotope substage 5e. Geology 21, 1079-1082.

Stirling, C.H., Esat, T.M., McCulloch, M.T., Lambeck, K., 1995. High-precision U-series dating of corals from Western Australia and implications for the timing and duration of the Last Interglacial. Earth and Planetary Science Letters 135, 115-130.

Stirling, C.H., Esat, T.M., Lambeck, K., McCulloch, M.T., 1998. Timing and duration of the Last Interglacial: evidence for a restricted interval of widespread coral reef growth. Earth and Planetary Science Letters 160, 745-762.

Stirling, C.H., Esat, T.M., Lambeck, K., McCulloch, M.T., Blake, S.G., Lee D.C., Halliday, A.N., 2001. Orbital forcing of the marine isotope stage 9 interglacial. Science 291 (5502), 290-293.

Scholz, D, Mangini, A, Felis, T., 2004. U-series dating of diagenetically altered fossil reef corals. Earth And Planetary Science Letters 218 (1-2), 163-178.

Thompson, W.G., Spiegelmann, M.W., Goldstein, S.L., Speed, R.C., 2003. An open-system model for U-series age determinations of fossil corals. Earth Planetary Science Letters 210, 365–38.

Teichert, C., 1947. Contributions to the geology of Houtman's Abrolhos. Proceedings of the Linnean Society of Western Australia. New South Wales 71, 145 – 196.

Teichert, C., 1950. Late Quaternary changes of sea level at Rottnest Island, Western Australia. Royal Society of Victoria Proceedings 59, 63 – 79. 275 – 298.

Van de Graaff, W.J.E., Denman, P.D., Hocking, R.M., 1976. Emerged Pleistocene marine terraces on Cape Range, Western Australia. Geological Survey of Western Australia Annual Report 1975, 62-69.

Veeh, H.H., 1966. Th/U and U/U ages of Pleistocene high sea level stand. Journal of Geophysical Research 71, 3379 – 3386.

Veeh, H.H., Sehwebel, D., van de Graaf, W.J.E., Denman, P.D., 1979. Uranium-series ages of eoralline terrace deposits in Western Australia. Journal of the Geological Society of Australia, 26, 285-292.

Villemant, B., Feuillet, N., 2003. Dating open systems by the 238U-234U-230Th method: application to Quaternary reef terraces. Earth and Planetary Science Letters 210, 105–118.

Zhu, Z.R., Wyrwoll, K-H., Collins L.B., Chen J.H., Wasserburg G.J., Eisenhauer A., 1993. High-precision U-series dating of Last Interglacial events by mass spectrometry: Houtman Abrolhos Islands, western Australia. Earth and Planetary Science Letters 118, 281–293.

SECTION A

Comparison of uncorrected and open-system corrected U-series coral ages from fossil reefs, Western Australia

A.1 ABSTRACT

West Australian fossil corals exhibit a high degree of open-system behaviour manifest in elevated ^{232}Th concentrations and high $\delta^{234}U_{initial}$ values. In an attempt to extract meaningful ages from corals that have undergone isotopic exchange, modeled alpha-recoil processes were used to calculate open-system ages. These open-system ages are based on the assumption that alpha-recoil mobilisation is the only diagenetic process operating within the coral or reef unit. This study attempted to independently verify the true accuracy of open-system corrections through the use of independent age controls including; 1) ages falling within the known duration of marine isotope stage (MIS) 5e, 2) ages that conform to stratigraphic superposition and, 3) age equivalence within individual corals. The corrected age data showed a poor correlation to independent age controls suggesting that; 1) there may be systematic errors built into the open-system model or, 2) alpha-recoil mobilisation is not the only isotopic exchange process operating within the corals. Without independent age verification, then U-series open-system correction must be approached with caution. We propose the following recommendations:

1. Analysis of multiple subsamples from individual corals as the best quantitative test in determining U-series age.

2. Where possible corals should be sampled in a stratigraphic context.

3. Open-system corrections should only be used in conjunction with independent age controls.

A.2 INTRODUCTION

Direct paleosea-level reconstructions rely heavily on dated fossil corals. Corals provide a fairly precise sea-level constraint with reef development principally controlled by water depth (Kennedy and Woodroffe, 2002; Cabioch *et al.*, 1999). The ^{238}U-^{234}U-^{230}Th decay series can provide an accurate chronometer extending over the last few hundred thousand years (Broecker, 1963; Edwards *et al.*, 1987a; Bard *et al.,* 1990 Stirling *et al.*, 1995) under optimal circumstances. Accurate dating is based on an assumption that corals have remained closed to isotopic exchange. With the introduction of thermal ionisation mass spectrometry (TIMS) (Chen *et al.*, 1986; Edwards *et al.*, 1987b) and more recently multi-collector inductively coupled plasma mass spectrometry (MC ICPMS) (Anderson *et al.*, 2004), there has been an increase in analytical precision by orders of magnitude, and a corresponding improvement in the ability to detect diagenetic alteration in isotopic ratios. This new analytical precision has shown corals to be more susceptible to open-system chemical and isotopic exchange than previously thought (Bard *et al.*, 1991). Consequently, the improvement in analytical precision has not lead to a corresponding improvement in age accuracy (Bard *et al.*, 1992). As a result, criteria have been established to screen corals for exposure to open-system U/Th exchange.

The primary criterion in determining the reliability of coral U-series ages has been to back calculate measured $\delta^{234}U$ activity ratios (Edwards *et al.*, 1987a; Chen *et al.*, 1991; Stirling *et al.*, 1995), which should correspond to a modern seawater $^{234}U/^{238}U$ activity of 146.6 ± 2.5‰ (Robinson *et al* 2004). Generally fossil corals exhibit higher initial $\delta^{234}U$ ($\delta^{234}U_{initial}$) values than is accounted for in living corals (Bender *et al.*, 1979; Bard *et al.*, 1991; Gallup *et al.*, 1994; Stirling *et al.*, 1995; Stirling *et al.*, 2001). These higher values may be the result of changing seawater $\delta^{234}U$ activities over successive interglacials, or a result of post mortality U/Th mobilization within the coral. Studies of $\delta^{234}U$ values in seawater show a variation of less than 15‰ over the last 360 ka (Henderson, 2002). In addition,

coeval corals that grew on the same reef, and multiple analyses of the same coral, can show variations in initial $\delta^{234}U$ ($\delta^{234}U_{initial}$) activity greater than the known variability of historical $\delta^{234}U$ seawater (Gallup *et al.*, 2002). We therefore assume that the variability observed in fossil corals is more likely the result of U/Th mobilization.

The are a number of mechanisms that may contribute to open-system behavior in corals including dissolution and precipitation reactions (Bar-Matthews *et al.*, 1993), decay dependent alpha-recoil mobilization (Fruijtier *et al.*, 2000; Henderson *et al.*, 2001) and solid state diffusion (Cherniak, 1997). While uranium solid-state diffusion is expected to be negligible on 10^4-10^5 year timescales and not an important process (Robinson *et al.*, 2006), mineralisation (Bar-Matthews *et al.*, 1993) and alpha-recoil processes (Thompson *et al.*, 2003) are known to produce the range of isotopic anomalies commonly observed in corals.

Primary coral skeletons are composed of metastable aragonite, most fossil corals older than ~ 2 x 10^4 years will show some evidence of calcite alteration and potential U/Th mobilization (Bar-Matthews *et al.*, 1993) depending on diagenetic history. A qualitative assessment of the degree of calcite contamination can be made through visual inspection and X-radiograph positive prints, which identify the more dense calcite bands in the coral (**Fig. 1**). Quantitative assessment can be made using X-ray diffraction where total calcite content for near pristine coral samples should measure less than 2%. It should also be noted that secondary aragonite precipitation is known to infill micropore space within the coral (Lazar *et al.*, 2004). This is a potential source of allochthonous uranium or thorium isotopes, detectable only by scanning electron microscopy and petrographic examination. However, the fact that apparently pristine coral samples exhibit $\delta^{234}U_{initial}$ values higher than modern seawater or modern corals (Ku *et al.*, 1990; Hamlin *et al.*, 1991), suggests that the isotopic systems operating in these corals are far

more subtle and sensitive to diagenetic change than indicated among general petrographic or geochemical parameters (Scholz *et al.*, 2004).

Alpha-decay of a radioactive parent isotope results in the recoil and displacement of the daughter isotope within the crystal lattice. The recoil distance is of the order of 10-110 nm for ^{238}U to ^{234}Th and results in a damage track inside the crystal lattice (Kigoshi, 1971). A recoil track that intersects the grain surface provides an easy path through which the decayed atom can move; in effect, recoil creates a thin layer with enhanced permeability. Permeability is selectively enhanced for the ^{234}U daughter isotope and the leaching process results in non-mass dependant isotope fractionation where the solid phase is depleted in ^{234}U/^{238}U and the liquid phase is enriched. Decay of dissolved uranium and alpha-recoil mobilization of uranium daughters will also produce particle-reactive ^{234}Th and ^{230}Th (Thompson *et al.*, 2003). The coupled addition of these thorium isotopes could simultaneously increase a coral's ^{234}U/^{238}U activity (elevate $\delta^{234}U_{initial}$ values) and ^{230}Th/^{238}U activity (producing older apparent ages), a trend commonly observed in fossil corals. Since all corals are subject to alpha-recoil processes, all measured coral ages will contain a systematic isotopic error. This isotopic error may be more statistically significant than the measured analytical error. As a result of such age uncertainties, there have been several attempts to correct for isotopic anomalies observed in corals using open-system models.

A.3 MODELLING OPEN-SYSTEM BEHAVIOR IN CORALS

The open-system U-series age model developed by Thompson *et al.* (2003) is based on alpha-recoil processes enhancing the mobility of daughter nuclides. The model assumes that alpha-recoil mobilisation is the only diagenetic process operating within the coral or reef unit. Recoil products are transported from an unspecified source into the coral skeleton, yielding the observed systematic, coupled enrichment trends in ^{230}Th/^{238}U

activities and $\delta^{234}U$. The model mathematically removes excess ^{234}U and ^{230}Th and re-calculates an open-system age that intercepts the seawater evolution curve; assuming an invariant $\delta^{234}U$ composition in the marine environment throughout the late Quaternary.

Extending the approach of Henderson *et al.* (2001), Villament and Feuillet (2003) propose a consistent model that accounts for possible initial ^{230}Th excess and where continuous selective redistribution (gain or loss) of ^{234}U, ^{234}Th and ^{230}Th is controlled by recoil processes. The model calculates one open-system U-series model age based on an integration of the data for all samples, making the critical assumption that all corals developed concurrently. This age assumption biases the integrated "average" age towards anomalous values if corals are of differing ages (Anderson *et al.*, in review).

The linear regression open-system isochron model of Scholz *et al.* (2004) examined a suite of corals exposed to meteoric waters through some of their post-mortem history. The authors applied episodic pulses of uranium loss and gain, with the $\delta^{234}U$ of the additional uranium determined by multiple measurements on sub-samples from the same coral. A model assuming different degrees of uranium addition and loss in different sub-samples of one coral produces straight lines (isochrons) on a $^{234}U/^{238}U$ vs. $^{230}Th/^{238}U$ plot and predicts that the true age of the coral can be calculated by intersecting this isochron with the seawater evolution curve.

Despite advances in dating techniques and improvements in the understanding of uranium and thorium exchange in corals, important aspects of the systematics which produce elevated $\delta^{234}U$ have yet to be satisfactorily explained. As a result, open-system models that successfully correct for U/Th exchange at one fossil locality do not resolve open-system behavior globally. Despite these modelling uncertainties open-system models are used to improve the timing and resolution of past sea-level highstands, e.g. Thompson and Goldstein (2005)

Here we report on 76 new MC ICPMS U-series coral dates from West Australian (WA) fossil reefs. This large database provides a unique opportunity to compare uncorrected U-series coral ages with open-system models. Corals were sampled along reef-growth-axis to provide stratigraphic age control prior to analysis. This provides a benchmark to test for reliability and accuracy in both uncorrected and modelled U-series coral dates.

Thus, this study has three distinct goals:

1. Using independent age controls, determine the reliability of geochemical parameters in screening for isotopic anomalies.

2. Using independent age controls assess the true accuracy of open-system age models.

3. Critically evaluate which measured coral ages can be considered reliable and used in further chronostratigraphic interpretations.

A.4 METHODS

A.4.1 Study region and coral samples

Emergent fossil reef terraces of the south and central coast of WA contain a continuous record of coral growth during MIS 5e. Many of these sites have been previously described (Farbridge 1950; Logan *et al.*, 1970; Van de Graaff *et al.*, 1976 Denman and Van de Graaff, 1977; Veeh *et al.*, 1979; Stirling *et al.*, 1995; Collins *et al.*,

1996; Eisenhauer *et al.*, 1996). In this study, morpho- and chronostratigraphy were the primary tools used at 14 surveyed sites (**Fig. 2**). Cross-terrace geomorphic profiles and vertical sections were constructed, logged and photographed. Hand-level and theodolite surveys established the elevation of the deposits relative to mean sea level. Positive elevations in this study are expressed simply as "+" (as +8 m) for height above present mean sea level.

Topographic profiles determined terrace elevation and aided in the reconstruction of the fringing reef growth histories. Corals in growth position were collected using rock-drills and cold-chisels across the reef flat, at cliff exposures and particularly at measured stratigraphic sections. We preferentially targeted corals from the Faviidae family for U-series dating because their well-developed wall structures are composed of dense aragonite and are generally free of detrital or recrystallised material. Where the family Faviidae was absent, coral from the genus, *Porites* and *Acropora* were sampled. Corals of these genera are less than ideal due to the porus nature of their skeleton, which limits effective precleaning (Scholz *et al.*, 2004).

Locality names were assigned based on the nearest topographic landmark on either 1:100 000 or 1:250 000 map sheets. Each sample-site was assigned a three-letter code e.g. LDS1c. The three letters indicate the region "L", and the specific site "DS" Dampier Salt, while the numerical is one of several samples collected at the site. A lower case letter LDS1 "c" indicates a sub-sample from a single coral.

A.4.2 Sample preparation and analytical procedures

A total of 76 West Australian coral samples were selected for U-series analysis. Samples were sectioned and micro-sampled to an approximate weight of 200 μg using a dental drill. Mechanical cleaning involved soaking in Milli-Q water and sonication. Samples were first dissolved in distilled water with a subsequent step addition of 10M

HNO_3 then spiked with a 50 mg "U-2" $^{233}Th/^{235}U$ isotope tracer and later evaporated to a minimum solution. A few drops of H_2O_2 were added to oxidise any remaining organic material. Samples were redissolved in 3 ml of 2M HNO_3 and transferred to bio-spin ®Tru.spec columns which separated U and Th from the solution. A 0.1 normal solution of HF/HCl was then passed though the columns to collect and concentrate U and Th. The solution was evaporated to dryness then redissolved with 2 ml 2% HNO_3, prior to injection.

All measurements were performed a using a MC-ICPMS at the Research School of Earth Sciences, Australian National University. Measurements were conducted using recently developed multiple-Faraday cup protocols reported in Andersen *et al.* (2004) Potter *et al.* (2005) and Stirling *et al.* (2005). This multiple-Faraday approach yields significantly better precision and reproducibility compared with the uncorrected use of less stable ion counter electron multipliers for the minor ^{234}U and ^{230}Th isotopes, thus reducing the U-series age uncertainties by up to a factor of ten (Stirling *et al.*, 2001).

A.4.3 Screening of U-series coral dates prior to open-system corrections

Following the procedures of earlier workers (Chen *et al.*, 1991; Stirling *et al.*, 1995; 1998; Robinson *et al.*, 2004), uncorrected coral measurements were screened for potential U/Th loss or gain based on the following criteria:

1) We consider the calculated $\delta^{234}U_{initial}$ to be the best quantitative test for open-system behavior in corals. For a coral age to be considered strictly reliable $\delta^{234}U_{initial}$ values should reflect a modern seawater value of 146.6 ± 4‰.

2) The total uranium concentration of fossil corals should approximate modern coral values of about 3 ± 0.5 ppm of uranium.

3) Fossil corals should be free of allochthonous ^{230}Th, as indicated by the absence of detrital ^{232}Th (< 1 ppb).

4) Corals should show primary aragonitic structures or have < 2% calcite concentration.

A.5 INDEPENDENT TESTS OF U-SERIES AGE RELIABILITY

A.5.1 Does coral age fall within the accepted duration of MIS 5e?

Emergent fossil reef terraces along the West Australian coastline are known to have grown during MIS 5e (Collins *et al.*, 1993a,b; McCulloch and Esat, 2000; Stirling *et al.*, 1995, 1998). Therefore, the most obvious test of whether uncorrected or corrected coral age is appropriate or accurate, is to see if measured ages fall within the known duration of this sea-level event. A large number of studies have attempted to define the onset, duration and termination of MIS 5e, but the results have been mixed. For example Muhs *et al.* (2002) give a range of 132 to 113 for coral from Oahu, while Stirling *et al.* (1998) suggest a period widespread reef growth occur between 128 and 121 ka with less robust reef development occurring up to 116 ka. Again these sorts of discrepancies are the likely result of U-series reliability issues. However in one of the more complete synthesis of MIS 5e U-series coral dates, Edwards *et al.* (2003) place the duration of MIS 5e at 130 ± 1 and termination at 116 ± 1 ka. Therefore, based on these age boundaries any of the 76 West Australian U-series ages that fall outside this interval may be imprecise regardless of reliability criteria or open-system corrections.

A.5.2 Do coral ages follow stratigraphic order?

In a stacked sequence of growth positions corals, true age should decrease from the base to the top. At Cape Cuvier, fringing reef development during MIS 5e occurred in shallow water. Once accommodation space was filled, reef growth would continue laterally (Kennedy and Woodroffe 2002). Based on this type of growth history age isochrons should be parallel to the reef front, meaning a relatively narrow but decreasing coral age range is expected up section (Kennedy and Woodroffe 2002). A total of 15 coral samples (LCC) were collected from a 3 m high vertical cliff section at Cape Cuvier. With approximately 30 m of reef-flat landward of the reef-crest there was an extended period of reef accretion prior to these corals growing, and the presence of Holocene notching suggests an active period of coastal erosion. This information provides a stratigraphic context for evaluating uncorrected or corrected U-series ages, using the fundamental principle of superposition and at the highest levels of stratigraphic resolution.

A.5.3 Do subsamples from a single coral colony yield equal ages?

The most stringent way to test the reliability of uncorrected U-series ages or open-system corrections is to analyse multiple samples from an individual coral. Because the coral grew during a very restricted time interval (annual banding can indicate growth age) this should be reflected in the U-series age. Coral LDS1 is a large head 3 m in diameter of the genus *Porites,* growth banding indicates its total lifespan to be less than 100 yrs. Under closed-system conditions we expect the 10 subsamples samples from LDS1 to show age equivalence. Multiple subsamples from a further 5 coral colonies also underwent U-series analysis.

A.6 RESULTS

A.6.1 Coral geochemistry

Coral $^{234}U/^{238}U$ vs. $^{230}Th/^{238}U$ activity do not plot on the seawater evolution curve (blue line), which describes the (closed-system) ingrowth and decay of ^{234}U and ^{230}Th isotopes from an initial seawater activity 1.1466; or more specifically, plot within the known duration of MIS 5e (red line segment) (**Fig. 3a,b**). This reveals that more than 85% of measured WA corals were subject to isotopic exchange, with a coupled shift towards elevated values for both $^{234}U/^{238}U$ and $^{230}Th/^{238}U$ activities. Uranium concentrations range from 1.24 to 5.32 ppm with an average of 2.91 ± 0.59 ppm (**Fig. 4**), within a range (2.0-3.5 ppm) typical of modern coral concentrations (Shen and Dunbar 1995).

^{232}Th concentrations proved highly variable with values ranging between 0.05 ppb up to 533 ppb. It was found that those corals with ^{232}Th concentrations >1 ppb exhibited greater age discrepancies (**Fig. 5**). In addition, corals with elevated ^{232}Th exhibit a positive correlation between increasing uranium concentrations and ^{234}U enrichment (**Fig. 4**). Evidence of ^{232}Th contamination may indicate the presence of allochthonous (non alpha-recoil) $^{230}Th_{nr}$ and/or ^{234}U isotopes. Thus, to best evaluate Thompson's modelling parameters, age corrections were only conducted on 53 coral samples with ^{232}Th concentrations below 1 ppb.

A.6.2 Corrected and uncorrected age and the duration of MIS 5e

West Australian corals returned an average uncorrected U-series age of 127.6 ± 4.5 ka (n=76). Only 10 coral samples or approximately 13% of the total sample population have a $\delta^{234}U_{initial}$, which falls within the 146.6 ± 4‰-confidence band (**Fig. 3b**) and have ages that cluster between 126 and 128 ka and around 122 ka. A total of 12 corals have ages older than the accepted duration of MIS 5e (>130 ka). The result of

open-system corrections is for an overall lowering of coral age to an average of 120.3 ± 5.3 ka (n=53) (**Fig. 6b**). This correction slightly improves the total number of ages that fall within the accepted duration of MIS 5e. However, 7 corals return ages that follow the termination of MIS 5e (<116 ka), all having $\delta^{234}U_{initial}$ values greater than 174‰. Since these corrected coral ages plot well outside the accepted duration of MIS 5e we question their reliability.

A.6.3 Uncorrected and corrected ages from a stacked coral sequence

Measured $^{230}Th/^{238}U$ isotope ratios exhibit fairly uniform values of 0.8 ± 0.01 down section. These near equivalent $^{230}Th/^{238}U$ activities produce coeval coral ages of around 130.5 ± 3 ka (**Fig. 6**). However, there does appear to be a slight younging up-section within the bottom 2/3's of the sequence, from 132.4 ± 1.5 ka at 2.25 m below the reef surface to 127.7 ± 1.1 ka at 1.15 m below the reef surface (**Fig. 6; Fig. 7**). This gives a vertical accretion rate of 0.25 mm/yr^{-1}. Open-system corrections lowered overall age to 116.7 ± 3.6, coinciding with the termination of MIS 5e. There was a very tight age correlation within the bottom 2/3's of the section where corals returned an average age of 117.4 ± 0.6 ka (**Fig. 6; Fig. 7)**. Either rapid vertical accretion or lateral reef growth can explain this age relationship.

A.6.4 Uncorrected and corrected ages from individual corals

A suite of 10 bulk (200 μg) coral samples analysed from LDS1 were found to be chemically distinct from each other (**Fig. 8**). Uranium concentrations ranged from 2.62 to 3.38 ppm, a trend commonly observed in modern corals (Shen and Dunbar 1995) (**Fig. 9**). However, crustal subsamples LDS1g and LDS1i were found to be highly enriched in ^{232}Th having concentrations of 235 and 533 ppb respectively (**Fig. 9**). A few centimetres below the crustal surface subsamples LDS1h and LDS1j show ^{232}Th

enrichment dropping to 2 and 7.7 ppb respectively. Subsamples collected from more pristine central parts of the coral LDS1d, e and f had ^{232}Th concentrations < 2 ppb and returned an average age of 124.2 ± 1.2 ka with a $\delta^{234}U_{initial}$ of 166.3 ± 2‰. Attempts to use an open-system correction on subsamples contaminated with ^{232}Th proved unsuccessful, coming no closer to yielding a single concise coral age (**Fig. 8**). However, even corals with minimal ^{232}Th contamination (< 2 ppb) as in samples LDS1d, e, f, and h, it made no improvement in the overall spread of ages. There was also a general trend for increasing uranium concentration to decrease ^{230}Th/^{238}U activities and increase ^{234}U/^{238}U activities (**Fig. 9**).

Multiple subsample analysis was made on 5 other corals (**Fig. 10**). Those with ^{232}Th concentrations > 1 ppm and $\delta^{234}U_{initial}$ values than > 180 are excluded from the plot. A single coral CRB1 has both its subsamples fall within the allowable 146.6 ± 4‰ range for reliable uncorrected ages, and an age difference of 800 yrs but is still within analytical error. All other coral subsamples have $\delta^{234}U_{initial}$ values fall outside the 146.6 ± 4‰ range so have been subject to isotopic exchange. Uncorrected subsamples from corals MSD3, SMM3 and HFB1 display equal age, despite having dissimilar $\delta^{234}U_{initial}$ values. The application of Thompson's open-system corrections did not improve age variability within individual corals.

A.7 DISCUSSION

A.7.1 The duration of MIS 5e

Uncorrected fossil corals with elevated ^{232}Th concentrations (> 1ppb) exhibit a broad scattering of U-series ages that range within and beyond the accepted duration of MIS 5e (**Fig.3b; Fig. 5**). This suggests that the presence of detrital ^{232}Th is evidence for the contemporaneous (non-subtle) addition of non-radiogenic ^{230}Th in samples older than 140 ka, or uranium uptake in samples younger than 110 ka (measured age).

However, corals with ^{232}Th < 1 ppb also exhibit evidence of isotopic exchange with elevated $\delta^{234}U_{initial}$ and ages that range beyond the accepted duration of MIS 5e (**Fig. 3b**). Based on the Thompson *et al.* (2003) model, these isotopic anomalies are the result of the coupled addition of particle reactive ^{234}Th and ^{230}Th, produced by the decay of dissolved uranium and alpha-recoil mobilisation of uranium daughters. By mathematically stripping of this excess ^{234}U and ^{230}Th, Thompson calculates an open-system age that intercepts the seawater evolution curve (**Fig. 3b**). While there are no geochemical protocols to test whether open-system ages are accurate, we provide evidence of open-system corrections in seven samples that fall outside the accepted duration of MIS 5e, suggesting the corrected ages remain inaccurate (**Fig. 3b**). There is no obvious evidence among elemental concentration or isotopic activity in these seven invalid ages that reveal alternative exchange processes, other than those reported in Thompson *et al.*, 2003. If 7 out of 53 ages are determined to be inaccurate, then how many other open-system corrections might ultimately be considered spurious?

A.7.2 The fundamental principle of stratigraphic superposition

Corals collected from a measured section at Cape Cuvier exhibit roughly equivalent ^{230}Th/^{238}U of activities of 0.8 ± 0.1, and produce a small range of ages centred at 130.5 ± 3.0 ka (**Fig. 6; Fig. 7**). Corals also produce progressively younger ages in the lower two thirds of the reef sequence. Ages of 132.4 ± 1.5 ka were determined at a depth of 2.25 m, and 127.7 ± 1.1 ka at 1.15 m depth, yielding a vertical reef accretion rate of 0.25 mm/yr^{-1}. Vertical accretion at this rate appears entirely reasonable for a reef framework dominated by coralgal boundstone considering the shallow water depth and potentially high wave energy at the site (Kennedy and Woodroffe 2002).

When open-system corrections (Thompson *et al.*, 2003) are applied to our uncorrected U-series ages, we observe a reduction in average age to 116.7 ± 3.6 ka (**Fig.**

6; Fig.7). The lower 2/3's of the age modelled section showed a tight cluster at 117.4 ± 0.6 ka suggesting either rapid vertical accretion > 8 mm/yr $^{-1}$ or, a more likely scenario, that of a dominant lateral accretion.

Based on the accepted duration of MIS 5e (116-130 ka) the uncorrected ages place timing of coral growth at the beginning of 5e. However the position of these corals within the reef framework clearly cannot represent the beginning of 5e. There is a 40 m wide reef flat landward of the sea cliff and even based on maximum vertical or lateral accretion rates, it would have taken several thousand of years before growth could reach this current mid-reef, morphostratigraphic position. So although uncorrected coral ages do display some relative age relationships up section, their overall age appears older than their stratigraphic location within the reef complex.

Open-system corrections also display relative age relationships, with the tight coeval age of 116.7 ± 3.6 ka and attributable to lateral reef accretion (**Fig. 6**). However, the overall ages do not agree with reef accretion and erosion processes. Erosion rates along tropical carbonate coastlines can range anywhere from 2 to 15 mm/yr and up to 33 mm/yr (Playford, 1997). Even using a conservative rate of 4 mm/yr (Trudgill, 1983), the lower emergent reef must have retreated by at least 30 m over the intervening Holocene period. The fossil corals now exposed at the shoreface should represent a growth period sometime prior to the termination of MIS 5e (coral ages > 116 ka) and the emergence of the reef. Hence corrected coral ages appear too young to represent the true coral age. Considering all aspects of this site and section we would expect a mid 5e age to be the most logical.

Despite the apparent variance in $\delta^{234}U_{initial}$, when $^{234}U/^{238}U$ and $^{230}Th/^{238}U$ are plotted on an activity ratio diagram, a linear isotopic array intersects the closed-system seawater evolution curve at around 124 ka (**Fig. 11**). This linear configuration suggests that coeval age corals gained different amounts of uranium with a fixed $\delta^{234}U$ value

around the same time, such as observed by Scholz *et al.* (2004). Corals that do not conform to this linear configuration may have been subjected to late uranium uptake or different $^{234}U/^{238}U$ groundwater activities. Based on the linear regression age model of Scholz *et al.* (2004), the intersection point of the modelled isochrons with the seawater evolution curve corresponds with evolution under a closed system and therefore approximates the true age of these corals. Cape Cuvier corals return an isochron age of 124 ka. The Scholz model suffers from fundamental condition that corals need to be coeval in age. However, the Scholz model does offer the most reasonable assessment for a mid MIS 5e coral age at this site.

A.7.3 Age equivalence in individual corals

The presence of chemical heterogeneity within a single *Porites* coral head (LDS1) has resulted in a range of uncorrected ages between 123.0 and 135.5 ka and $\delta^{234}U_{initial}$ of 156.19 ‰ to 173.62 ‰ (**Fig. 8; Fig. 9**). These subsamples generally have ^{232}Th concentrations >1 ppb. It would therefore appear that ^{232}Th enrichment also incorporated $^{230}Th_{nr}$, which yields an older age for DLS1i. However, the lowering of $\delta^{234}U_{initial}$ in LDS1j towards modern seawater values could have resulted only from the complementary addition of ^{238}U ($^{234}U/^{238}U$ activities < 1) or preferential loss of ^{234}U ($^{234}U/^{238}U$ activities > 1). This shows that presence of detrital ^{232}Th is a strong indicator for chemical or isotopic exchange in corals. We argue that open-system corrections were not able to return any sensible ages due to the presence of detrital ^{232}Th. It would also appear that the surrounding continental dune complex that buried parts of the reef in which the *Porites* was collected as a likely source of the detrital ^{232}Th.

Analysis of 5 other corals showed equivalent uncorrected ages despite having different $\delta^{234}U_{initial}$ values (**Fig. 10**). It would appear that heterogeneous enrichment in $\delta^{234}U_{initial}$ has not affected the $^{230}Th/^{238}U$ activity (overall age). This would require the

addition of ^{234}U without ^{238}U or ^{230}Th; this is not possible under normal alpha-recoil process. Corrected U-series ages did not improve internal age variability in individual corals. Five out of the six age corrected corals actually showed an increase of between 500 and 1500 yrs between the minimum and maximum subsample age within individual corals. In these samples, despite elevated $\delta^{234}U_{initial}$ values, the uncorrected ages exhibited tighter subsample age equivalence than was achievable using open-system corrections

A.7.4 Potential miscalculations in the Thompson's alpha-recoil

Because alpha-recoil mobilization results in the coupled addition of ^{234}U and ^{230}Th, those corals with higher $\delta^{234}U_{initial}$ should yield older U-series ages (see Fig. 9 for an example). However, we observe in Figure 8, that there are at least 3 examples where coral subsamples with different $\delta^{234}U_{initial}$ values yield equal ages. This is possible only through the addition of ^{234}U without ^{238}U or ^{230}Th. Robinson *et al.*, (2006) identified a uranium enriched ferromanganese layer (>10 ppm) on the surface of fossil corals as a potential source of excess ^{234}U. Robinson *et al.* (2006) modeled alpha-recoil diffusion across this ferromanganese rich surface layer. Using a diffusion coefficient of 0.1 _m^2yr^{-1}, Robinson found whole-coral $\delta^{234}U_{initial}$ values increased to 147‰ after 20 ka and 164‰ after 200 ka without affecting the overall coral age. Thus, alpha-recoil diffusion from a high uranium surface coating can cause increase in $\delta^{234}U_{initial}$ values with minimal changes to the modeled age. It appears that this process may be responsible for the apparent difference in $\delta^{234}U_{initial}$ from replicate coral subsamples that exhibit equal ages (**Fig. 10**). Robinson *et al.* (2006) stress that without detailed knowledge of the U/Th distribution within a specific coral sample, it is not possible to convert closed-system ages to open-system ages.

A.7.5 How best to use U-series coral ages

The primary criterion in determining the reliability of coral U-series ages has been to back calculate measured $\delta^{234}U$ activity ratios (Edwards *et al.*, 1987a; Chen *et al.*, 1991; Stirling *et al.*, 1995), which should correspond to a modern seawater $^{234}U/^{238}U$ activity of 146.6 ± 2.5‰ (Robinson *et al* 2004). The more elevated the $\delta^{234}U_{initial}$ the more unreliable the age. Based on independent age controls in this study it has been determined that higher $\delta^{234}U_{initial}$ values do not always equate to more erroneous ages (**Fig. 3b; Fig. 8; Fig 11; Fig 12**). It was found that the presence of > 1ppb of detrital ^{232}Th produces the largest discrepancy in age (**Fig. 5; Fig. 6; Fig. 8; Fig. 9**). We propose that this criterion should be used as a primary determinant in age reliability. It was also observed that equal-age subsamples from the same coral could have different $\delta^{234}U_{initial}$ values (**Fig. 8 Fig. 10**), suggesting that an increase in $\delta^{234}U_{initial}$ may not lead to a corresponding increase in age. Similar relationships were also observed in a recent study of deep-sea scleractinian corals (Robinson *et al.*, 2006).

This study recommends the use of the following protocols in determination and assessment of the reliability of U-series coral ages:

1. Analysis of multiple subsamples from individual corals as the best quantitative test in determining U-series age;

2. Detrital ^{232}Th concentrations should be < 1ppb;

3. Allowable error in back calculated $\delta^{234}U_{initial}$ should be extended from 146.6 ± 4 ‰ to 146.6 ± 10 ‰;

4. Uranium concentrations should be between 2.5 and 3.5 ppm; and

5. Open-system corrections should only be used in conjunction with rigorous independent age tests.

A.8 CONCLUSIONS

The coupled shift in $^{234}U/^{238}U$ and $^{230}Th/^{238}U$ activity observed in pristine coral samples (that results in elevated $\delta^{234}U_{initial}$ and older apparent ages) has been attributed to alpha-recoil mobilization of particle reactive ^{234}Th and ^{230}Th by Thompson *et al.* (2003) and Thompson and Goldstein (2005). This study questions the accuracy and reliability of the open-system model, used to correct for alpha-recoil-based anomalies commonly observed in fossil corals. Until this study, independent tests to validate the accuracy of open-system corrections were lacking. Without an independent measure of accuracy, corrected U-series age is required to be accepted at face value. We evaluated open-system corrections against independent age controls such that; 1) corrected ages fall within the accepted duration of MIS 5e, 2) corrected coral age correspond with stratigraphic order, and 3) coral subsamples from a single coral colony produce a reasonably tight cluster of ages. We find that open-system corrections fail to satisfy any of these age tests. It is also apparent that there are no isotopic indicators that identify spurious coral age among our several tests. Moreover, even if a number of corrected coral ages agree with the test criteria, they still may not represent true and accurate coral ages. These findings not only call into question the validity of the Thompson *et al.* (2003) open-system correction, but also the use of such corrections to alter or modify Upper Pleistocene sea-level history.

A.9 REFERENCES

Andersen, M.B., Stirling, C.H., Potter, E.K., Halliday, A.N., 2004. Toward epsilon levels of measurement precision on $^{234}U/^{238}U$ by using MC-ICPMS. International Journal of Mass Spectrometry 237 (2-3), 107-118.

Andersen M.B., Stirling C.H., Potter E-K., Halliday, A.N., Blake, S.G., McCulloch M.T., Ayling B.F., O'Leary M.J., *in review*. Direct chronology of the Marine Isotope Stage 15 (~600 ka) estimated from high-precision U-series ages from Henderson Island, south Pacific.

Bard, E., Hamelin, B., Fairbanks, R.G., 1990. U/Th ages obtained by mass-spectrometry in corals from Barbados: sea level during the past 130,000 years. Nature 346 (6283), 456-458.

Bard, E., Fairbanks, R.G., Hamelin, B., Zindler, A., Huong, C.T., 1991. ^{234}U anomalies in corals older than 150,000 years. Geochimica et Cosmochimica Acta 55, 2385-2390.

Bard, E., Fairbanks, R.G., Hamelin, B., 1992. How accurate are the U/Th ages obtained by mass spectrometry on coral terraces, in: G.J. Kukla, E. Went (Eds.), Start of a Glacial, NATO ASI Series 13, Springer, Berlin, pp. 15-21.

Bar-Matthews, M., Wasserburg, G. J., Chen, J.H., 1993. Diagenesis of fossil coral skeletons: correlation between trace-elements, textures, and $^{234}U/^{238}U$. Geochimica et Cosmochimica Acta 57, 257-276.

Bender, M.L., Fairbanks, R.G., Taylor, F.W., Matthews, R.K., Goddard, J.G., Broecker, W.S., 1979. Uranium-series dating of Pleistocene reef tracts of Barbados, West Indies. Geological Society of America Bulletin 90, 577-594.

Broecker, W.S., 1963. A preliminary evaluation of uranium series in equilibrium as a tool for absolute age measurement on marine carbonates. Journal of Geophysical Research 68, 2817-2834.

Cabioch, G., Montaggioni, L.F., Faure, G., Ribaud-Laurenti, A., 1999. Reef coralgal assemblages as recorders of paleobathymetry and sea level changes in the Indo-Pacific province. Quaternary Science Reviews 18, 1681-1695.

Chen, J.H., Edwards, R.L., Wasserburg, G.J., 1986. ^{238}U, ^{234}U and ^{232}Th in seawater, Earth and Planetary Science Letters 80 (3-4), 241-251.

Chen, J.H., Curran, H.A., White, B., Wasserburg, G.J., 1991. Precise chronology of the Last Interglacial period: $^{234}U^{230}Th$ data from fossil coral reefs in the Bahamas. Geological Society of America Bulletin 103, 82-97.

Cherniak, D.J., 1997. An experimental study of strontium and lead diffusion in calcite, and implications for the carbonate diagenesis and metamorphism. Geochimica et Cosmochimica Acta 61, 4173-4179.

Collins, L.B., Zhu, Z.R., Wyrwoll, K.H., Hatcher, B.G., Playford, P.E., Chen, J.H., Eisenhauer, A., Wasserburg, G.J., 1993a. Late Quaternary evolution of coral reefs

on a cool-water carbonate margin: the Abrolhos carbonate platforms, Southwest Australia. Marine Geology 110, 203-212.

Collins, L.B., Zhu, Z.R., Wyrwoll, K.H., Hatcher, B.G., Playford, P.E., Eisenhauer, A., Chen, J.H., Wasserburg, G.J., Bonani, G., 1993b. Holocene growth history of a reef complex on a cool-water carbonate margin: Easter Group of the Houtman Abrolhos, eastern Indian Ocean. Marine Geology 115, 29-46.

Collins, L.B., Zhu, Z.R., Wyrwoll, K.-H., 1996. The structure of the Easter Platform, Houtman Abrolhos Reefs: Pleistocene foundations and Holocene reef growth. Marine Geology 135, 1-13.

Denman, P.D., Van de Graaff, W.J.E., 1976. Emergent Quaternary marine deposits in the Lake MacLeod area, Western Australia. Western Australia Geological Survey Annual Report 1977, 32-36.

Eisenhauer, A., Zhu, Z.R., Collins, L.B., Wyrwoll, K.H., Eichstatter, R., 1996. The Last Interglacial sea-level change: new evidence from the Abrolhos Islands. West Australia. Geol Rundsch 85, 606-614.

Edwards, R.L., Chen, J.H., Wasserburg, G.J., 1987a. ^{238}U, ^{234}U, ^{230}Th, ^{232}Th systematics and the precise measurement of time over the past 500,000 years. Earth and Planetary Science Letters 81, 175-192.

Edwards, R.L., Chen, J.H., Ku T.-L., Wasserburg, G.J., 1987b. Precise timing of the last inter-glacial period from mass spectrometric analysis of ^{230}Th in corals. Science 236, 1547-1553.

Edwards, R.L., Cutler, K.B., Cheng, H., Gallup, C.D., 2003. Geochemical evidence for Quaternary sea-level change. Treatise on Geochemistry 6:13, 343-364.

Fairbridge, R.W., 1950. The geology and geomorphology of Point Peron, Western Australia. Royal Society of Western Australia Journal 34, 35-72.

Fruijtier, C., Elliot, T., Schlager, W., 2000. Mass-spectrometric $^{234}U/^{230}Th$ ages from the Key Largo Formation, Florida Keys, United States: Constraints on diagenetic age disturbance. Geological Society of America Bulletin 112, 267-277.

Gallup, C.D., Edwards, R.L., Johnson, R.G., 1994. The Timing of high sea levels over the past 200,000 years. Science 263, 796-800.

Gallup, C. D., Cheng, H., Taylor, F. W., Edwards, R.L., 2002. Direct determination of the timing of sea-level change during Termination II. Science 295, 310-313.

Hamelin, B., Bard, E., Zindler, A., Fairbanks, R.G., 1991. $^{234}U/^{238}U$ mass spectrometry of corals: How accurate is the U-Th age of the last interglacial period? Earth and Planetary Science Letters 106, 169-181.

Henderson, G. M., Slowey, N. C.,Fleisher, M.Q., 2001. U/Th dating of carbonate platform and slope sediments. Geochemica et Cosmochemica Acta 65, 2757-2770.

Henderson, G.M., 2002. Seawater $^{234}U/^{238}U$ during the last 800 thousand years. Earth and Planetary Science Letters 199, 97-11.

Kennedy, D.M., Woodroffe, C.D., 2002. Fringing reef growth and morphology: a review Earth-Science Reviews 57 255-277.

Kigoshi, K., 1971. Alpha-recoil thorium-234: dissolution into water and the uranium-234/ uranium-238 disequilibrium in nature. Science 173 (3991), 47-48.

Ku, T.-L., Ivanovich, M., Luo, S., 1990. U-series dating of Last Interglacial high sea stands: Barbados revisited. Quaternary Research 33, 129-147.

Lazar, B., Enmar, R., Schossberger, M., Bar-Matthews, M., Halicz, L., Stein, M., 2004. Diagenetic effects on the distribution of uranium in live and Holocene corals from the Gulf of Aqaba. Geochimica et Cosmochimica Acta 68 (22), 4583-4593.

Logan, B.W., Read, J.R., Davies, G.R., 1970. History of carbonate sedimentation, Quaternary Epoch, Shark Bay, Western Australia. American Association of Petroleum Geologists Memoir 13: 38-85.

McCulloch, M.T., Esat T., 2000. The coral record of last interglacial sea levels and sea surface temperatures. Chemical Geology 169, 107-129.

Muhs, D.R., Simmons, K.R., Steinke, B., 2002. Timing and warmth of the Last Interglacial period: new U-series evidence from Hawaii and Bermuda and a new fossil compilation for North America. Quaternary Science Reviews 21 (12-13), 1355-1383.

Playford, P.E., 1997. Geology and hydrology of Rottnest Island, Western Australia, in: Vacher, H.L., T. Quinn, (Eds.), Geology and Hydrology of Carbonate Islands, Developments in Sedimentology 54, Elsevier, London, pp. 783–810

Potter, E.K., Stirling, C.H., Andersen, M.B., Halliday, A.N., 2005. High precision Faraday collector MC-ICPMS thorium isotope ratio determination. International Journal of Mass Spectrometry 247 (1-3), 10-17.

Robinson, L.F., Belshaw, N. S., Henderson G.M., 2004. U and Th concentrations and isotope ratios in modern carbonates and waters from the Bahamas. Geochimica et Cosmochimica Acta 68, 1777–1789.

Robinson, L.F., Adkins, J.F., Fernandez, D.P., Burnett, D.S., Wang, S-L., Gagnon, A.C., Krakauer, N., 2006. Primary U-distribution in scleractinian corals and its implications for U-series dating. Geochemistry Geophysics Geosystems 7 (5), 1-20.

Scholz, D., Mangini, A., Felis, T., 2004. U-series dating of diagenetically altered fossil reef corals. Earth and Planetary Science Letters 218 (1-2), 163-178.

Shen, G.T., Dunbar, R.B., 1995. Environmental Controls on Uranium in Reef Corals. Geochimica et Cosmochimica Acta 59 (10), 2009-2024.

Stirling, C.H., Esat, T.M., McCulloch, M.T., Lambeck, K., 1995. High-precision U-series dating of corals from Western Australia and implications for the timing and duration of the Last Interglacial. Earth and Planetary Science Letters 135, 115-130.

Stirling, C.H., Esat, T.M., Lambeck, K., McCulloch, M.T., 1998. Timing and duration of the Last Interglacial: evidence for a restricted interval of widespread coral reef growth. Earth and Planetary Science Letters 160, 745-762.

Stirling, C.H., Esat, T.M., Lambeck, K., McCulloch, M.T., Blake, S.G., Lee D.C., Halliday, A.N., 2001. Orbital forcing of the marine isotope stage 9 interglacial. Science 291 (5502), 290-293.

Stirling, C.H., Halliday A.N., Porcell, D., 2005. In search of live Cm-247 in the early solar system. Geochimica et Cosmochimica Acta 69 (4), 1059-1071.

Thompson, W.G., Spiegelmann M.W., Goldstein S.L., Speed R.C., 2003. An open-system model for U-series age determinations of fossil corals. Earth Planetary Science Letters 210, 365-38.

Thompson, W.G., Goldstein, S.L., 2005. Open-system coral ages reveal persistent suborbital sea-level cycles, Science 308 (5720), 401-404.

Trudgill, S.T., 1983. Preliminary estimates on intertidal limestone erosion, One Tree Island, Southern Great Barrier Reef, Australia. Earth Surface Processed and Landforms 8 (2), 189-193.

Veeh, H.H., Van de Graaff, W.J.E., Denman, P.D., 1979. Uranium-series ages of coralline terrace deposits in Western Australia. Journal of the Geological Society of Australia 26, 285-292.

Van de Graaff, W.J.E., Denman, P.D., Hocking, R.M., 1976. Emerged Pleistocene marine terraces on Cape Range, Western Australia. Geological Survey of Western Australia Annual Report 1975, 62-69.

Villemant, B., Feuillet, N., 2003. Dating open systems by the 238U-234U-230Th method: application to Quaternary reef terraces. Earth and Planetary Science Letters 210, 105-118.

A.10 FIGURES 1-11

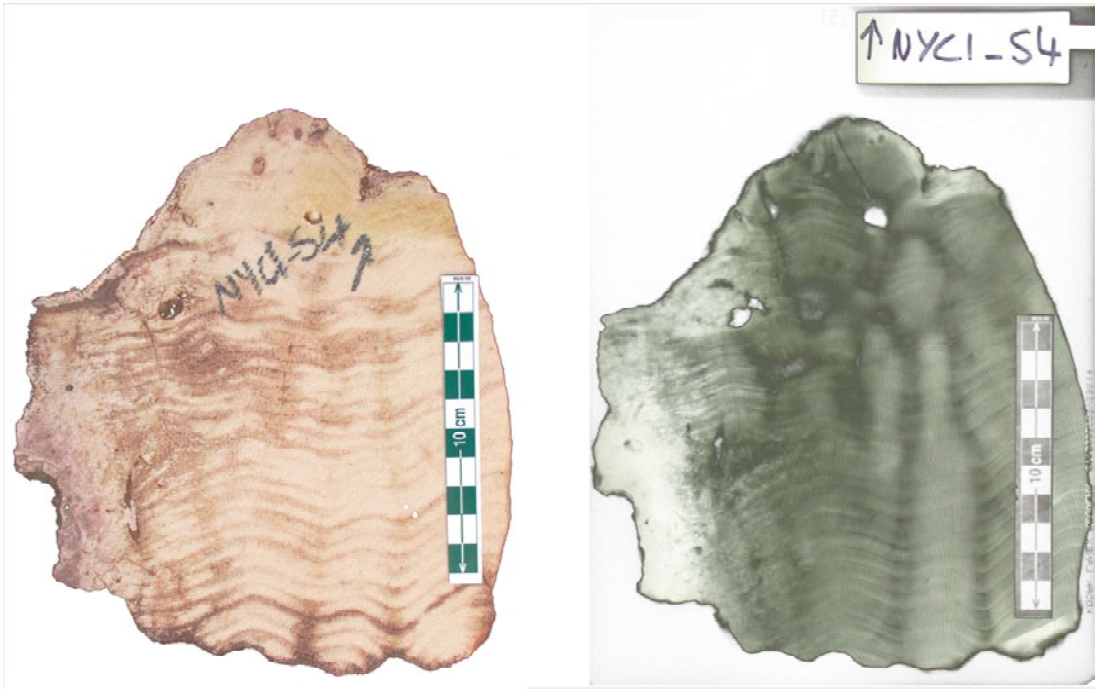

Figure 1: A *Porites* coral (NYC) collected a few metres above sea level at the mouth of Yardie Creek, Cape Range. A sliced 7 mm thick section (left) and its X-radiograph positive print (right). The lighter areas on the X-ray print represent denser areas of the coral and are associated with calcite alteration. Brown staining observed on the sliced section is sediment contamination sourced through pore water movement along less dense growth banding within the coral.

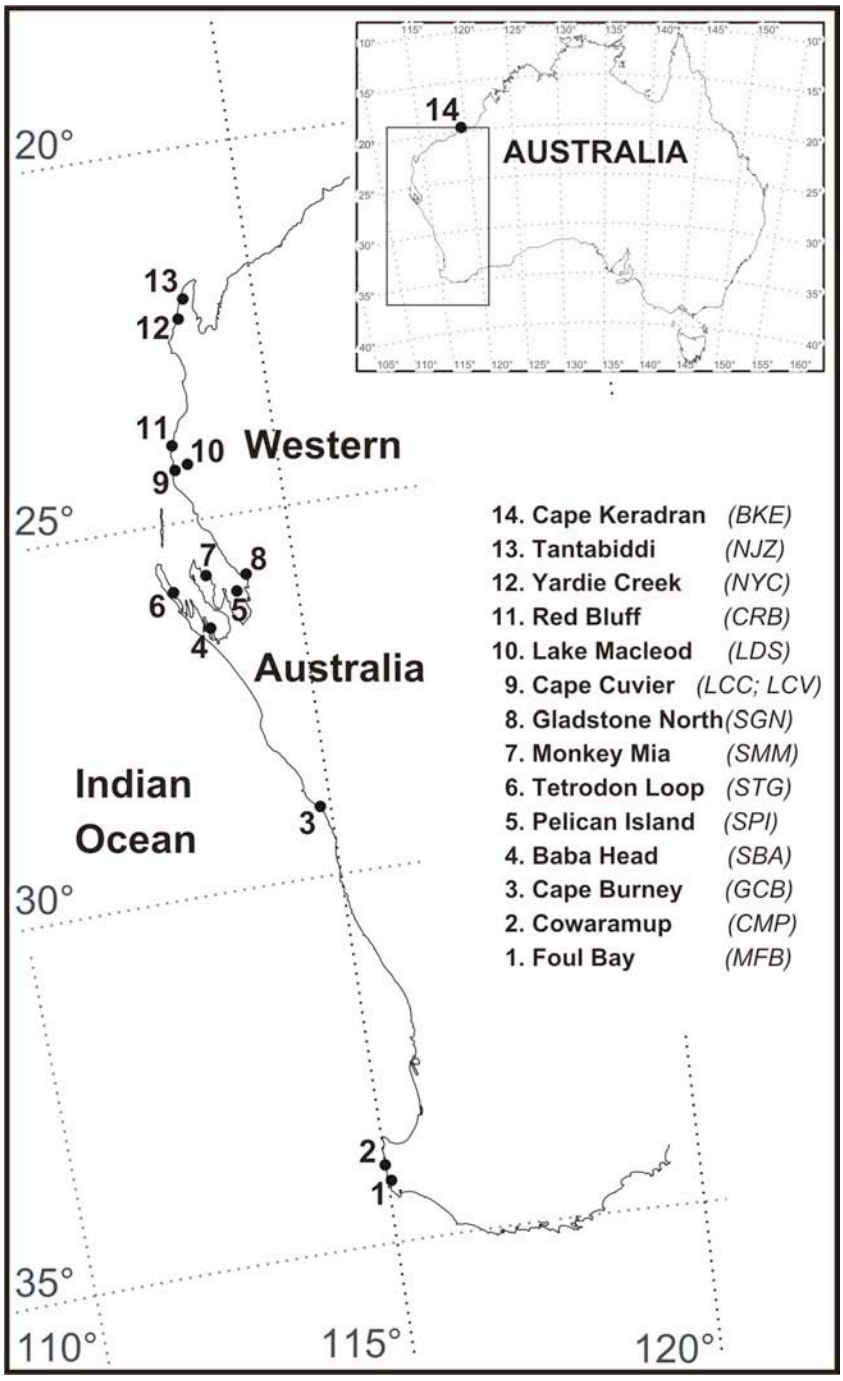

Figure 2: Map of Western Australia showing fossil reef and sample locations.

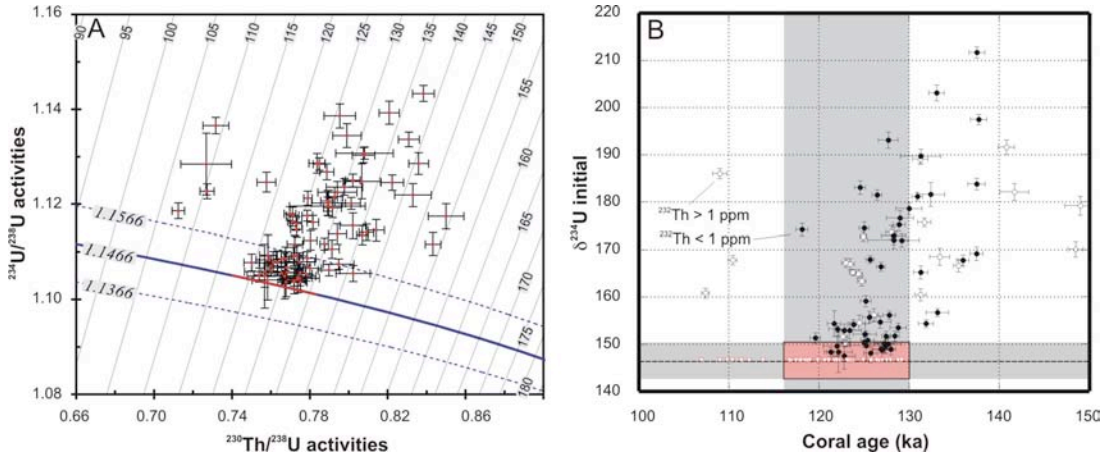

Figure 3: A) Compilation of Western Australian U-series data plotted on a $^{234}U/^{238}U$ activity ratio diagram. The blue line represents closed system evolution with and modern seawater $^{234}U/^{238}U$ activity of 1.1466 and the red segment represents the duration of MIS 5e. The sub-vertical lines are lines of equal ^{230}Th age B) $^{234}U/^{238}U$ activity at the time of coral growth versus ^{230}Th-age. The horizontal grey shaded area represents zone of age reliability where $\delta^{234}U_{initial} = 146.6 \pm 4‰$ (horizontal dotted line). Vertical shaded area represents the known duration of MIS 5e based on Edwards *et al.* (2003). Reliable uncorrected (black circle) and open-system corrected ages (triangles) should plot within the red box. Open-system ages corrected to a $\delta^{234}U_{initial}$ seawater value of 146.6.

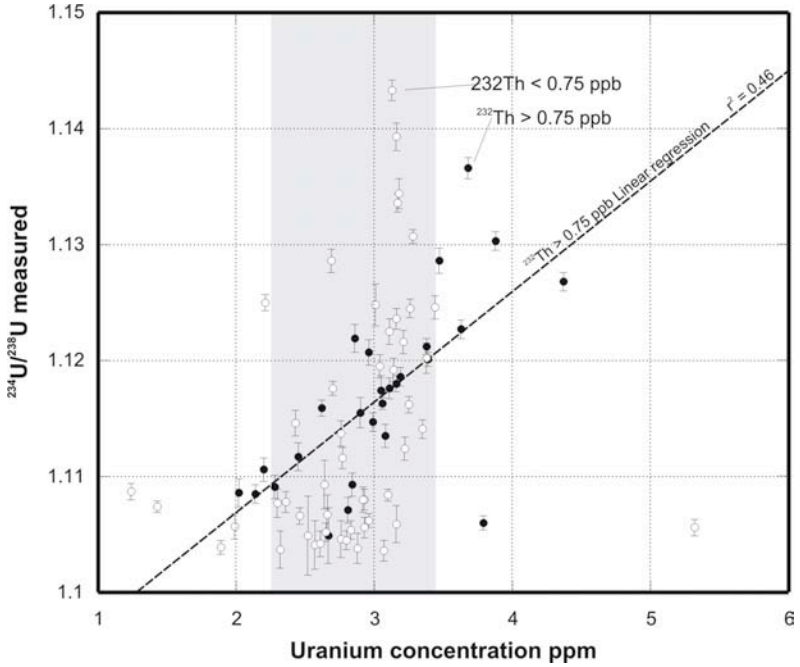

Figure 4: A plot of uranium concentration vs. measured $^{234}U/^{238}U$ activity. The solid circles are corals with ^{232}Th concentrations >0.75 ppb and the open circles corals with ^{232}Th concentrations <0.75 ppb. The shaded area represents the average spread of uranium concentrations for modern corals (Shen and Dunbar 1995). A positive correlation of increasing $^{234}U/^{238}U$ activities with increasing uranium concentrations is observed in corals with ^{232}Th > 0.75 ppb.

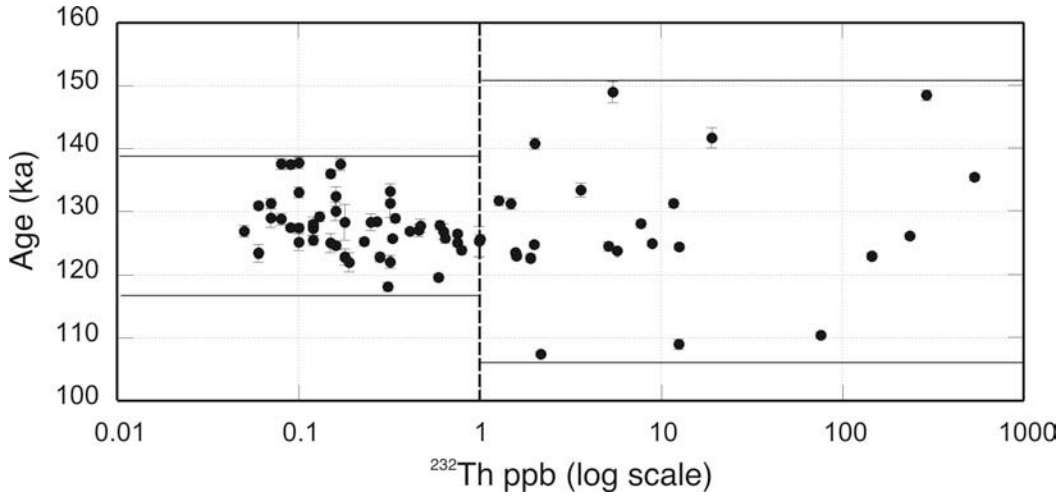

Figure 5: A plot of ^{232}Th concentrations (log scale) vs. age. Corals with ^{232}Th concentrations > 1 ppb exhibit greater age variability than corals with ^{232}Th <1 ppb. This suggest that allochthonous ^{230}Th, ^{238}U or ^{238}U may have be incorporated along with ^{232}Th into the coral skeleton.

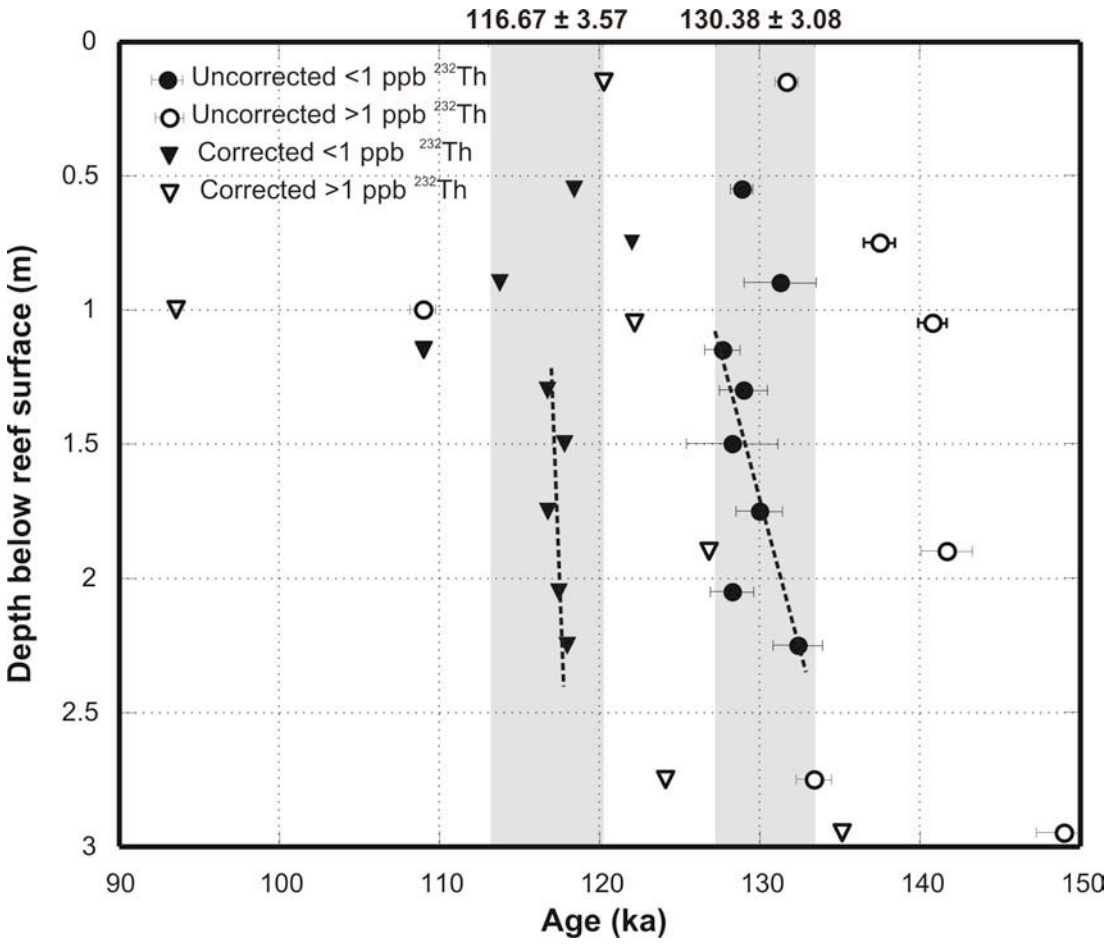

Figure 6. Coral age collected from a vertical reef section at Cape Cuvier. Circles represent uncorrected coral age, open for ^{232}Th > 1 ppb and closed for ^{232}Th < 1 ppb. Triangles represent open-system corrected coral age, open for ^{232}Th > 1 ppb and closed for ^{232}Th < 1 ppb.

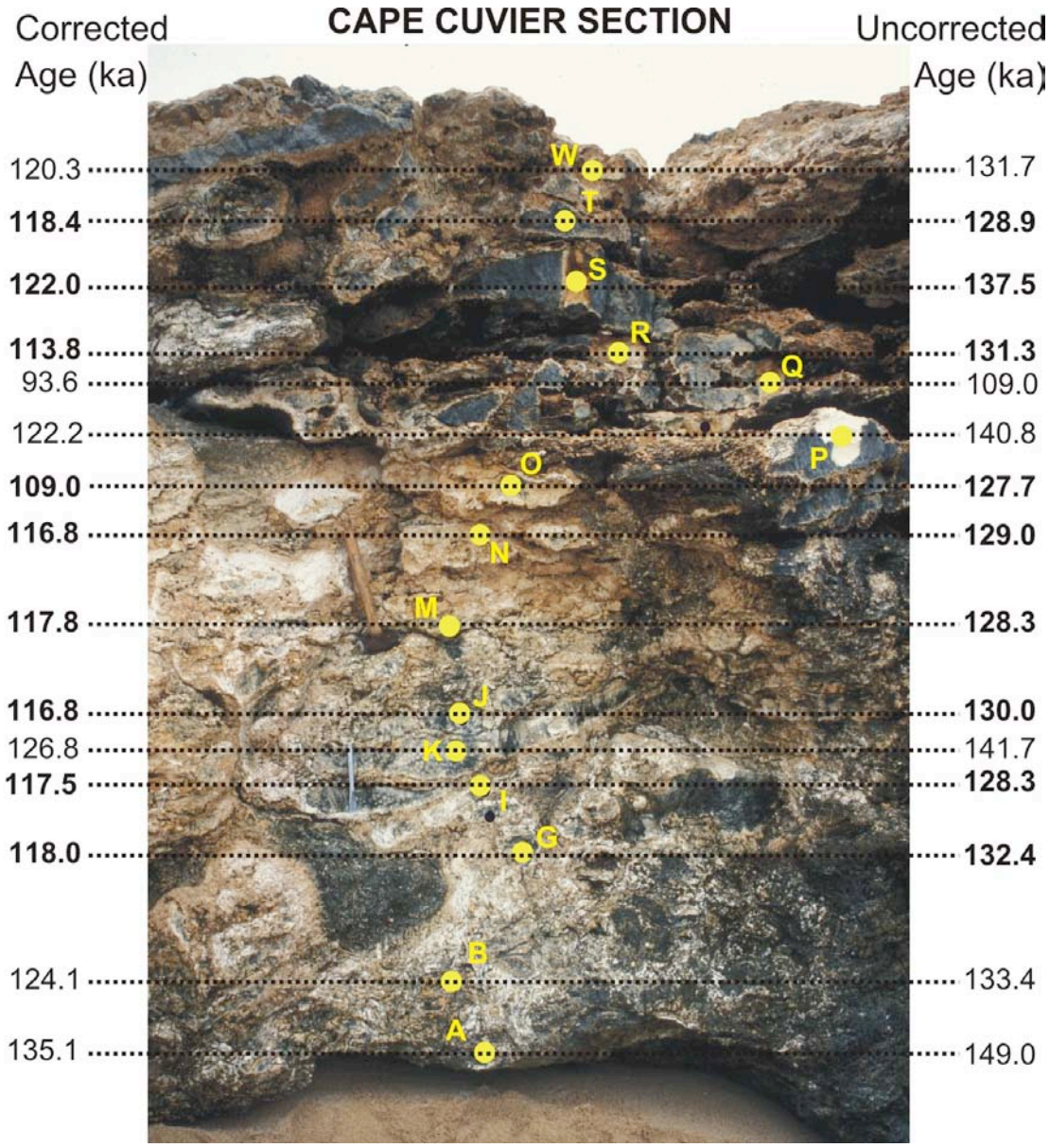

Figure 7. U-series dating results from a Holocene sea cliff cut into a MIS 5e reef terrace at Cape Cuvier.. Yellow dots represent the sample location, both corrected and uncorrected ages are reported. All measured samples had elevated $\delta^{234}U_{initial}$, bold numbers indicate coral samples with ^{232}Th < 1ppb.

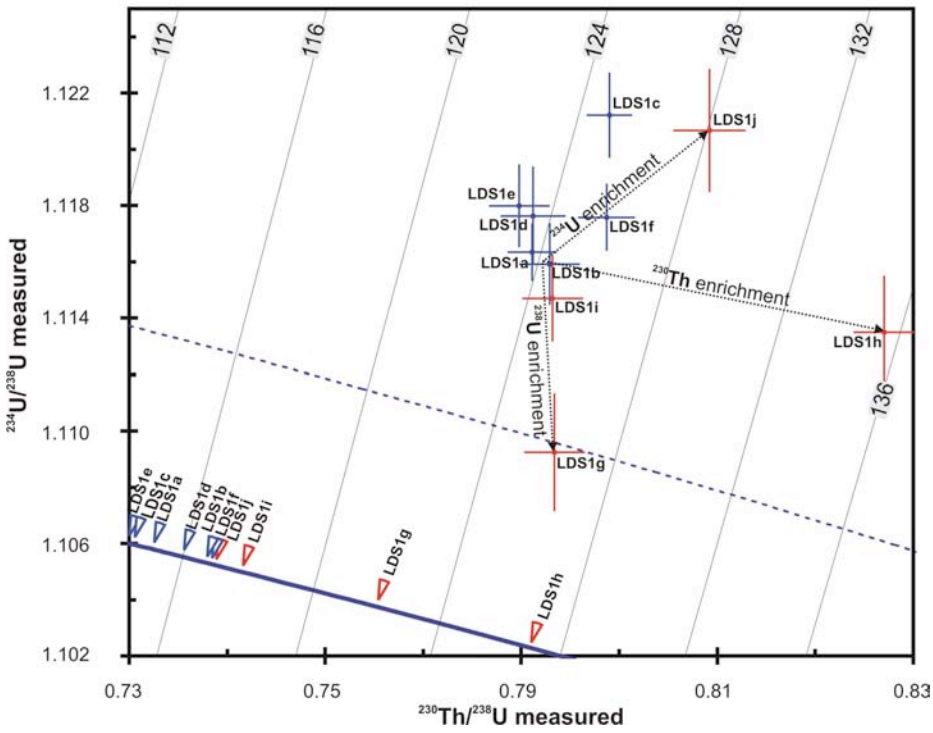

Figure 8: Compilation of LDS1 *(Porites)* U-series subsample data plotted on a $^{234}U/^{238}U$ activity ratio diagram. Red indicates surface coral subsamples and blue apparent pristine interior subsamples. The triangles represent open-system corrections. Blue line represents closed system evolution with and modern seawater $^{234}U/^{238}U$ activity of 1.1466. Blue dotted line represents closed system evolution with and modern seawater $^{234}U/^{238}U$ activity of 1.1566.

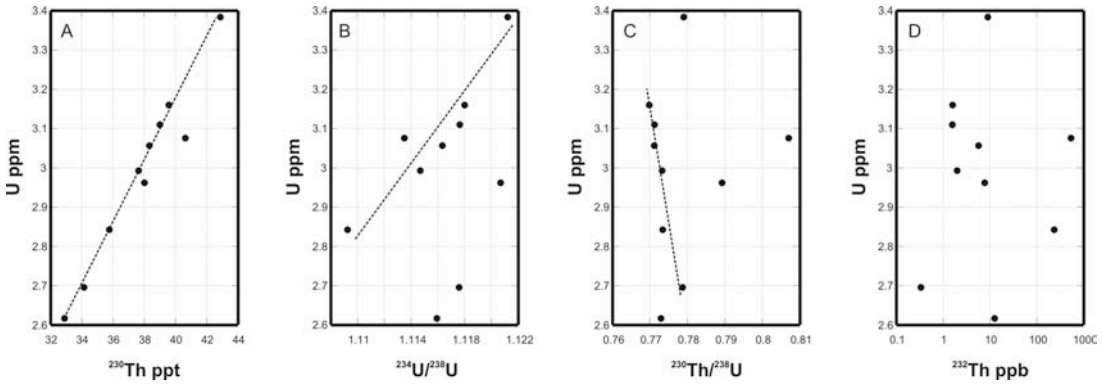

Figure 9: U and Th Isotopic ratios vs. uranium concentration in multiple coral subsamples taken from LDS1.

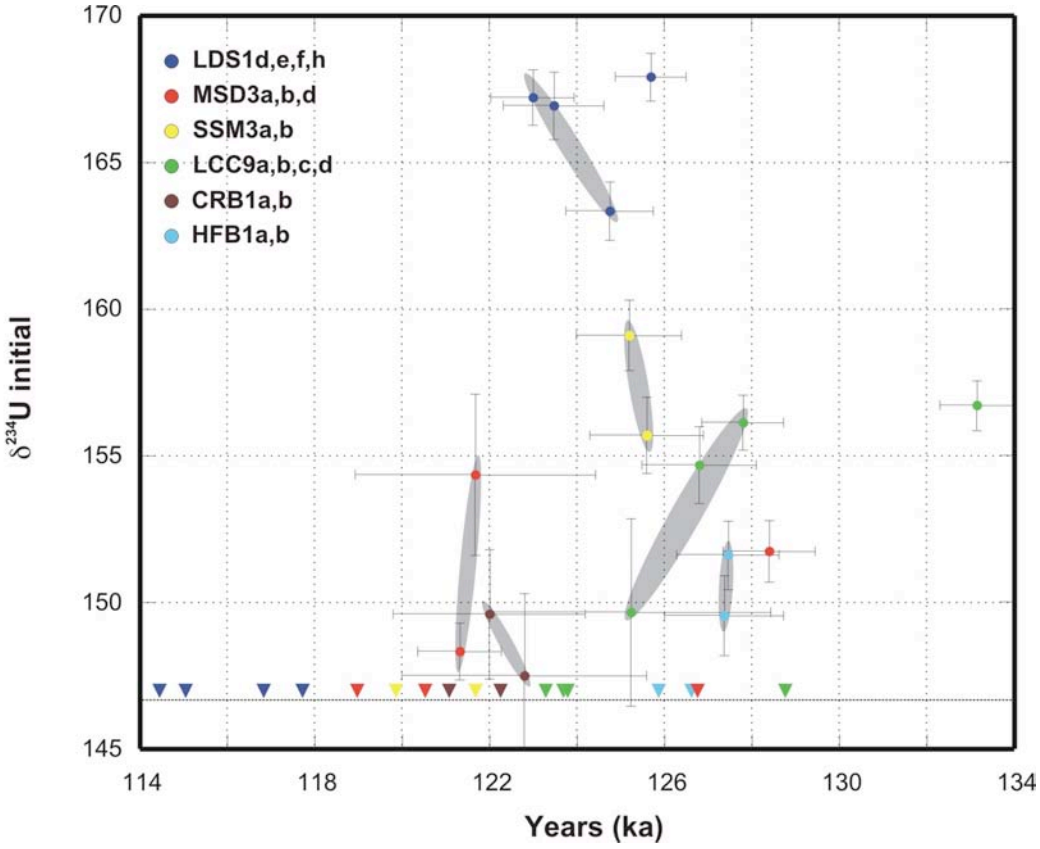

Figure 10. Coral subsamples showing $\delta^{238}U_{initial}$ at the time of coral growth vs. ^{230}Th-age. Different colours represent a different individual coral. Triangles represent open-system ages corrected to a $\delta^{234}U_{initial}$ seawater value of 146.6‰. Grey shaded areas indicate subsamples from the same coral showing age equivalence.

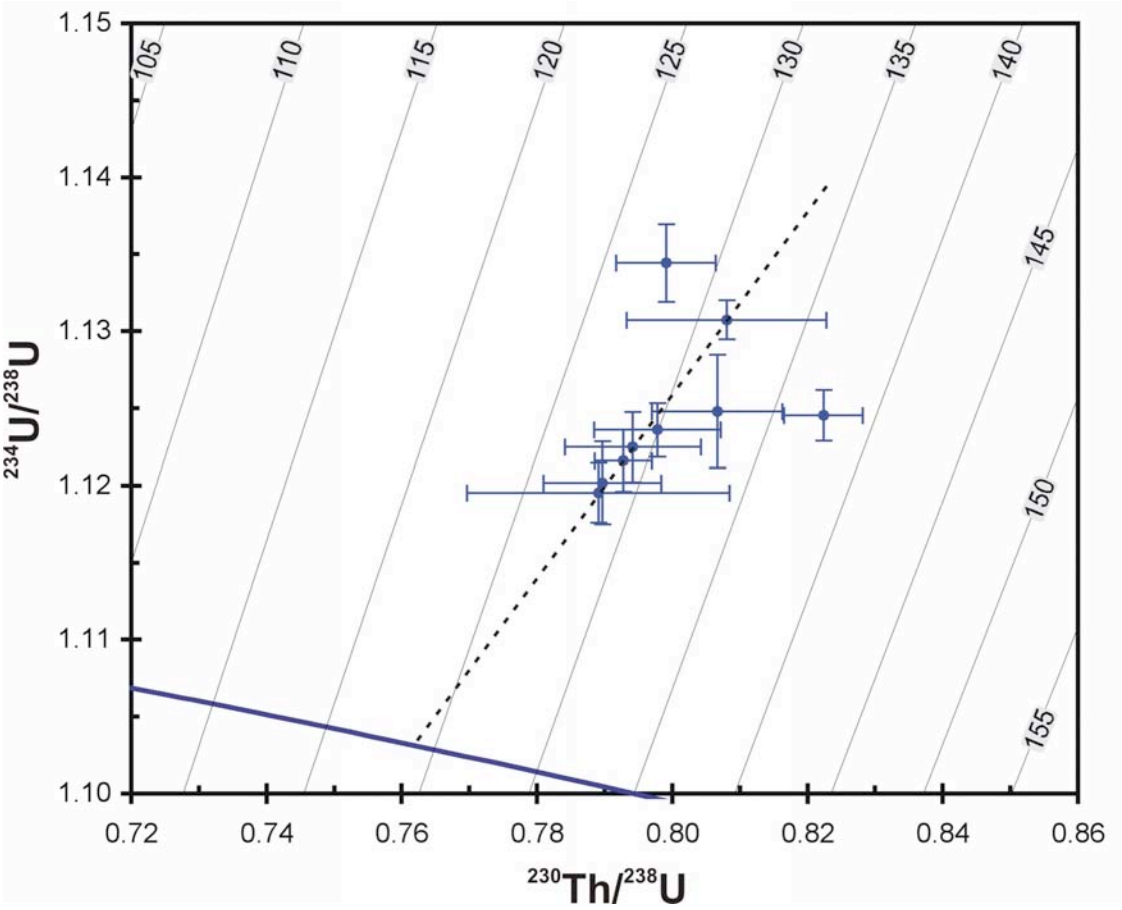

Figure 11. A compilation of Cape Cuvier corals on a $^{234}U/^{238}U$ activity ratio diagram. Blue line represents closed system evolution with and modern seawater $^{234}U/^{238}U$ activity of 1.1466. The dashed line indicates a linear compositional array representative of those Cape Cuvier corals.

Table 1: U-series analysis

Sample Code	U ppm[1]	Th ppt[2]	^{232}Th ppb[3]	^{234}U/^{238}U	± 2σ	δ ^{234}U[4]	± 2σ	^{230}Th/^{238}U[5]	± 2σ	^{232}Th/^{230}Th	Conv. Age[6]	± 2σ	Initial δ^{234}U[7]	± 2σ	Corr. Age[8]
LDS1a	3.06	38.32	5.70	1.1163	0.0005	116.34	0.49	0.7711	0.0012	1260	123.75	0.35	165.23	0.65	115.991
LDS1b	2.62	32.89	12.52	1.1159	0.0007	115.92	0.71	0.7729	0.0015	492	124.39	0.47	164.91	0.91	116.727
LDS1c	3.38	42.86	8.92	1.1212	0.0007	121.21	0.74	0.7790	0.0011	900	124.92	0.36	172.72	0.97	114.186
LDS1d	3.11	38.99	1.57	1.1176	0.0009	117.63	0.86	0.7712	0.0016	4666	123.47	0.48	166.93	1.15	115.050
LDS1e	3.16	39.56	1.59	1.1180	0.0007	117.99	0.72	0.7698	0.0015	4693	122.99	0.46	167.21	0.95	114.459
LDS1f	2.70	34.14	0.33	1.1176	0.0006	117.58	0.58	0.7787	0.0014	19112	125.69	0.48	167.91	0.81	116.836
LDS1g	2.84	35.75	234.99	1.1093	0.0010	109.25	1.03	0.7734	0.0015	31	126.09	0.52	156.19	1.32	121.950
LDS1h	2.99	37.63	1.99	1.1147	0.0008	114.69	0.75	0.7732	0.0015	3964	124.75	0.46	163.34	1.00	117.727
LDS7i	3.08	40.63	532.53	1.1135	0.0010	113.49	0.99	0.8070	0.0015	15	135.48	0.54	166.64	1.32	126.987
LDS7j	2.96	38.00	7.72	1.1207	0.0011	120.67	1.08	0.7892	0.0018	993	128.05	0.59	173.62	1.42	116.971
LCV1a	2.20	28.33	11.63	1.1106	0.0010	110.59	0.98	0.7914	0.0019	457	131.27	0.64	160.45	1.28	125.356
LCV1b	3.35	44.07	0.15	1.1141	0.0008	114.10	0.84	0.8091	0.0019	54759	135.98	0.68	167.76	1.17	127.030
LCV2a	3.17	42.81	0.10	1.1336	0.0008	133.64	0.76	0.8309	0.0027	78065	137.73	0.90	197.47	1.09	116.980
LCV2b	3.88	50.91	1.48	1.1303	0.0008	130.34	0.80	0.8076	0.0029	6441	131.25	0.87	189.10	1.15	113.987
LCV2c	4.37	56.01	0.75	1.1268	0.0008	126.80	0.84	0.7887	0.0018	13939	126.46	0.53	181.48	1.10	112.270
LCC9a	1.24	15.67	0.60	1.1087	0.0007	108.68	0.70	0.7787	0.0022	4938	127.80	0.69	156.13	0.93	123.689
LCC9b	2.93	36.75	0.63	1.1080	0.0009	107.97	0.93	0.7748	0.0039	10949	126.80	1.22	154.68	1.30	123.290
LCC9c	1.43	18.40	0.32	1.1074	0.0005	107.44	0.54	0.7948	0.0040	10814	133.15	1.25	156.71	0.84	128.766
LCC9d	2.67	33.17	0.99	1.1049	0.0024	104.93	2.40	0.7672	0.0080	6282	125.24	2.41	149.66	3.19	123.789
LCV6a	2.21	28.88	0.06	1.1250	0.0007	124.98	0.68	0.8021	0.0019	89622	130.93	0.59	181.14	0.90	116.747
LCV7_1	2.69	34.21	0.16	1.1286	0.0010	128.60	1.03	0.7837	0.0021	39635	124.57	0.61	183.07	1.41	109.826
LCV7_2	3.14	40.36	0.13	1.1192	0.0010	119.20	1.02	0.7917	0.0023	56496	129.18	0.73	171.92	1.38	118.688
LCV7_3	3.22	40.83	0.75	1.1124	0.0010	112.43	1.01	0.7803	0.0017	10213	125.02	0.53	174.50	1.31	121.161
LCV7_4	3.44	42.37	0.31	1.1246	0.0010	124.62	1.04	0.7577	0.0024	25669	118.13	0.66	174.19	1.33	106.959
LCV3a	3.13	42.64	0.08	1.1433	0.0009	143.32	0.85	0.8384	0.0028	94188	137.53	0.88	211.66	1.20	111.401
LVC3b	3.16	42.17	0.10	1.1393	0.0012	139.27	1.21	0.8208	0.0026	76512	133.06	0.86	203.08	1.68	110.379
LCC_a	3.05	42.01	5.39	1.1174	0.0013	117.45	1.33	0.8500	0.0046	1462	149.00	1.70	179.20	2.00	135.140
LCC_b	2.90	37.65	3.59	1.1155	0.0013	115.49	1.34	0.8021	0.0033	1966	133.40	1.10	168.50	1.80	124.136
LCC_g	3.01	39.30	0.16	1.1248	0.0018	124.80	1.84	0.8067	0.0048	46520	132.40	1.55	181.60	2.50	117.981
LCC_i	3.38	43.25	0.25	1.1202	0.0013	120.18	1.34	0.7897	0.0044	32419	128.30	1.35	172.90	1.85	117.462
LCC_j	2.86	38.52	18.92	1.1219	0.0012	121.89	1.21	0.8330	0.0047	382	141.70	1.60	182.10	1.80	126.837
LCC_k	3.16	40.76	0.16	1.1236	0.0009	123.60	0.87	0.7978	0.0047	48364	130.00	1.45	178.60	1.30	116.779
LCC_m	3.04	38.83	0.18	1.1195	0.0010	119.54	0.97	0.7891	0.0097	40107	128.30	2.85	172.00	1.80	117.807
LCC_n	3.11	40.02	0.07	1.1225	0.0011	122.49	1.13	0.7942	0.0050	113410	129.00	1.50	176.60	1.60	116.771
LCC_o	3.18	41.08	0.47	1.1344	0.0013	134.44	1.26	0.7991	0.0037	16419	127.70	1.10	193.10	1.70	109.027
LCC_p	3.47	46.98	2.01	1.1286	0.0011	128.56	1.14	0.8359	0.0025	4378	140.80	0.89	191.60	1.55	122.185
LCC_q	3.68	43.63	12.48	1.1366	0.0009	136.55	0.85	0.7317	0.0033	655	109.00	0.79	186.00	1.10	93.573
LCC_r	3.28	42.88	0.32	1.1307	0.0006	130.74	0.64	0.8080	0.0074	25336	131.30	2.25	189.70	1.45	113.780
LCC_s	3.26	43.33	0.17	1.1245	0.0008	124.52	0.82	0.8224	0.0029	46762	137.50	0.97	183.80	1.20	122.030
LCC_t	3.21	41.22	0.34	1.1216	0.0010	121.59	1.00	0.7928	0.0021	22684	128.90	0.69	175.20	1.30	118.410
LCC_w	3.39	44.03	1.27	1.1201	0.0006	120.14	0.64	0.8013	0.0023	6511	131.70	0.73	175.70	0.91	120.279
SBA1	2.81	34.79	1.90	1.1071	0.0011	107.07	1.10	0.7601	0.0018	3427	122.64	0.56	151.59	1.46	120.146
STG5	2.88	35.94	0.46	1.1038	0.0013	103.81	1.30	0.7720	0.0032	14766	127.00	1.00	148.80	1.75	126.385
STG1	2.46	31.09	0.08	1.1066	0.0007	106.57	0.66	0.7801	0.0030	72614	128.80	0.92	153.50	0.95	125.720
STG4	1.99	24.70	0.12	1.1057	0.0011	105.73	1.14	0.7683	0.0025	39536	125.40	0.76	150.80	1.50	123.447
SPI4	2.92	35.93	0.28	1.1080	0.0011	107.96	1.05	0.7612	0.0022	23948	122.80	0.65	152.90	1.40	119.998
SPI5	2.36	28.64	0.59	1.1078	0.0009	107.80	0.88	0.7500	0.0019	9177	119.60	0.58	151.30	1.15	117.471
SGN1	2.76	35.47	0.07	1.1137	0.0011	113.75	1.05	0.7942	0.0023	90678	131.30	0.79	165.20	1.40	123.137
SGN3	3.25	41.08	0.41	1.1162	0.0007	116.18	0.72	0.7816	0.0015	18740	126.87	0.47	166.40	0.95	118.586

SMM3a	2.28	28.43	1.00	1.1091	0.0010	109.06	0.97	0.7717	0.0024	5347	125.60	0.75	155.70	1.30	121.684
SMM3b	2.77	34.65	0.23	1.1116	0.0009	111.61	0.90	0.7723	0.0020	27791	125.20	0.60	159.10	1.20	119.861
SMM4	3.79	46.69	144.53	1.1060	0.0006	106.04	0.57	0.7603	0.0016	61	122.94	0.46	150.20	0.76	121.256
NJZ1	2.02	25.26	5.10	1.1086	0.0012	108.60	1.22	0.7675	0.0022	929	124.47	0.70	154.55	1.58	121.021
NJZ2	2.14	26.58	0.79	1.1085	0.0008	108.52	0.81	0.7653	0.0020	6291	123.84	0.61	154.16	1.04	120.553
NYC1a	2.32	28.94	0.64	1.1037	0.0016	103.67	1.55	0.7678	0.0021	8483	125.74	0.76	148.07	2.02	124.944
NYC1b	2.45	33.59	290.00	1.1117	0.0012	111.65	1.19	0.8433	0.0020	22	148.48	0.84	170.09	1.64	138.339
MFB1c	3.19	36.96	2.16	1.1186	0.0008	118.58	0.83	0.7124	0.0016	3212	107.42	0.42	160.79	1.05	102.224
HFB1a	2.61	32.79	0.10	1.1042	0.0011	104.22	1.06	0.7736	0.0021	63382	127.37	0.68	149.55	1.36	126.625
HFB1b	2.93	36.90	0.09	1.1056	0.0009	105.64	0.92	0.7751	0.0013	76807	127.46	0.47	151.61	1.17	125.871
HFB2	3.63	42.96	75.59	1.1227	0.0008	122.70	0.79	0.7272	0.0018	1048	110.43	0.49	167.80	0.99	102.479
MSD3a	2.65	32.50	xxx	1.1052	0.0008	105.16	0.75	0.7540	0.0014	33540	121.32	0.43	148.33	0.96	121.076
MSD3b	2.64	32.60	xxx	1.1093	0.0021	109.32	2.11	0.7585	0.0021	30011	121.68	0.74	154.35	2.75	118.978
MSD3c	2.52	31.00	xxx	1.1049	0.0034	104.91	3.37	0.7568	0.0045	34249	122.18	1.54	148.33	4.31	121.942
MSD3d	2.83	36.58	0.27	1.1054	0.0008	105.44	0.76	0.7780	0.0016	25486	128.40	0.52	151.74	1.05	126.760
MFB1a	2.96	38.00	xxx	1.1062	0.0006	106.19	0.59	0.7898	0.0028	48270	131.88	0.83	154.33	0.85	129.167
MFB1b	3.07	38.63	0.12	1.1036	0.0009	103.61	0.92	0.7752	0.0017	62265	127.98	0.57	148.93	1.21	127.518
MFB2	2.80	35.06	0.12	1.1045	0.0008	104.48	0.79	0.7748	0.0051	54395	127.66	1.49	150.04	1.22	126.725
MFB3	1.89	23.62	0.05	1.1039	0.0006	103.93	0.56	0.7718	0.0029	85830	126.87	0.92	148.92	0.80	126.394
MFB4	5.32	65.96	0.15	1.1056	0.0007	105.62	0.67	0.7656	0.0052	80212	125.00	1.50	150.40	1.10	123.525
MFB6	2.66	33.08	0.10	1.1067	0.0017	106.70	1.70	0.7680	0.0043	59630	125.10	1.30	152.10	2.20	123.287
CMP1	3.10	38.30	0.32	1.1084	0.0005	108.38	0.47	0.7591	0.0033	4380	122.05	0.97	153.19	0.74	119.834
BKE1	2.43	32.10	0.09	1.1146	0.0011	114.56	1.12	0.8141	0.0021	68127	137.49	0.72	169.16	1.43	127.945
GCB2	2.76	34.52	0.12	1.1046	0.0016	104.63	1.60	0.7738	0.0036	52810	127.30	1.10	150.10	2.10	125.670
CRB1a	3.16	38.70	0.19	1.1059	0.0016	105.88	1.64	0.7568	0.0051	39590	122.00	1.50	149.60	2.20	120.527
CRB1b	2.57	31.60	0.18	1.1041	0.0021	104.12	2.12	0.7583	0.0040	33400	122.80	1.25	147.50	2.80	122.255
CRB2	2.30	28.44	0.06	1.1077	0.0012	107.73	1.25	0.7633	0.0045	83981	123.40	1.35	152.90	1.70	120.678

Notes to Table 1.

[1] Uranium concentrations are measured in part per million (ppm) equivalent to ng/g.

[2] ^{230}Th concentrations measured in parts per trillion (ppt) equivalent to fg/g

[3] ^{232}Th concentrations measured in parts per billion (ppb) equivalent to pg/g

[4] $\delta^{234}U = \{[(^{234}U/^{238}U)/(^{234}U/^{238}U)_{eq}]-1\} \times 10^3$. $(^{234}U/^{238}U)_{eq}$ is the atomic ratio at secular equilibrium and is equal to $\lambda_{238}/\lambda_{234} = 5.4891 \times 10^{-5}$, where λ_{238} and λ_{234} are the decay constants for ^{238}U and ^{234}U, respectively, adopting half-lives of Cheng *et al.*, (1998)

[5] $[^{230}Th/^{238}U]_{act} = (^{230}Th/^{238}U)/(\lambda^{238}/\lambda^{230})$.

[6] U-series ages are calculated iteratively using

$$1 - \left[\frac{^{230}Th}{^{238}U}\right]_{act} = e^{-l_{230}T} - \left(\frac{d^{234}U(0)}{1000}\right)\left(\frac{l_{230}}{l_{230}-l_{234}}\right)\left(1 - e^{(l_{234} - l_{230})T}\right)$$

where T is the age in years and l_{230} is the decay constant for ^{230}Th. $l_{238} = 1.551 \times 10^{-10}$ y^{-1}; $l_{234} = 2.826 \times 10^{-6}$ y^{-1}; $l_{230} = 9.158 \times 10^{-6}$ y^{-1}.

[7] The initial value is given by $\delta^{234}U_i = \delta^{234}Ue^{l_{234}T}$, where T is the age in years.

[8] For open system equation model see Thompson *et al.*, 2003

Table 2: XRD analysis

AAC Run No	Sample Code	Quartz SiO_2	Aragonite $CaCO_3$	Calcite $CaCO_3$	HMC $(Ca,Mg)CO_3$	Dolomite $CaMg(CO_3)_2$	Ankerite $Ca(Mg,Fe)(CO_3)_2$	Sodium Chloride NaCl
5547-02	LDS1i	4%	79%	2%	10%	5%		
5547-03	LDS1j							
5547-09	LDS1g	3%	61%	2%	2%		31%	
5547-19	LDS1h	1%	98%	1%				
5547-01	LCV7_1		99%			1%		
5547-15	LCV7_3	1%	99%					
5547-04	NYC1a	2%	71%	24%		3%		
5547-07	NYC1b	3%	86%	9%		3%		
5547-08	NYC1c		71%	26%		3%		
5547-11	NYC1d		84%	15%	1%			
5547-05	LCV1b		86%	9%	3%	2%		
5547-16	LCV1c		99%	1%				
5547-12	LCV2a		96%	1%	2%	1%		
5547-13	LCV2b	4%	14%	26%	54%			2%
5547-20	LCV2c	1%	99%	0%				
5547-18	LCV2d	1%	99%	1%				
5547-06	MFU1a			3%	97%			
5547-21	MFU1b		99%	1%				

SECTION B

Morphostratigraphic evidence for Unstable sea levels during marine isotope stage 5e: Cape Cuvier, Western Australia

B.1 ABSTRACT

Geomorphologic and morphostratigraphic investigations of an emergent fringing reef complex at Cape Cuvier, Western Australia reveals two geomorphically distinct marine units. We record a lower coralgal reef platform between 3 and 5.5 m above MLWS (mean low water spring) and an upper thin, coralgal rim and planation surface at 8.5 to 10.5 m above MLWS. The difference in morphology and elevation suggests reef development occurred at different times and under environmentally discrete conditions. In an attempt to better refine the timing of emplacement of each marine unit, high-precision U-series dating of 27 corals collected along vertical and lateral reef growth axis was undertaken. All measured corals exhibited elevated $\delta^{234}U_{initial}$ values, suggesting that there was pervasive uptake of ^{234}U-enriched uranium. This open-system behaviour resulted in older apparent U-series ages that conflict with the known duration of MIS 5e and the apparent growth history of the reef. Open-system corrections were applied to these corals in an attempt to improve their age reliability, however, they also returned ages that conflicted our empirical data.

B.2 INTRODUCTION

At Cape Cuvier (**Fig 1**), an emergent fringing reef complex provides stratigraphic and geomorphic evidence of a complex sea-level highstand during marine isotope stage (MIS) 5e. Two marine erosion terraces were previously identified (Denman and Van de Graff, 1977): a lower well-developed coralgal reef at 3 to 5.5 m above mean low water springs (all subsequent elevations are noted as "+" relative to this datum), and an upper erosional unit at about +10 m with in situ coral at +9.4 m. Based on field evidence, Veeh *et al.* (1979) considered that the two marine units observed at Cape Cuvier may be the result of a bimodal rather than single sea level high stand event. Alternatively they postulated that the difference in elevation between lower and upper reef deposits could be an artefact of tectonic uplift.

Early U-series dates (Veeh *et al.* 1979) utilizing alpha counting methods returned ages for the lower terrace of 123 ± 11 ka (n=2) and 134 ± 8, 120 ± 10 and 140 ± 12 ka for the higher coral/algal rim. More recently, TIMS coral ages (Stirling *et al.*, 1998) from a location to the north of Cape Cuvier at + 6.75 m and + 8.61 m returned dates of 128 ± 0.7 ka and 126 ± 0.5 ka respectively. However both these ages are considered unreliable due to elevated initial $\delta^{234}U$ ($\delta^{234}U_{initial}$) values. Although it has not proved possible to constrain the timing of the lower and upper marine units into separate sea level events due to low-precision or reliability issues, it is however possible to place a last interglacial (MIS 5e) age to these marine deposits.

This study addresses eustatic and tectonic issues regarding the age and elevation of these emergent marine deposits by better defining the timing of emplacement and duration of growth. This will be achieved through field interpretation of fringing reef development, utilization of high-precision dating methods and open-system corrections to obtain precise age information.

B.3 CLIMATE AND OCEANOGRAPHIC SETTING

Cape Cuvier (24° 13.45' S 113° 23.42' E) is located on the central west coast of WA and is one of three prominent headlands situated along the 180 km long north south trending coastal Quobba Ridge (**Fig. 1**). Modern fringing reefs extend from Point Quobba in the south into the Ningaloo reef tract at Cape Range 300 km to the north. Sea surface temperatures at Cape Cuvier are regulated by the southward migration of the warm low salinity Leeuwin current during winter months (Thompson, 1984) and the northward flowing Ningaloo current during the summer (Taylor and Pearce, 1999). This combination of ocean currents results in a narrow range of annual sea surface temperature from 26.3°C in April to 21.4°C in September. Such marine conditions are suitable for hermatypic coral growth.

The 3 pm wind rose for Carnarvon (**Fig. 2**) (located 40 km south of Cape Cuvier) records frequent fresh to strong, south-to-south west winds throughout most of the year. During the summer these winds generate moderate seas characterised by a significant wave height of 2.0 - 2.5 ± 0.7 m with a mean wave period of 8.8 s. During winter months mid latitude depressions can generate a ground swell of >5 m for 60 to 90 days per year (*World Wave Atlas;* http://www.knmi.nl/waveatlas*)*. Consequently, modern fringing reefs along the Cape Cuvier coastline are frequently exposed to very high wave energies.

B.4 METHODS

B.4.1 Surveying, site descriptions and sample collection

Reef framework was described and photographed, and when possible, corals were identified to species level. The lower emergent reef flat (**Fig. 3a**) was surveyed using a transit. The top surface of the adjacent modern fringing reef, representing MLWS was assigned the 0 m benchmark. The measured transect

incorporated the broadest section of reef, from the seaward edge of the terrace (perpendicular to the coast) that had corals exposed at the surface. The upper coralgal rim (**Fig. 3b**) was traced from the exposed southern side to the protected northern side of the cape, with elevations measured using a survey staff. An actively eroding 3 m high sea cliff section at the base of the lower emergent platform was measured and logged in detail (**Fig. 3c**).

Coral and coralline algal samples were collected using a petrol powered rock drill, with 15 mm diameter barrel and diamond-impregnated bit. Drill penetration averaged between 15 and 20 cm. A total of 15 stratigraphically oriented coral cores were taken from the measured sea cliff section, while 7 cores were drilled across the lower emergent reef flat transect. Due to the limited exposure of corals along the upper coralgal rim only two samples were collected using a chisel and hammer.

B.4.2 Sample preparation and analytical procedures

A representative suite of 7 corals were analysed using XRD to assess the degree of calcite alteration. Thirty-two coral samples were selected for U-series analysis. Samples were sectioned and micro-sampled to an approximate weight of 200 mg with a dental drill. Due to the porous nature of the coral skeleton (**Fig. 3d**), it proved very difficult to identify or remove any potential secondary mineral crystallization of detrital contamination. As a result, bulk coral samples had to be analysed. Mechanical cleaning involved soaking in MilliQ water and sonication.

Samples were first dissolved in distilled water by step addition of 10M HNO_3 then spiked with a 50 mg "U-2" $^{229}Th/^{233}U$ isotope tracers and evaporated to a minimum solution. A few drops of H_2O_2 were added to oxidise any remaining organic material. Samples were redissolved in 3 ml of 2M HNO_3 and transferred to bio-spin ®Tru.spec columns which separated U and Th from solution. A 0.1 normal solution of

HF/HCl was then passed though the columns to collect and concentrate U and Th. The solution was evaporated to dryness then redissolved with 2 ml 2% HNO_3, prior to injection.

U-series measurements were performed using a Neptune MC-ICPMS at the Research School of Earth Sciences, Australian National University. Measurements were conducted using a combination of simultaneous multiple-Faraday cup and ion counter protocols based on those previously described for TIMS (Stirling *et al.*, 1998 and McCulloch and Esat 2000). The main difference being that ion counting/faraday gains where determined by reference to an external standard (SRM 960) for determination of $^{234}U/^{235}U$ ratios where ^{234}U is measured using ion counting. For the low abundance isotopes ^{230}Th and ^{229}Th (spike) these where both measured using the central ion counter, but simultaneously with ^{235}U and ^{238}U and ^{232}Th on Faraday cups allowing corrections for both beam instability as well as mass bias. For detailed protocols see McCulloch and Mortimer (in prep). This multiple-Faraday approach yield higher precision in conjunction with a significantly reduced sample size requirement, lowering age uncertainties by up to a factor of five (Stirling *et al.*, 2001) compared to single cup procedures. Although higher precision measurements are possible using multiple Faraday only procedures (Bernal *et al.* (2002), Andersen *et al.* (2004) Potter *et al.* (2005) and Stirling *et al.* (2005)), these suffer from the disadvantage of requiring much larger, gram size samples. For the labour intensive preparation of carefully selected portions of coral walls adopted in this study, the measurement of relatively small samples (<50 mg) is a distinct advantage.

B.4.3 Reliability criteria for $^{234}U/^{230}Th$ coral ages

Following the procedures of earlier workers (Chen et al., 1991; Stirling et al., 1995 and 1998; Robinson et al., 2004), corals were screened for potential U and Th loss or gain based on the following criteria:

1. We consider the calculated $\delta^{234}U_{initial}$ to be the best quantitative test for open system behaviour in corals. For a coral age to be considered strictly reliable $\delta^{234}U_{initial}$ values should reflect a modern seawater value of 146.6 ± 4‰.
2. The total uranium concentration of fossil corals should approximate modern coral values of about 3 ± 0.5 ppm of uranium.
3. Fossil corals should be free of allochthonous ^{230}Th, as indicated by the absence of detrital ^{232}Th (< 1 ppb).
4. Corals should show primary aragonitic structures or have < 2% calcite concentration.

B.4.4 Open system corrections

The pervasive nature of coral diagenesis means that most Pleistocene corals have been subjected to at least some degree uranium or thorium gain or loss. There have been several attempts to model open-system behaviour in corals, most notably, Thompson *et al.* (2003), Villemant and Feuillet (2003) and Scholz *et al.* (2004). Thompson *et al.* (2003) uses a quantitative model where the positive correlation between $(^{234}U/^{238}U)_{meas.}$ and $(^{230}Th/^{238}U)_{meas.}$ activity ratios is explained by coupled addition of particle-reactive ^{234}U and ^{230}Th, which is produced by decay and alpha-recoil mobilisation ^{238}U and its daughters. This study does, however, provide an excellent opportunity to investigate the utility and reliability of U-series open-system corrections from Cape Cuvier fossil corals. All corals exhibiting open system behaviour were corrected using the Thompson *et al.* (2003) model, which can be most usefully applied to single dates from individual corals with low initial non-radiogenic ^{230}Th collected from the same reef system.

B.5 RESULTS

B.5.1 Coral reef geomorphology

A measured transect finds the windward edge of the lower emergent reef at 3.2 m above the modern reef terrace (**Fig. 4**). The reef flat slopes landward at 1.5° over 50 m with the surface covered predominantly in CCA, where corals are exposed at the surface they generally represent an erosional surface (**Fig. 3e**). Reef gradient steepens to 3.3° over the next 50 m up to 7.4 m with a thin veneer of coralline algal material overlying an eroded Tertiary eolianite surface. Drainage gutters and rills found on the lower emergent reef terrace have a similar surface morphology to that of the modern reef (**Fig. 3f**).

A poorly preserved rim of coralgal material at +8.4 to +10.5 m is found encrusting a paleosea cliff on both the lee and windward side of the Cape, also described by Denman and Van de Graaf (1976). On the exposed southern side of the Cape, a cobble conglomerates at +8-10 m and encrusted with CCA are found to lie unconformably over an erosional terrace cut into the Tertiary calcarenite (**Fig. 3g**). Coarse indurated carbonate deposits with shallow seaward dipping planar beds at +7.4 and +12 m are interpreted to be a beach facies (**Fig. 3h**).

The modern sea cliff exposes the internal structure of the lower emergent platform and is found to comprise of medium to coarse-grained detrital sediments and CCA bindstone, which then grades into a metre high alternating sequence of monospecific coral (*Acropora humulis)* and detrital sediment packages. The upper half of the section is dominated by an alternating coral and CCA bindstone which is then capped at the surface by CCA.

B.5.2 XRD analysis

The results of XRD analysis conducted on corals from lower reef flat and the upper coralgal rim are shown in Table 1. Corals LCV7_1 and LCV7_3 collected from the exposed surface of the main reef terrace were found to be 99% aragonite. Corals from the upper coralgal rim showed some evidence of calcite alteration with samples LCV2_1

and LCV1_2 composed of 96 and 86% aragonite respectively. Samples LCV1e_3, LCV2e_2, LCV2e_3 and LCV2e_4 were composed of 99% aragonite.

B.5.3 U-series coral dates

The results of 27 U-series coral dates from Cape Cuvier are shown in Table 2 and (**Fig. 5**). Uranium concentrations for all corals but one fall within the 2.5 - 3.5 ppm range that is anticipated for modern corals (Edwards *et al.*, 1988; Eisenhauer *et al.*, 1993; Stirling *et al.*, 1995). The one outlying coral, LCV2e_4 from the upper coralgal rim had a uranium concentration of 4.37 ppm. Of the 27 corals analysed, 20 had ^{232}Th concentrations < 1 ppb suggesting minimal non-radiogenic ^{230}Th contamination. Those 7 corals with suspected detrital contamination had ^{232}Th concentrations ranging between 1.27 and 18.92 ppb, visually showed red staining (though initial micro-sampling attempted to avoid these areas) and generally gave higher U-series ages (**Fig. 5**). These corals were not used in any age interpretations or open system corrections. All corals analysed had elevated $\delta^{234}U_{initial}$ values ranging from 168 to 211‰, and as such all dates are considered unreliable (**Fig. 5**). The reliability of both uncorrected and corrected coral ages was also tested against our current understanding of timing, duration and oscillations of 5e sea levels and how that relates of the timing and nature of fringing reef development.

B.5.4 The reliability of U-series ages in stratigraphic succession

The reliability of both uncorrected and corrected coral ages was also tested against our current understanding of timing, duration and oscillations of 5e sea levels and how that relates of the timing and nature of fringing reef development.

Ten coral samples collected from a 3 m high vertical cliff section provide the fundamental test of stratigraphic superposition for U-series ages (**Fig. 6a,b,c**). Measured

$^{230}Th/^{238}U$ isotope ratios exhibit fairly uniform values of 0.8 ± 0.01 up section (**Fig. 6b**). These near equivalent $^{230}Th/^{238}U$ values produce near equivilent coral ages of 130.5 ± 3 ka (**Fig. 6c**). This is despite having elevated $\delta^{234}U_{initial}$ values of 181.6 to 195.1‰, which are the product of more variable $^{234}U/^{238}U$ isotopic ratios (**Fig. 6a**). Based on an earlier MIS 5e sea level curve by Stirling *et al.* (1995 and 1998), these conventional (uncorrected) coral ages coincide with the early stages of the highstand.

Open-system corrections were applied to these corals in an attempt to correct for post mortality uranium and thorium mobilization. The result was a systematic lowering of mean coral age from 130.5 ± 3 to 117.3 ± 3.5 ka, a shift of some 13 ka. Once again there was a tight correlation in coral age down section, where the mean age of lower 5 corals was 117.4 ± 0.6 ka. The minor age inversions observed in the upper half of the section may be the result of sampling bias, where corals were collected approximately 1 m off section. These corrected ages place suggest the timing of coral growth occured at the end of MIS 5e.

B.5.5 Lateral reef accretion and U-series ages

The age of the reef flat should correspond to the time the reef reached sea level and was no longer able to accrete vertically. Five corals collected along a measured transect across the lower reef terrace and had ages ranging from 118 ka to 138 ka and had $\delta^{234}U_{nitial}$ values of between 171.92 and 211.66‰. These uncorrected coral ages do not display a uniform sequence of stratigraphic age across the reef flat (**Fig. 4**).

As a result of open system corrections, coral age increases landward of the current seaward edge of the reef terrace from 109.82 ka to 121.16 ka at the back reef (**Fig. 4**). This age sequence conforms with the laterally prograding reef model

(Kennedy and Woodroffe, 2002), however coral age appears younger than the excepted duration of MIS 5e (Edwards et al., 2003)

B.5.6 Incipient reef development and U-series ages

Due to the exposed setting and poor preservation, corals collected from the upper coralgal rim samples were less than pristine. Of the 5 corals analysed only LCV1e_3 and LCV2e_3 had equivalent modern uranium concentrations and minimal calcite alteration (**Table 1**; **Table 2**). The loss of skeletal definition may be the result of secondary aragonite or calcite precipitation. These two corals returned conventional ages of 136.0 ± 0.7 and 131.3 ± 0.9 ka and $\delta^{234}U_{initial}$ values of 167.76 and 189.10‰ respectively. Open system corrections returned ages for LCV1e_3 and LCV2e_3 of 127.0 and 114.0 ka

B.6 DISCUSSION

B.6.1 Reef morphology, evolution and neotectonics

Two geomorphically distinct emergent marine units are evident at Cape Cuvier, a lower mature reef terrace and an incipient upper coralgal rim. The lower reef unit represents a prolonged interval of stable sea level, while the under-developed nature of the upper unit represents a brief seal level hiatus. The difference in elevation between these two units has been attributed to tectonic displacement (Stirling *et al.*, 1998) but local geomorphic evidence points to a multiple eustatic sea-level highstand event at Cape Cuvier.

Western Australia has a tectonically stable coastal margin (Murray-Wallace, 2002). Its position as an intraplate continental margin in the far field of former ice sheets minimizes the potential for vertical displacement as a result of glacio-isostatic or tectonic

processes. Well-developed early MIS 5e reef flat, terrace, or subtidal features are well documented in WA. That they show no significant variation across 2500 km of coastline (Hearty *et al.*, 2004) is testament to this stability. However, suggestions have been made that significant warping and faulting has occurred during the Quaternary, particularly in Cape Range (Van de Graff *et al.*, 1976), Shark Bay (Playford, 1990) and Cape Cuvier (Stirling *et al.*, 1998). Even so, Cape Cuvier also reveals features common to many stable coastlines around the world such as Bermuda and the Bahamas, including a mature MIS5e reef terrace at an elevation of +3.5 to +5.5 m. This suggests that this site has not been subject to tectonic displacement. Therefore the upper coral rim at +8 to 10 m, found just inboard of the lower reef, which is geomorphically distinct from the lower platform, must have resulted from a brief eustatic sea level event at this new elevation and not tectonic displacement.

B.6.1.1 Lateral reef accretion

The presence of a marine planation terrace beneath parts of the lower emergent reef is revealed where modern erosive processes have excavated deep grooves across the seaward face of the emergent reef, exposing sections perpendicular the shoreline. This indicates that coastal erosion took place prior to reef development, with coral growth occurring close to the shoreline in a shallow water high-energy setting. The resulting lack of vertical accommodation space would have produced a laterally accreting reef sequence (Kennedy and Woodroffe 2002). Based on this type of growth history age isochrons should be parallel to the reef front, meaning progressively older corals will be exposed on the reef surface landward of the crest.

The surface of the lower reef is veneered by a ~ 10cm thick coralline algae crust of *Hydrolithon* or *Neogoniolithon* (**Fig. 3f**), which are commonly found in shallow water

high-energy environments (Cabioch *et al.*, 1999). This again highlights the high-energy setting in which the reef developed. Drainage gutters are exposed across the reef flat and where corals do outcrop at the surface they appear to be truncated (**Fig. 3e,f**). This suggests that the reef flat was at times an active zone of both accretion and erosion, likely influenced by minor oscillations in sea level and local changes in the intensity of mechanical and bioerosive processes. Age isochrons across the reef flat may be more varied as a result.

B.6.1.2 Sea cliff retreat

The present seaward limit of the emergent reef at Cape Cuvier does not represent the true maximum lateral extent of the fossil reef flat. Recent erosive processes within the mid and upper literal zone have resulted in the notching and retreat of the lower emergent reef terrace (**Fig.3a**). It is difficult to calculate erosion rates on limestone coasts, requiring the quantification of a number of variables including: 1) diversity and density of bioeroding species; 2) the chemical action of seawater; 3) the mechanical action of wave-laden sediment; 4) substrate density (Spencer and Viles, 2002); and 5) freshwater dissolution. Erosion rates along tropical carbonate coastlines can range anywhere from 2 to 15 mm/yr and up to 33 mm/yr (Playford, 1988). Even using a conservative rate of 4 mm/yr (Trudgill, 1983) would mean that the lower emergent reef has retreated by at least 30 m during the Holocene. The fossil corals now exposed at the shoreface should represent a growth period sometime prior to the termination of MIS 5e (coral ages > 116 ka) and the emergence of the reef.

*B.6.1.3 Cor*algal *rim development*

At Cape Cuvier geomorphic features infer a brief but rapid sea level rise of between 4 and 6 metres during MIS 5e. Evidence includes an erosional terrace (+10 m) in situ coral (+9.4 m), coralline algal rim (+10.5 m) and beach deposits (+7.4 and +12.5 m) (Denman and Van de Graaff 1976). The difference in elevation and morphology of the upper coralgal rim compared the lower emergent reef terrace indicate vastly different development histories. The mature nature of the lower reef terrace points to an extensive growth history during a period of relative stable sea level, while the underdeveloped nature of the upper coralgal rim points to a rapid sea level rise brief hiatus then rapid fall. Neumann and Hearty (1996) argued on the basis of bioerosion rates of a Bahamian +6 m notch that this peak 5e sea level event may have lasted for less than 600 years. This period of time was insufficient to promote abundant coral growth at this new elevation or for the lower reef terrace to fill the newly available accommodation space. The short duration of this peak sea level event should result in a brief period of coral growth and consequently a tight cluster of coral ages.

B.6.2 U-series dates and reef development

B.6.2.1 Stratigraphic integrity of uncorrected and corrected U-series ages

Corals collected from the eroded sea cliff provide a stratigraphic context for the measured U-series ages. Age isochrons of a laterally accreting reef should be parallel to the reef front. Therefore, corals collected from the sea cliff section should be approximately similar in age. Of the 10 corals collected, nine display comparatively similar ages of 130.5 ± 3.0 ka (**Fig. 6c**), and correspond to measured isotopic ratios, which exhibit roughly equivalent values up section (**Fig 6a,b**). These concordant age and

isotope values are in contrast to their $\delta^{234}U_{initial}$ values, which range between 172 and 193 ‰.

Despite the apparent variance in $\delta^{234}U_{initial}$, when $^{234}U/^{238}U$ and $^{230}Th/^{238}U$ are plotted on an activity ratio diagram there appears a linear array of isotopic anomalies intersecting the closed-system seawater evolution curve at around 124 ka (**Fig 7**). A linear array such as this suggests that coeval age corals gained different amounts of uranium with a fixed $\delta^{234}U$ value around the same time (Scholz *et al.*, 2004). Those corals that do not lie on the linear array may have been subjected to late uranium uptake or different $^{234}U/^{238}U$ groundwater activities, or detrital ^{230}Th contamination.

When an open system correction (Thompson *et al.*, 2003) is applied to these conventional U-series ages, we observe an over all reduction in age to 116.7 ± 3.6 ka. Again based on the known duration of MIS 5e (116-132 ka) these corrected ages place timing of coral growth at the end of 5e. We know that modern erosive processes have conservatively removed over 1/3 of the original total width of the reef. Consequently, the current seaward extent of the lower reef terrace cannot represent the final position of the 5e reef crest, as an age of 116 ka would suggest. Therefore, these corrected ages are again too young to correlate with the predicted growth history of this laterally accreting fringing reef.

*B.6.2.2 Later*al *reef growth and uncorrected and corrected U-series ages*

Assuming a laterally accreting growth history for the lower emergent reef, U-series coral ages are expected to become progressively older landward of the shoreface. This trend was not expressed in the U-series analyses of five corals collected from a surveyed cross reef transect (**Fig. 4**). The lack of consistency across the reef flat could be explained by differential erosion and vertical accretion, resulting in a mixture of coral

ages exposed at the reef surface. However elevated $\delta^{234}U_{initial}$ values, a consequence of U/Th exchange, can also produce errors in U-series age calculations and stratigraphic age inversions (**Fig. 6**).

When an open system correction (Thompson *et al.*, 2003) is applied to these conventional U-series ages, the cross reef flat age succession conforms to the laterally accreting reef growth model. The closest shore face coral returned an age of 109.82 ka increasing incrementally to a back reef age of 121.16 ka. These open system age corrections despite showing age order across the reef flat open would seem to have underestimated the actual coral age by about 10 ka, based on the established duration of MIS 5e of 116 ± 1 to 129 ± 1 ka (Edwards *et al.*, 2003).

*B.6.2.3 Open system age corrections from the co*ralgal *rim*

The incipient nature the upper coralgal rim suggests a brief period of coral growth at this new sea level elevation, and a tight clustering of coral ages is expected. Unfortunately, due to the exposed nature of the deposit all samples were subject to U/Th exchange, expressed in elevated $\delta^{234}U_{initial}$ values and ages ranging from between 126.46 ± 0.53 and 137.73 ± 0.9 ka. Open system corrections were applied to the two remaining corals with minimal ^{232}Th contamination or elevated U concentrations and returned ages of 127 ka for LV1_3 and 116 ka for LCV2_1. The timing of this peak 5e sea level event is believed to have occurred at the end of 5e (Hearty and Neumann *et al.*, 2001), and although LCV2_1 (116 ka) does return a corrected age that agrees with the timing of this sea level event the other coral LCV1_3 (127 ka) does not. There is nothing in these corals geochemistry that could distinguish why one corrected coral age should be considered more reliable than the other corrected coral age. Consequently, as a result of

advanced diagenesis and U/Th mobilisation and ambiguous open-system corrections from coralgal rim corals, no reliable age data could be obtained from this upper unit.

B.7 CONCLUSIONS

1. Emergent marine units at Cape Cuvier can be divided in two morphostratigraphic units. Lower terrace reef growth initiated close to shore atop an erosional terrace. The lack of vertical accommodation space forced the reef to accrete laterally creating a seaward thickening wedge of carbonate sediment. Reef structure is composed primarily of coral framestone and coralgal bindstone. The well-developed nature of the reef suggests it developed during an extended sea level stillstand. Coral and coralline algae are found encrusting paleosea cliff 5 to 7 m above the height of lower reef terrace. The incipient nature of the deposit and the fact that the lower terrace was not able to utilize the newly available accommodation space points to a brief but rapid sea level excursion to this new elevation; in line with observations from other stable carbonate platforms.

2. U-series dating of fossil corals were undertaken in order better define the timing and duration of multiple sea level events at Cape Cuvier. All measured corals exhibited elevated $\delta^{234}U_{initial}$ values, suggesting that there was at pervasive uptake of ^{234}U-enriched uranium within the reef system. A result of this open system behaviour was for corals to exhibit older apparent ages that conflicted with the known duration of MIS 5e and the apparent growth history of the reef.

3. Open system corrections were applied to these corals in an attempt to improve their age reliability. However, like the conventional U-series ages, these corrected

ages do not correspond to either the known duration of MIS 5e or the apparent growth history of the reef. Whereas the conventional ages are too old by several thousand years, the corrected ages appear too young by several thousand years.

B.8. REFERENCES

Andersen, M.B., Stirling, C.H., Potter E.K., Halliday, A.N., 2004. Toward epsilon levels of measurement precision on $^{234}U/^{238}U$ by using MC-ICPMS. International Journal of Mass Spectrometry 237 (2-3), 107-118.

Bard, E., Fairbanks, R.G., Hamelin, B., Zindler, A., Huang, C.T., 1991. ^{234}U anomalies in corals older than 150,000 years. Geochimica et Cosmochimica Acta 55, 2385-2390.

Cabioch, G., Montaggioni, L.F., Faure, G., Ribaud-Laurenti, A., 1999. Reef coralgal assemblages as recorders of paleobathymetry and sea level changes in the Indo-Pacific province. Quaternary Science Reviews 18, 1681-1695.

Chen, J.H., Curran, H.A., White, B., Wasserburg, G.J., 1991. Precise chronology of the Last Interglacial period: $^{234}U^{230}Th$ data from fossil coral reefs in the Bahamas. Geological Society of America Bulletin 103, 82-97.

Denman, P.D., Van de Graaff, W.J.E., 1976. Emergent Quaternary marine deposits in the Lake MacLeod area, Western Australia. Western Australia Geological Survey Annual Report 1977, 32-36.

Eisenhauer, A., Zhu, Z.R., Collins, L.B., Wyrwoll, K.-H., Eichstatter, R., 1993. The Last Interglacial sea level change: new evidence from the Abrolhos Islands, West Australia. Geol. Rundsch. 85, 606-614.

Edwards, R.L., Taylor, F.W., Wasserburg, G.J., 1988. Dating earthquakes with high-precision thorium-230 ages of very young corals. Earth and Planetary Science Letters 90, 371-381.

Edwards, R.L., Cutler, K.B., Cheng, H., Gallup, C.D., 2003. Geochemical evidence for Quaternary sea-level change. Treatise on Geochemistry 6:13, 343-364.

Hamelin, B., Bard, E., Zindler, A., Fairbanks, R.G., 1991. $^{234}U/^{238}U$ mass spectrometry of corals: How accurate is the U-Th age of the last interglacial period? Earth and Planetary Science Letters 106, 169-18.

Hearty, P.J., Neumann, A.C., 2001. Rapid sea level and climate change at the close of the Last interglaciation (MIS 5e): evidence from the Bahamas Islands. Quaternary Science Reviews 20, 1881-1895.

Hearty, P.J., O'Leary M.J., 2004 Stratigraphy of Quaternary Peri-continental carbonate and quartz dunes of W. Australia. 17th Australian Geological Convention, Hobart, Tasmania.

Henderson, G.M., 2002. Seawater ($^{234}U/^{238}U$) during the last 800 thousand years. Earth and Planetary Science Letters 199, 97-110.

Kennedy, D.M., Woodroffe, C.D., 2002. Fringing reef growth and morphology: a review Earth-Science Reviews 57 255-277.

McCulloch, M.T., Esat T., 2000. The coral record of last interglacial sea levels and sea surface temperatures. Chemical Geology 169, 107-129.

Murray-Wallace, C. V. 2002. Pleistocene coastal stratigraphy, sea-level highstands and neotectonism of the southern Australian passive continental margin - a review. Journal of Quaternary Science 17, 469 - 489.

Neumann, A.C., Hearty, P.J., 1996. Rapid sea-level changes at the close of the last interglacial (substage 5e) recorded in Bahamian island geology. Geology 24 (9), 775-778.

Playford PE. 1988. Guidebook to the Geology of Rottnest Island. Excursion Guidebook No. 2, Western Australia Division of the Geological Society of Australia: Perth; 67 pp.

Playford, P.E., 1990. Geology of the Shark Bay area, Western Australia. In: Berry, P.F., Bradshaw, S.D. & Wilson, B.R. (Eds.). Research in Shark Bay. Report of the France-Australe Bicentenary Expedition Committee. Western Australian Museum, Perth, 13-31.

Potter, E.K., Stirling, C.H., Andersen, M.B., Halliday, A.N., 2005. High precision Faraday collector MC-ICPMS thorium isotope ratio determination. International Journal of Mass Spectrometry 247 (1-3), 10-17.

Robinson, L.F., Belshaw, N. S., Henderson G.M., 2004. U and Th concentrations and isotope ratios in modern carbonates and waters from the Bahamas. Geochimica et Cosmochimica Acta 68, 1777 - 1789.

Scholz, D., Mangini, A., Felis, T., 2004. U-series dating of diagenetically altered fossil reef corals. Earth And Planetary Science Letters 218 (1-2), 163-178.

Stirling, C.H., Esat, T.M., McCulloch, M.T., Lambeck, K. 1995. High-precision U-series dating of corals from Western Australia and implications for the timing and duration of the Last Interglacial. Earth and Planetary Science Letters 135, 115-130.

Stirling, C.H., Esat, T.M., Lambeck, K., McCulloch, M.T. 1998. Timing and duration of the Last Interglacial: evidence for a restricted interval of widespread coral reef growth. Earth and Planetary Science Letters 160, 745-762.

Stirling, C.H., Halliday A.N., Porcell, D., 2005. In search of live Cm-247 in the early solar system. Geochimica et Cosmochimica Acta 69 (4), 1059-1071.

Stirling, C.H., Esat, T.M., Lambeck, K., McCulloch, M.T., Blake, S.G., Lee D.C., Halliday, A.N., 2001. Orbital forcing of the marine isotope stage 9 interglacial. Science 291 (5502), 290-293.

Spencer, T., Viles, H., 2002. Bioconstruction, bioerosion, and disturbance on coral reefs and rocky carbonate coasts. Geomorphology 48, 23-50.

Taylor, J.G., Pearce, A.F., 1999. Ningaloo Reef Current observations and implications for biological systems: Coral spawn dispersal, zooplankton and whale shark abundance. Journal of the Royal Society of Western Australia 82, 57-65.

Thompson, R.O.R.Y., 1984. Observations of the Leeuwin Current off Western Australia. Journal of Phyical Oceanography 14, 623-628.

Thompson, W.G., Spiegelmann, M.W., Goldstein, S.L., Speed, R.C., 2003. An open-system model for U-series age determinations of fossil corals. Earth and Planetary Science Letters 210, 365-380.

Trudgill, S.T., 1983. Preliminary estimates on intertidal limestone erosion, One Tree Island, Southern Great Barrier Reef, Australia. Earth Surface Processed and Landforms 8 (2), 189-193.

Van de Graaff, W.J.E., Denman, P.D. and Hocking, R.M., 1976. Emerged Pleistocene marine terraces on Cape Range, Western Australia. Geological Survey of Western Australia Annual Report, 62-69.

Veeh, H.H., Schwebel, D., van de Graaff, W.J.E., Denman, P.D., 1979. Uranium series ages of coralline terrace deposits in Western Australia. Journal of the Geological Society of Western Australia, 26 285-292.

Villemant, B., Feuillet N., 2003. Dating open systems by the 238U-234U-230Th method: application to Quaternary reef terraces. Earth and Planetary Science Letters. 210, 105-118.

B.9 FIGURES 1-7

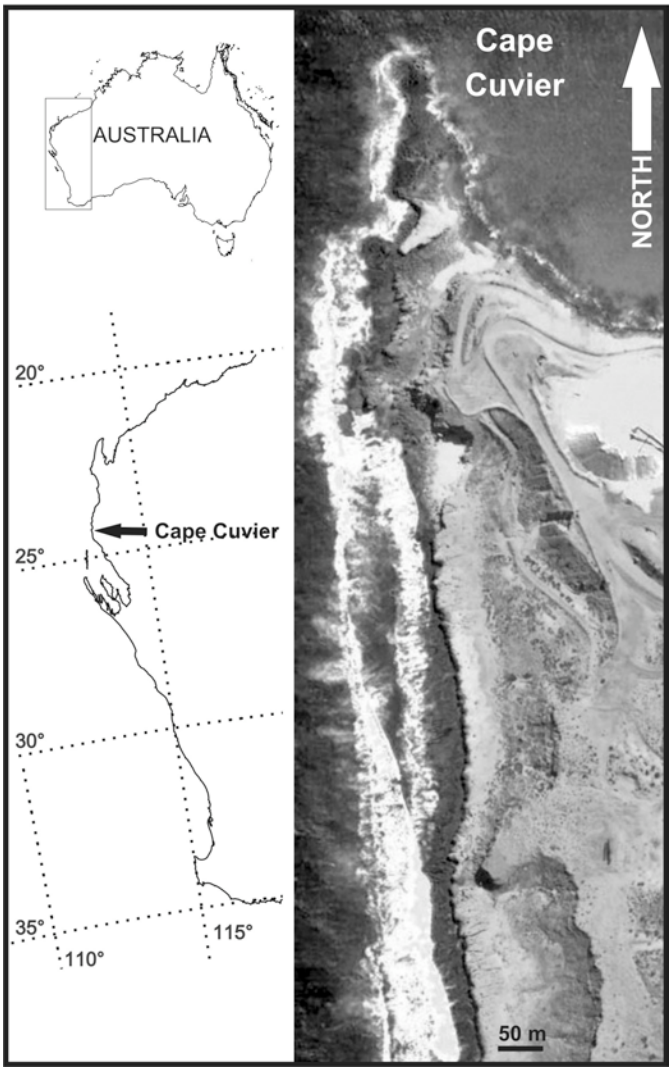

Figure 1: Location of Cape Cuvier, Western Australia

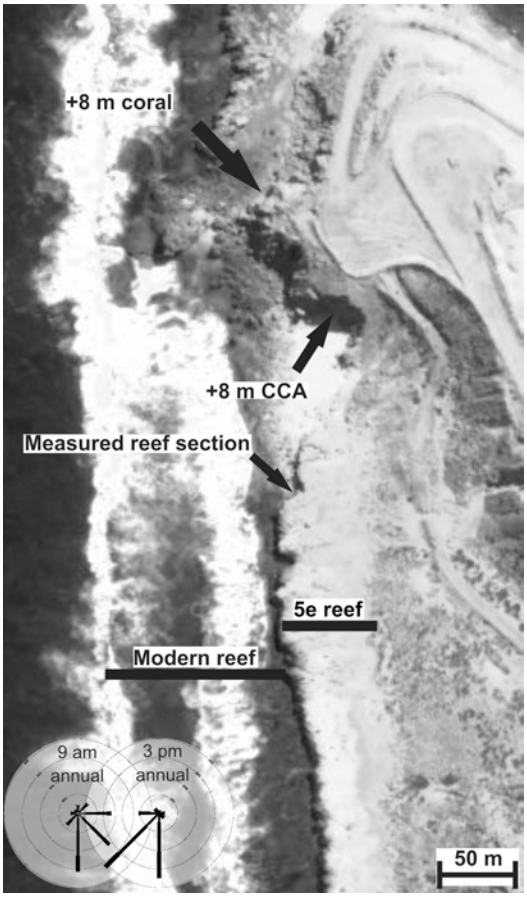

Figure 2: An aerial photograph of Cape Cuvier showing the lower MIS 5e reef platform and upper coralgal rim. The 9am and 3pm wind rose are also shown.

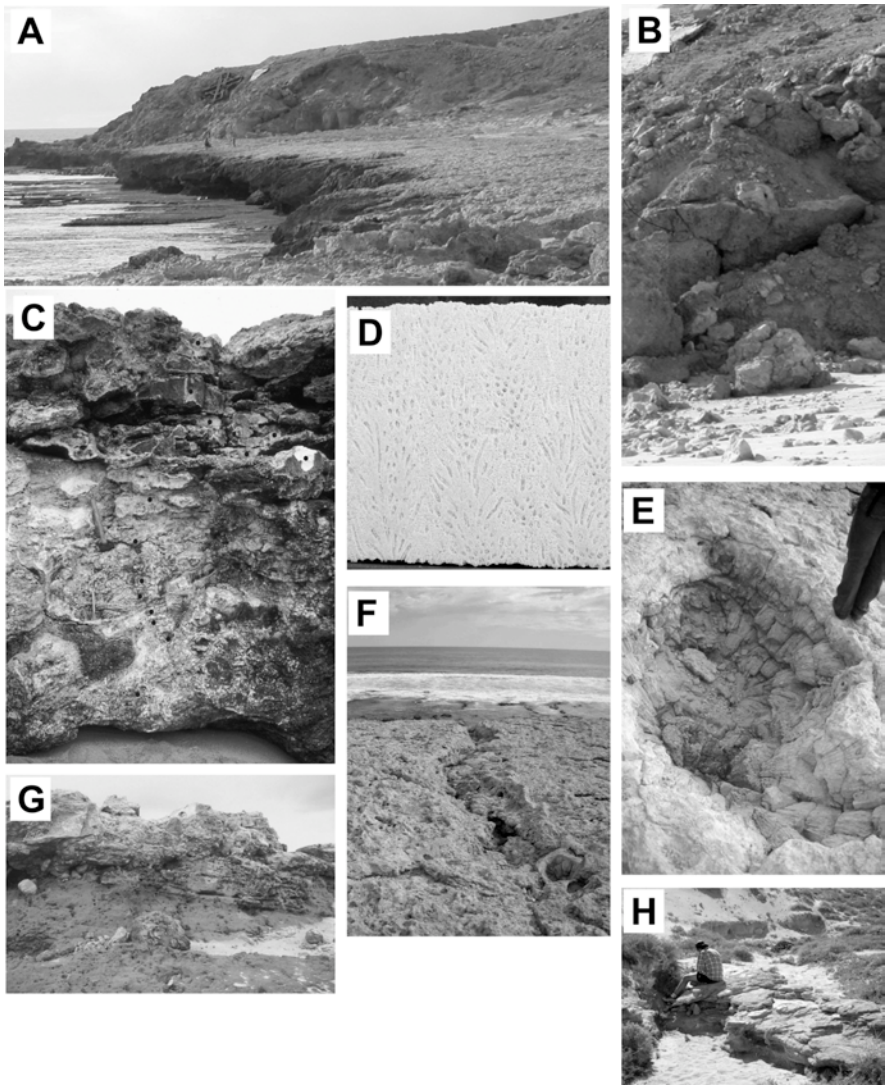

Figure 3: A) Modern and emergent reef platform at Cape Cuvier (looking north) at low tide, coralline algae can be seen encrusting the fossil reef in the foreground, cliffs in the background host the upper coralgal rim. B) 3 m high sea cliff section, thick coral (*A. digitifera*) plates can be observed with black dots representing a coral drill core. C) Seaward looking view of the emergent reef flat, a drainage gutter displays similar morphology to the modern reef flat in the background. D) Coralline algae can be seen encrusting the paleo-sea-cliff mid way up photo. E) A sectioned sample of *A. Digitifera* collected from the sea cliff. F) a large favid coral exposed on the surface of the emergent reef flat, it appears truncated and capped by coralline algae. G) Wave cut coral terrace at an elevation of +10 m capped by a coralline algal conglomerate. H) Fossil beach at 7.4 m.

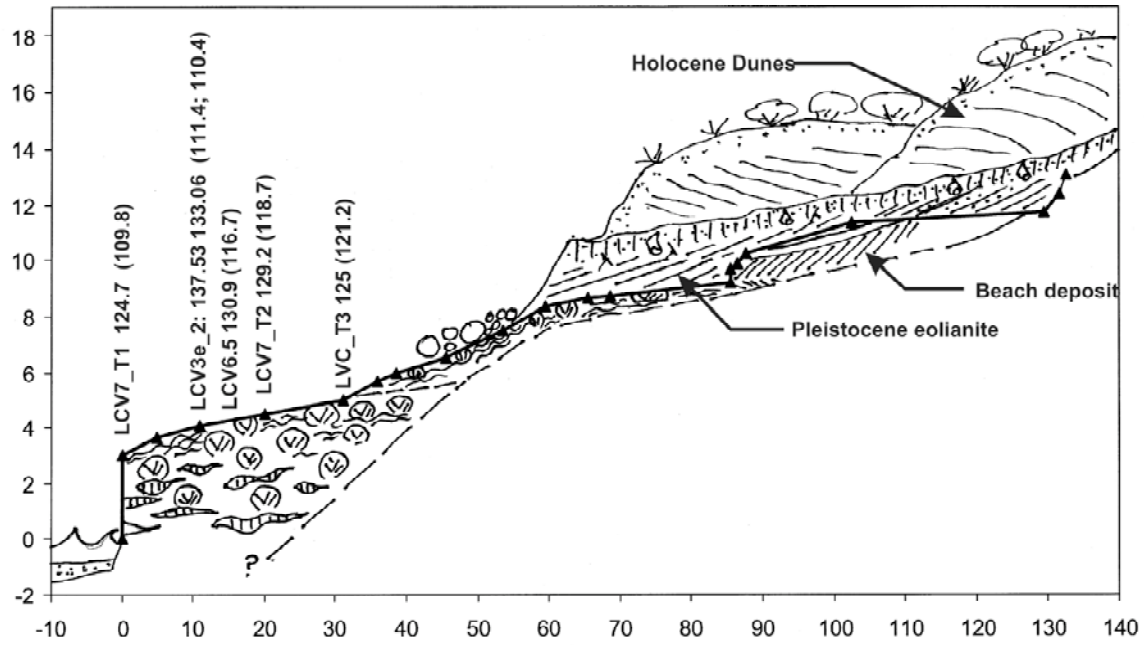

Figure 4: Surveyed transect of the emergent reef terrace at Cape Cuvier and U-series ages (000). Corrected U-series ages are bracketed.

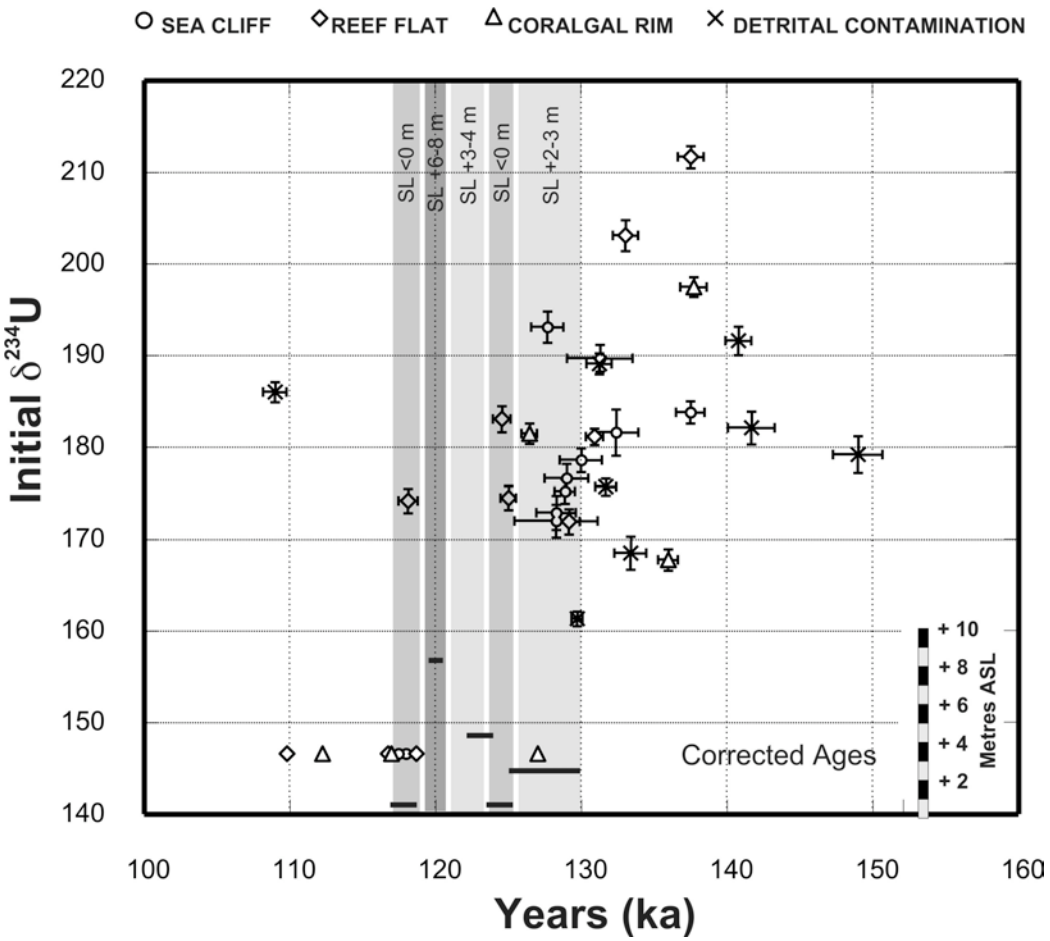

Figure 5: $\delta^{234}U_{initial}$ vs. ^{230}Th-age. The duration and elevation of MIS 5e sea levels (based on data from Hearty and Neumann 2001) are also plotted (shaded areas). All corals exhibit $\delta^{234}U_{initial}$ values that are greater than modern seawater, which has a $^{234}U/^{238}U$ activity of 146.6‰. Thompson *et al.* (2003) open-system model was used to correct those corals with elevated $\delta^{234}U$ to modern seawater activity of 146.6‰. The corrected ages would suggest coral growth occurred almost exclusively at the end of MIS 5e.

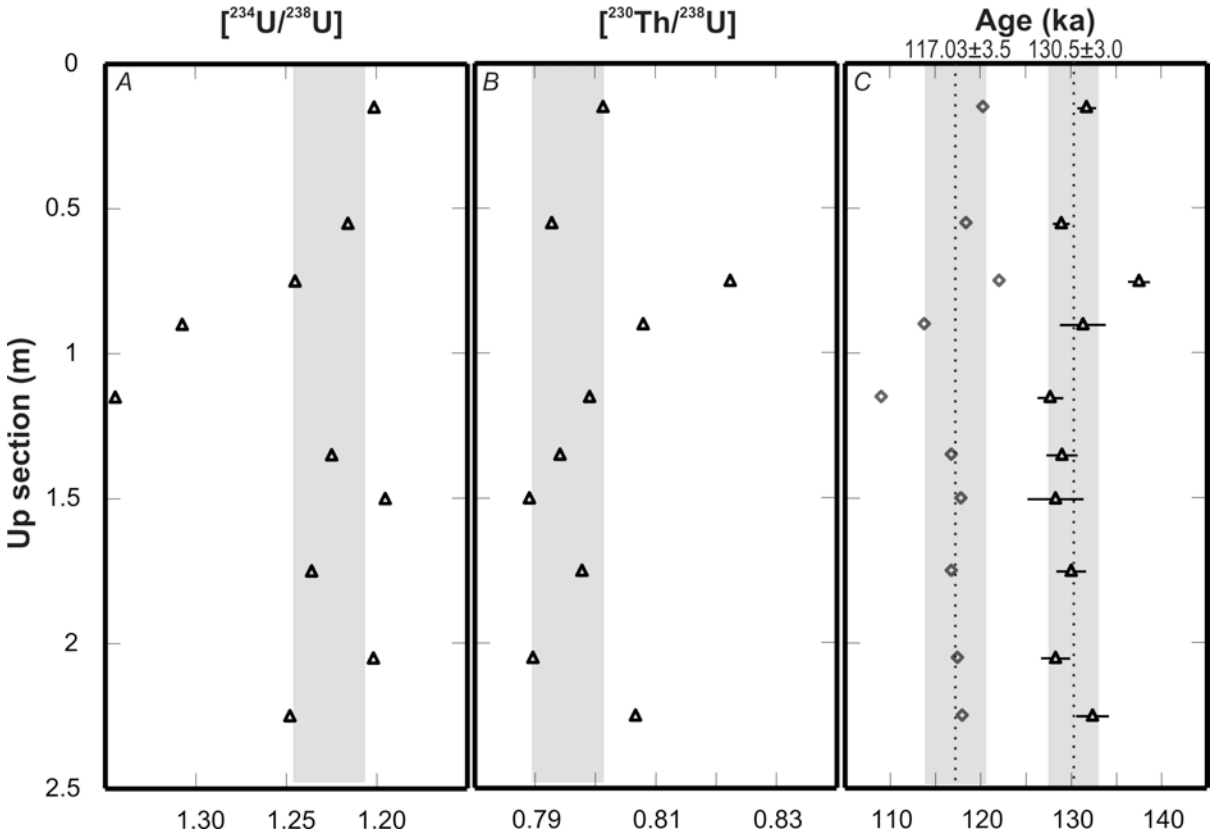

Figure 6: Isotopic ratios and ^{230}Th age for corals collected up a 3 m measured section at Cape Cuvier. 5a) ^{234}U/^{238}U isotopic ratios, 5b) ^{230}Th/^{238}U isotopic ratios, 5c) conventional (triangle) and corrected (diamond) U-series age in thousands of years (ka). Shaded represents average values with 1 SD.

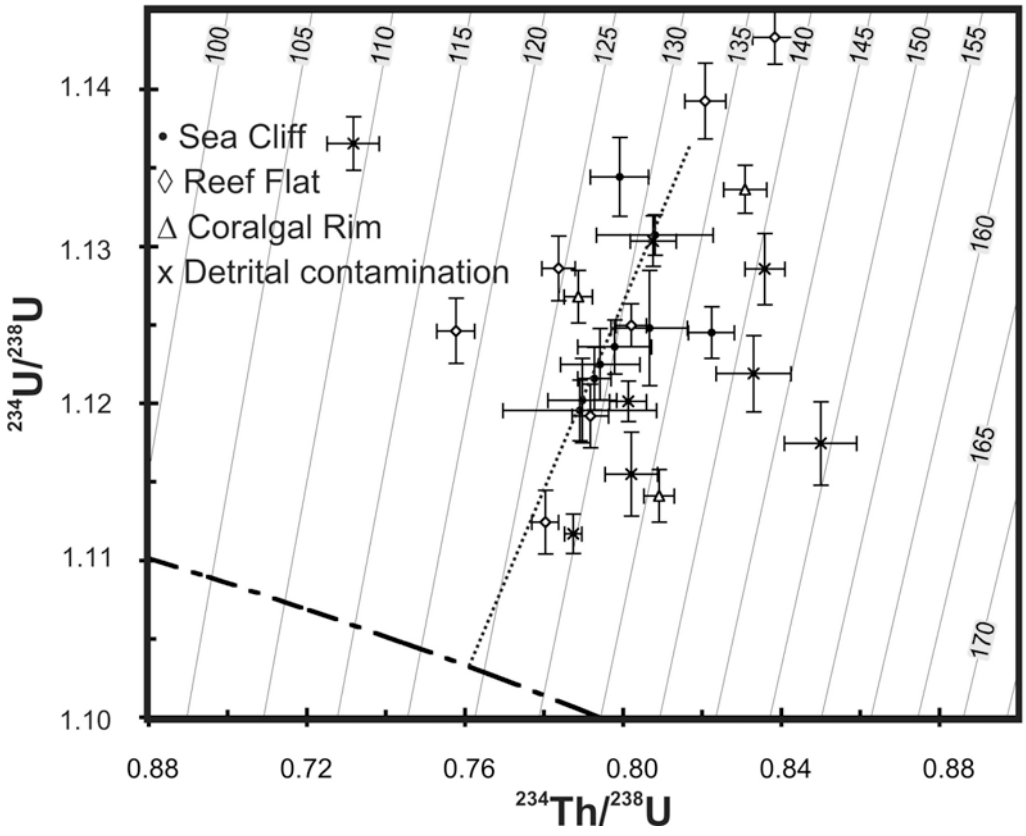

Figure 7: Compilation of the U-series data of the MIS 5e corals on a $^{234}U/^{238}U$ activity ratio diagram. The thick dashed line represents closed system evolution with and initial modern seawater value of 1.1466. The subvertical lines are age isochrons. The dashed line indicates a linear compositional array, which intersects the closed-system evolution curve at 124 ka.

Table 1: XRD analysis

PHASE AAC Run No	Your Ref	Quartz SiO2	Aragonite CaCO3	Calcite CaCO3	High Mg calcite (Ca,Mg)CO3	Dolomite CaMg(CO3)2
5547-01	LCV7_1		99%			1%
5547-05	LCV1_2		86%	9%	3%	2%
5547-12	LCV2_1		96%	1%	2%	1%
5547-15	LCV7_3	1%	99%			
5547-16	LCV1_3		99%	1%		
5547-18	LCV2_4	1%	99%	1%		
5547-20	LCV2_3	1%	99%	0%		

Table 2: U-series data

Summary	U ppm[1]	^{230}Th ppt[2]	^{232}Th ppb[3]	δ^{234}U Meas.[4]	± 2σ	^{230}Th/ ^{238}U[5]	± 2σ	[^{230}Th/ ^{232}Th]	Age (ka)[6]	± 2σ	Initial δ^{234}U[7]	± 2σ	Modelled Age[8]
Sea cliff coral ages													
LCCg_C	3.01	39.30	0.16	124.80	1.84	0.8067	0.005	46520	**132.40**	1.55	**181.60**	2.50	117.98
LCC1i_C	3.38	43.25	0.25	120.18	1.34	0.7897	0.004	32419	**128.30**	1.35	**172.90**	1.85	117.46
LCCk_C	3.16	40.76	0.16	123.60	0.87	0.7978	0.005	48364	**130.00**	1.45	**178.60**	1.30	116.78
LCC1m_C	3.04	38.83	0.18	119.54	0.97	0.7891	0.010	40107	**128.30**	2.85	**172.00**	1.80	117.81
LCC1n_C	3.11	40.02	0.07	122.49	1.13	0.7942	0.005	113409	**129.00**	1.50	**176.60**	1.60	116.77
LCC1o_C	3.18	41.08	0.47	134.44	1.26	0.7991	0.004	16419	**127.70**	1.10	**193.10**	1.70	109.03
LCCp_C	3.47	46.98	2.01	128.56	1.14	0.8359	0.003	4377	**140.80**	0.89	**191.60**	1.55	122.19
LCC1r_C	3.28	42.88	0.32	130.74	0.64	0.8080	0.007	25335	**131.30**	2.25	**189.70**	1.45	113.78
LCCs_C	3.26	43.33	0.17	124.52	0.82	0.8224	0.003	46761	**137.50**	0.97	**183.80**	1.20	122.03
LCCt_C	3.21	41.22	0.34	121.59	1.00	0.7928	0.002	22683	**128.90**	0.69	**175.20**	1.30	118.41
LCCw_C	3.39	44.03	1.27	120.14	0.64	0.8013	0.002	6511	**131.70**	0.73	**175.70**	0.91	120.28
Detrital ^{232}Th													
LCCa_C	3.05	42.01	5.39	117.45	1.33	0.8500	0.005	1462	**149.00**	1.70	**179.20**	2.00	135.14
LCCb_C	2.90	37.65	3.59	115.49	1.34	0.8021	0.003	1965	**133.40**	1.10	**168.50**	1.80	124.14
LCC1j_C	2.86	38.52	18.92	121.89	1.21	0.8330	0.005	381	**141.70**	1.60	**182.10**	1.80	126.84
LCCq_C	3.68	43.63	12.48	136.55	0.85	0.7317	0.003	655	**109.00**	0.79	**186.00**	1.10	93.57
LCV_1e_2	2.20	28.28	11.63	111.69	0.63	0.7874	0.001	454	**129.74**	0.37	**161.34**	0.79	123.48
Upper coralgal rim													
LCV_1e_3	3.35	44.07	0.15	114.10	0.84	0.8091	0.002	54759	**135.98**	0.68	**167.76**	1.17	127.03
LCV_2e_1	3.17	42.81	0.10	133.64	0.76	0.8309	0.003	78065	**137.73**	0.90	**197.47**	1.09	116.98
LCV_2e_3	3.88	50.91	1.46	130.34	0.80	0.8076	0.003	6441	**131.25**	0.87	**189.10**	1.15	113.99
LCV_2e_4	4.37	56.01	0.75	126.80	0.84	0.7887	0.002	13939	**126.46**	0.53	**181.48**	1.10	112.27
Reef flat													
LCV 6.5	2.21	28.88	0.06	124.98	0.68	0.8021	0.002	89622	**130.93**	0.59	**181.14**	0.90	116.75
LCV7 T1	2.69	34.21	0.16	128.60	1.03	0.7837	0.002	39635	**124.57**	0.61	**183.07**	1.41	109.83
LCV7 T2	3.14	40.36	0.13	119.20	1.02	0.7917	0.002	56496	**129.18**	0.73	**171.92**	1.38	118.69
LCV7 T3	3.22	40.83	0.75	112.43	1.01	0.7803	0.002	10213	**125.02**	0.53	**174.50**	1.31	121.16
LCV7e_3c	3.44	42.37	0.31	124.62	1.04	0.7577	0.002	25669	**118.13**	0.66	**174.19**	1.33	106.96
LCV3e_2a	3.13	42.64	0.08	143.32	0.85	0.8384	0.003	94188	**137.53**	0.88	**211.66**	1.20	111.40
LVC3e_2b	3.16	42.17	0.10	139.27	1.21	0.8208	0.003	76512	**133.06**	0.86	**203.08**	1.68	110.38

Notes to Table 2.

[1] Uranium concentrations are measured in parts per million (ppm).

[2] ^{230}Th concentrations measured in parts per trillion (ppt).

[3] ^{232}Th concentrations measured in parts per billion (ppb).

[4] $\delta^{234}U = \{[(^{234}U/^{238}U)/(^{234}U/^{238}U)_{eq}]-1\} \times 10^3$. $(^{234}U/^{238}U)_{eq}$ is the atomic ratio at secular equilibrium and is equal to $\lambda_{238}/\lambda_{234} = 5.4891 \times 10^{-5}$, , where λ_{238} and λ_{234} are the decay constants for ^{238}U and ^{234}U, respectively, adopting half-lives of Cheng *et al.*, (1998)

[5] $[^{230}Th/^{238}U]_{act} = (^{230}Th/^{238}U)/(\lambda^{238}/\lambda^{230})$.

[6] U-series ages are calculated iteratively using:

1- $[^{230}Th/^{238}U]_{act} = \exp^{\lambda_{230}T} - (\delta^{234}U(0)/1000)(\lambda_{230}/(\lambda_{230}-\lambda_{234}))(1-\exp(^{\lambda_{234}-\lambda_{230}T})$ where T is the age in years and λ_{230} is the decay constant for ^{230}Th. $\lambda_{238} = 1.551 \times 10^{-10}$ y^{-1}; $\lambda_{234} = 2.826 \times 10^{-6}$ y^{-1}; $\lambda_{230} = 9.158 \times 10^{-6}$ y^{-1}. Strictly reliable ages will have $^{234}U_{initial}$ 146.6 ± 5‰

[7] The initial value is given by $\delta^{234}U_i = \delta^{234}U(0)\exp(\lambda_{234}T)$, where T is the age in years.

[8] Open system ages were modelled after Thompson *et al.*, 2003.

SECTION C

Coral reef and stromatolite development in Shark Bay during Recent and Marine Isotope Stage 5e sea level high-stands

C.1 ABSTRACT

Field observations and U-series ages reveal that Shark Bay, Western Australia (WA) has been flooded on at least 3 occasions during the Upper Pleistocene/Holocene period, resulting in a succession of marine deposits around the Bay. The exact age of these deposits has until now been problematic due to a lack of reliable and accurate age data. This study reports 17 new U-series coral dates from emergent reef deposits around Shark Bay which together with new field data, point to an extended period of coral reef development during the peak of the last interglacial, marine isotope stage (MIS) 5e. There is little direct evidence of fossil reef development occurring during interglacials of the Middle/Upper Pleistocene (MIS 9/11). This places most of the fossil reefs currently assigned to the Dampier Formation (Middle Pleistocene) such as those observed at Tetrodon Loop and Monkey Mia into the Bibra Formation, which is shown to be of Last Interglacial (MIS 5e) age.

Coral reef communities in Shark Bay were significantly more widespread during MIS 5e compared to those of the present day, despite similar architecture of the bay and coastal configuration. This can be attributed to higher sea levels and an absence of major sill and bank structures that together with increased water depth, resulted in an enhancement of marine circulation within the reaches and basins. The youngest geomorphic features in Shark Bay are bathymetrically controlled, and include the formation of Faure and Fork Flat sills, a result of extensive carbonate sedimentation during the Holocene. Stromatolites are absent from the geological record within Shark Bay until the Holocene; suggesting that sea levels and marine sedimentary processes that have operated during the present sea-level highstand are unique to this period.

C.2 INTRODUCTION

Present-day Shark Bay on the central west coast of Australia (25.5° to 26.5° South latitude) has a depauperate (to non-existent in inner bay waters) coral fauna when compared to Ningaloo reef in the North and the Houtman-Abrolhos in the south (**Fig. 1a**). The presence of large barrier islands to the east and north, as well as the length and shallowness of the embayments restrict oceanic circulation within Shark Bay (Logan and Cebulski, 1970). As a result, strong, permanent high salinities and steep temperature gradients limit the occurrence of modern coral growth to the seaward margins of the embayments (Marsh, 1990). There is however evidence of reef development occurring well within the present metahaline and hypersaline embayments during previous interglacials (Logan *et al.*, 1970).

Although limiting present-day coral growth, the hypersaline environments such as those present today in the southern end of Hamelin Pool, Shark Bay, are ideal for the development of microbial communities responsible for building stromatolites. Although they are amongst the oldest form of life being recorded back to the early Archean, stromatolites have an extremely limited present-day occurrence being restricted to a few other hypesaline lakes along the Western Australian coastline and a restricted occurrence in the Bahamas. Thus understanding the evolution of the Shark Bay environment is critical to understanding this unique and once prolific form of life.

The history of the evolution and carbonate sedimentation of Shark Bay is summarised by Playford (1990) and reported in two American Association of Petroleum Geologists (AAPG) Memoirs, "Carbonate Sedimentation and Environments, Shark Bay, Western Australia", No. 13, 1970 and "Evolution and Diagenesis of Quaternary Carbonate Sequences, Shark Bay", Western Australia No. 22, 1974. While the sedimentological aspects of both AAPG memoirs are highly detailed and descriptive, the terminology and chronology of the marine highstand events is

questionable due to the absence of reliable dating techniques and a limited understanding of timing and amplitude of Quaternary sea-level change.

The early work of Logan *et al.* (1970) recognized that the ancestral dune landscape of Shark Bay was flooded on three separate occasions during the latter part of the Quaternary. Evidence for these marine transgressions is revealed in marine carbonate sequences that outcrop along the Shark Bay coastline. These marine transgressions are referred to in order of decreasing age: 1) Middle Pleistocene Dampier marine phase; 2) the Upper Pleistocene Bibra marine phase; and 3) the Holocene-Recent marine phase (Logan *et al.*, 1970). An exact chronology of these events has not been previously established; therefore the correlation of carbonate outcrops across the bay has remained problematic (**Table 1**).

Thus objectives of this study are to:

1. Develop a stratigraphic succession and a chronological framework for emergent marine units in order to establish the frequency, timing and duration of Pleistocene marine incursions into Shark Bay.

2. Provide insight into the evolution of oceanographic processes within Shark Bay, based on timing and emplacement of major morphological features.

3. Offer scenarios and models that might explain the occurrence of stromalites in the present-day hypersaline environment of Hamelin Pool and the much more widespread distribution of corals within Shark Bay generally during MIS 5e, using modern environmental parameters as a point of reference.

C.3 MODERN ENVIRONMENTAL SETTING

C.3.1 Coastal geomorphology

Shark Bay is Australia's largest semi-enclosed coastal embayment with 1,100 km of coastline and an open water area of approximately 10,000 km^2. It is bounded to the west by Edel Land and Dirk Hartog Island, to the north by Bernier and Dorre Islands and to the east by the Australian mainland (**Fig. 1b**). The Peron Peninsula, a large Lower to Middle Pleistocene relic transverse dune complex (Hocking *et al.*, 1987) bisects the bay, forming two shallow NW-SE trending reaches. Upper Pleistocene ooid rich carbonates flank much of the peninsulas western headlands (Donald, 2003). The 40-km-long Hopeless Reach in the east has a coastal strip consisting of extensive supratidal flats, and a low-lying coastal plain, backed on the east by a Tertiary limestone escarpment. The adjoining 49,600 km2 catchment feeds the ephemeral rivers the Gascoyne and the Wooramel. Fluvial contribution from surface runoff into Shark Bay is severely restricted by arid conditions (<200 mm/y), high evaporation rates, permeable soils and highly intermittent rainfall.

The Tamala Limestone (Playford *et al.*, 1976) dominates exposures across much of Edel Land, is bounded on the west by the 150 m to 250 m high Zuytdorp cliffs fronting the Indian Ocean. The coastline along Freycinet Reach consists of partially submerged, north-south orientated, longitudinal dune ridges and interdune valleys. The north-south trending Bernier and Dorre Islands are composed of Pleistocene age carbonate eolianites with large scale cross bedding.

C.3.2 Oceanography

Seawater exchange between continental shelf waters (including the Leeuwin Current) and Shark Bay waters occurs through the 25 km, 60 m deep Naturaliste Channel, and the 35 km and

50 m deep Geographe Channel (**Fig. 1b**). These channels shoal rapidly to an average depth of 15 m as they enter the bay. During the winter and spring, when the predominantly southerly winds periodically swing to the north, continental-self waters penetrate northern Shark Bay through the Geographe Passage (Burling *et al.*, 1999). Extensive shallow carbonate banks and seagrass beds further restrict circulation within Shark Bay. The largest bank is the Faure Sill, which effectively divides Hopeless Reach, forming L'Haridon Bight and the larger Hamlin Pool in the south (**Fig. 1b**). The 2 km wide 6 m deep Herald Loop Channel permits limited seawater exchange between the two basins. Restricted marine circulation combined with an annual evaporation rate of 2000 mm, 10 times greater than the annual precipitation, has resulted in strong lateral salinity gradients within Shark Bay. Normal oceanic salinities of 35 to 40 persist in the northern parts of the bay, this changes to metahaline (40 to 56) through to hypersaline (56 to 70) in L'Haridon Bight and Hamlin Pool in the south (**Fig. 1b**). These extreme salinity values were found to be permanent within Hamlin Pool suggesting that the salt production, due to evaporation, is balanced by the rate of salt discharge into the rest of the bay (Logan and Cebulski, 1970).

C.4 REEF BIOGEOGRAPHY AND DEVELOPMENT

C.4.1 Shark Bay coral communities

Areas of greatest coral diversity occur along the protected headlands of Bernier and Dorre Islands and to a lesser extent the lee side of Dirk Hartog island, where 55 species from 23 genera form narrow fringing or patch reefs in close proximity to the open sea (Marsh, 1990; Hatcher, 1991) (**Fig. 1b**). Coral communities are conspicuously absent from northern open water areas of Shark Bay were extensive mobile carbonate banks and seagrass beds limit the availability of suitable substrate. However, where scattered hardgrounds are found, generally

along the western fringe of Denham Sound, communities of *Turbinaria* dominate (Marsh, 1990) (**Fig. 2i**). A further reduction in coral diversity occurs within the metahaline regions of Freycinet Reach were minor solitary stands of *Goniastrea aspera*, *Favites pentagona*, *Favia sp. Goniopora lobata* and *Turbinaria spp.* are present (Marsh, 1990). Moving south into Henri Freycinet Harbour, along Hopeless Reach and into hypersaline Hamlin Pool there are no extant coral communities.

C.4.2 Shark Bay stromatolite communities

Lithified and laminated organo-sedimentary structures (stromatolites) occur along the intertidal and subtidal shorelines of Hamlin Pool and L'Haridon Bight (**Fig. 1b; Fig. 2h**). Their occurrence coincides with ecologically harsh (hypersaline) environments where potential competitors for substrate, such as corals or seagrass (Kendrick *et al.*, 1990), or predators such as gastropods (Playford, 1990), are severely restricted. Vertical accretion of Shark Bay stromatolites, facilitated by sediment trapping, is on the order of ~0.5 mm/year (Playford, 1990), but can be as low as 0.3 mm/year within the higher energy intertidal zone where potential for erosion is increased (Chivas *et al.*, 1990). With such slow accretion rates there is a danger of burial during periods of rapid sediment deposition. However, one of the factors that allow stromatolites to dominate Hamlin Pool and L'Haridon Bight, and is intrinsically linked to hypersaline zones, is the lack of biogenic sedimentation due to a reduction in the abundance of carbonate producing flora and fauna (Walker and Woelkering, 1988). Additionally, due to the extremely low tidal velocities there is little potential for sediment transport; when high-energy events such as cyclones do occur sediments tend to bypass the intertidal or subtidal zones to form onshore storm (coquina) ridges (Playford, 1990; Nott, 2006).

C.5 MATERIALS AND METHODS

Place names of study sites were derived from the Point Quobba to Geraldton nautical chart (Aus 331), Monkey Mia Special, Yaringa, Wooramel and Carnarvon Special topographic and geologic maps.

C.5.1 Stratigraphic logs

Many previously described localities in and around Shark Bay (Logan *et al.*, 1970) were revisited and stratigraphically logged, along with several new localities. Elevations of emergent marine units were measured using a theodolite or hand-level, and approximate (± 0.2 cm) mean sea level (MSL), calculated from know tidal elevations, was assigned the 0 m benchmark. The composition of the sedimentary strata both underlying and overlaying emergent marine units was described.

C.5.2 Sample collection

Access to many of the remote sites was possible only by small boat, four-wheel drive or on foot. A petrol powered rock drill, incorporating a water swivel 15 mm diameter barrel with an impregnated diamond bit was used to collect coral specimens. Drill penetration averaged between 150 to 200 mm. Eolianite samples were collected using a rock hammer.

Much effort was made to sample corals in the field without bias towards a particular period of coral growth i.e., sampling at multiple locations around the bay and spatially exclusive points from an outcropping reef. However, it is highly likely that periods of reef growth may be missing from the geologic record through marine erosion (Tetrodon Loop), buried under active dunes or intertidal sand sheets (Gladstone North), or concealed by stromatolite growth

(Nilemah). It was envisaged that by sampling corals from multiple locations around the bay, that a more complete picture of reef development may be revealed.

C.5.3 Geochronology

U-series measurements were performed using a Neptune MC-ICPMS at the Research School of Earth Sciences, Australian National University. Measurements were conducted using a combination of simultaneous multiple-Faraday cup and ion counter protocols based on those previously described for TIMS (Stirling *et al.*, 1998 and McCulloch and Esat 2000) . The main difference being that ion counting/faraday gains where determined by reference to an external standard (SRM 960) for determination of $^{234}U/^{235}U$ ratios where ^{234}U is measured using ion counting. For the low abundance isotopes ^{230}Th and ^{229}Th (spike) these where both measured using the central ion counter, but simultaneously with ^{235}U and ^{238}U and ^{232}Th on faraday cups allowing corrections for both beam instability as well as mass bias. For detailed protocols see McCulloch and Mortimer (in prep). This multiple-Faraday approach yield higher precision in conjunction with a significantly reduced sample size requirement, lowering age uncertainties by up to a factor of five (Stirling *et al.*, 2001) compared to single cup procedures. Whilst higher precision measurements are possible using multiple faraday only procedures reported in Andersen *et al.* (2004) Potter *et al.* (2005) Stirling *et al.* (2005) and Bernal *et al.*, (2002), these suffer from the disadvantage of requiring much larger, gram size samples. For the labour intensive preparation of carefully selected portions of coral walls adopted in this study, the measurement of relatively small samples (<50 mg) is a distinct advantage.

C.5.4 Reliability of $^{234}U/^{230}Th$ coral ages

The accuracy of ^{234}U-^{230}Th series dating method relies on corals incorporating U with contemporaneous $\delta^{234}U$ seawater activities and negligible ^{230}Th into their aragonite skeletons

during precipitation of their carbonate and that they subsequently remain closed to uranium and thorium loss or gain. However, in fossil coral ^{234}U and ^{230}Th activities do not always reflect closed system evolution from a system with $^{234}U/^{238}U$ seawater ratio. These anomalous values could reflect: 1) changes in seawater $\delta^{234}U$ activities over glacial/interglacial cycles (Henderson, 2002); or 2) internal diagenesis of their aragonite skeleton and/or secondary aragonite crystallization (Hamelin *et al.*, 1991); or 3) direct U/Th exchange within pore waters (Thompson *et al.*, 2003). The potential for such processes generally increases with age, but preservation of closed U-Th isotopic systematics is highly site specific (e.g. McCulloch and Esat, 2000, Bard *et al.*, 1991) and can vary for coral to coral as well as within the different structural elements of an individual coral.

Following the procedures of earlier workers (Chen *et al.*, 1991; Stirling *et al.*, 1995 and 1998; Robinson *et al.*, 2004) corals were screened for potential U and Th loss or gain based on the following criteria:

- We consider the calculated $\delta^{234}U_{initial}$ to be the best quantitative test for open system behaviour in corals. For a coral age to be considered strictly reliable $\delta^{234}U_{initial}$ values should reflect a modern seawater value of 146.6 ± 10‰.
- The total uranium concentration of fossil corals should approximate modern coral values of about 3 ± 0.5 ppm of uranium.
- Fossil corals should be free of allochthonous ^{230}Th, as indicated by the absence of detrital ^{232}Th (< 1 ppb).
- Corals should show primary aragonitic structures or have at most < 2% calcite concentration.

C.6 RESULTS

A total of 13 U-series measurements of coral ages from various locations around Shark Bay (**Fig. 1b**) are presented in **Table 2**. A single flowstone was also dated from the Zuytdorp Cliffs at the Womerangee Hill type section as well as a stromatolite sample.

C.6.1 Baba Head

Baba Head is located on the northeastern headland of Disappointment Inlet (Edel Land) 26˚60.2' S 113˚69.2' E, within the metahaline Freycinet Basin (**Fig. 1b; Fig. 2a**). The lithology of the area was described by Read (1974) as unconsolidated, to strongly-lithified calcarenite with large-scale crossbedding. A wave cut terrace and notch composed of a well-indurated, Mid-Pleistocene, red/yellow oolite form the basal unit. A well-indurated coquina beach with coral rubble lay unconformably above the terrace at +0.5 to +1.0 m and partly in fills the notch. Read (1974) correlates the marine coquina and coral rubble unit with the Bibra formation. A non-in situ coral fragment collected from the coquina deposit returned a U-series age of 122.6 ± 5 ka with a $\delta^{234}U$ value of 151.6‰ indicating a reliable age.

C.6.2 Tetrodon Loop

Located on the eastern shore of Dirk Hartog Island, Tetrodon Loop, 25˚57' S 113˚08' E is presently within the oceanic marine zone, and downwind of a large mobile dune system (**Fig. 1b; Fig. 2b**). The only modern coral communities found in the area are those surrounding Egg Island at the northern end of Tetrodon Loop. These consist primarily of the genus *Turbinaria.* Emergent fossil reefs outcrop along the western shore and at the head of the Tetrodon Loop and are dominated by *Platygyra, Porites* and *Galaxia* species. Reef elevation sits approximately +1.5 to +2.5 m, forming a small erosional scarp. Logan *et al.* (1970) originally defined the Tetrodon

reef as Dampier formation or Middle Pleistocene. However, U-series dating of three in situ corals from this study along with two previously dated corals from Stirling *et al.* (1995) and Stirling (1996) return an average age of 126.5 ± 1.5 ka, placing the age of formation firmly within MIS 5e, and correlating with the Bibra marine formation. Like Baba Head, a wave cut terrace at a height of 0.8 metres above MSL composed of a well-indurated, Mid-Pleistocene, red/yellow oolites forms the basal unit.

C.6.3 Gladstone North

The type section of the MIS 5e (Bibra formation) is located at Gladstone North, a few kilometres south of the Wooramel delta, 25° 55.059' S, 114° 15.383' E (**Fig. 1b; Fig 2c**). At this locality in situ Porites and Faviideae coral heads outcrop within the intertidal zone but are mostly buried beneath onlapping Holocene sediments. U-series dating of two large in situ coral heads returned ages of 127.3 ± 1.1 and 126.9 ± 0.5 with δ^{234}U values of 150‰ and 166‰ respectively placing the timing of coral growth during early MIS 5e although the latter sample has only a marginally acceptable δ^{234}U value. The upper surfaces of these corals show no evidence of bioerosion or subaerial exposure, suggesting they grew below the level of mean low water springs and therefore do not represent the true maximum MIS 5e elevation of sea-level. The coastal cliffs at Gladstone North are composed of an alternating sequence of bioclastic and ooid rich beach ridge deposits. A coral fragment was collected (approx. 4 m above MSL) from the Wooramel Cliff section at the southern end of the Wooramel delta; it returned an age of 313 ka placing its growth sometime during MIS 9. However, an elevated initial δ^{234}U of 196‰ and a ^{232}Th concentration of 145.3 ppb place some doubt over the accuracy of this age.

C.6.4 Monkey Mia

Continental dunes (Peron sand) dominate the western fringe of the Peron Peninsular and form a 6-8 m high sea-cliff, a result of modern marine erosion. Marine carbonates onlap the shore as Holocene beach and coastal ridge deposits. Beachrock is found outcropping along a 100 m section of beach approximately 2km North of Monkey Mia at 25° 47.05' S, 113° 41.12 E, between 0 and +1.5 m (**Fig.1b; Fig. 2d**). As the formation of beach rock usually occurs within the intertidal zone (Bricker, 1971), its presence above this zone suggests it was formed during a higher than present sea-level event. Early Holocene sea-levels in Shark Bay are known to have been between 0.5 and 1 m above present elevations (Playford, 1990) however, coral rubble cemented within the beach rock returned two U-series ages of 125.6 ± 0.75 ka and 125.2 ± 0.6 ka with δ^{234}U values of 155.7‰ and 159.2‰ respectively.

A coquina rich beach deposit outcrops at the base of the Peron dunes 2 to 3 m above MSL, 50 m to the north of the beachrock unit. A Turbinaria coral fragment from within the deposit returned an age of 122.94 ± 0.46 ka, with δ^{234}U values of 150.2‰, confirms a younger MIS 5e age. The MIS 5e age for the beachrock and coquina beach deposit at Monkey Mia places the MIS 5e shoreline along the Monkey Mia coast in close proximity to the present shoreline, but at 2-3m higher levels suggesting a stable coastline with little erosion or dune accretion.

C.6.5 Pelican Island

Pelican Island is an elongate low relief (< 3 m above MSL) ooid rich carbonate sand cay situated on the northern edge of the Faure Sill, 25° 50.1' S, 114° 01' E (**Fig. 1b; Fig 2e**). Fossil reefs outcrop along the intertidal zone with many of the surfaces recolonised by calcareous algae. U-series dating of two corals returned ages of 122.8 ± 0.65 ka and 119.6 ± 0.58, with δ^{234}U values of 152.9‰ and 151.3 ‰ respectively, indicating that Pelican Island was a shoal or bank

feature during MIS 5e with coral growth becoming established in this location towards the end of the MIS 5e highstand.

C.6.6 Nilemah

Nilemah is located at the head of Hamlin Pool, in an area of extensive stromatolite growth. A small stromatolite mound (SHP1) was collected from Nilemah prior to the conformation of Shark Bay world heritage status in 1990, and stored at the Department of Geology, Australian National University. The exact elevation of this sample is unknown except to say the stromatolite was collected from within the littoral zone. The sample was impregnated with resin prior to sectioning. It was found that the stromatolite grew on top of a *faviideae* (**Fig. 1b; Fig. 2f**). The coral returned an Upper Pleistocene age of 283 ka, and the stromatolite a mid-Holocene age of 6 ka (**Table 2**). The reliability of the ages is questioned due to the high $\delta^{234}U$ values of 190‰ of the Upper Pleistocene coral, and the high ^{232}Th contents and very low $^{230}Th/^{232}Th$ ratio and hence relatively large contribution to ^{230}Th from detrital contamination in the stromatolite. However, despite significant uncertainties in interpretation of the U-series ages, the stromatolite U-series age is clearly an upper limit and thus constraining its growth to the recent Holocene with the coral being constrained to MIS 5e or possibly the penultimate highstand.

C.7 DISCUSSION

C.7.1 Chronological framework

As a part of a wider study of the Quaternary stratigraphy and sedimentology of Shark Bay, Logan *et al.* (1970) defined two marine transgressions, which he named the Dampier (older)

and the Bibra (younger) formations. Playford (1990) recognised that the Bibra formations were likely formed during the peak of the last interglacial, MIS 5e. However, due to a lack direct dating, much of the emergent shallow marine deposits within Shark Bay have been assigned to the Middle Pleistocene Dampier formation. U-series coral dates from sites across Shark Bay (**Fig. 3**) show that these emergent coral reef deposits were in fact lain down exclusively during MIS 5e, which correlates to the Bibra formation. The very-well-indurated nature of shallow marine (oolitic) and beach ridge deposits, outcropping intermittently along the coastal plane of Shark Bay (Logan *et al.*, 1970) provide evidence of active diagenetic processes associated with marine incursions during the Middle and Upper Pleistocene (MIS 9/11).

C.7.2 Timing of emplacement of major morphological features

By far the most dominant feature along Shark Bay's oceanic coastline is the 150 to 250 m high Zuytdorp sea cliffs of Edel Land. Woomerange Hill, at 270 m is the highest point along this section of coast and is also the type section for the Tamala Limestone. Although not quantitatively dated it has been assigned Middle to Upper Pleistocene age (Playford, 1990). It is likely, based on its size and indurated nature, that Edel Land and the Zuytdorp sea cliffs would have presented a distinct barrier feature during MIS 5e.

Dirk Hartog Island is an equally massive feature comprising Tamala eolianites and separated from Edel Land by the 3 km wide South Passage. Evidence of emergent MIS 5e fringing reefs along the southern tip of Dirk Hartog Island (Stirling, 1996) suggests that this seaway was active at that time. Like its modern analogue, currents through the passage would have been tidally driven, limiting the incursion of oceanic waters into Freycinet Reach. This would leave a northern entrance as the only viable route by which marine waters could penetrate deep into the bay. Therefore knowledge of the timing of emplacement of Bernier and Dorre Islands are critical to the understanding of ocean dynamics in Shark Bay during MIS 5e.

To assign an age to either Bernier or Dorre is difficult as there has been little detailed study of the stratigraphy or lithology apart from what appears in the Geological Survey of Western Australia 1:250,000 geological series (SG49-4 and SG49-8, 1983) (Hocking *et al.*, 1987). As yet no last interglacial marine deposits have been identified from either of these islands. This might suggest the islands were formed post MIS 5e or simply that emergent reef deposits have been completely eroded by modern marine processes.

The question as to whether these Islands existed during the last interglacial is therefore difficult to answer. However, the current correlation of stratigraphic units on Bernier and Dorre Islands to those on Edel Land and Dirk Hartog Islands suggests that they were distinct barrier features during the last interglacial. If this is so how might have oceanic water penetrated deep within Shark Bay's embayments during MIS 5e?

C.7.3 Coastal Physiography

If the western northern reaches of Shark Bay were in fact barred, then an increase in oceanic circulation within the bay may have been facilitated by a modified coastal physiography. Where MIS 5e marine units and shoreline deposits do outcrop it is usually proximal to the modern shoreline (**Fig. 1b; Fig. 2**). This indicates that at least in these locations there was minimal dune migration or desert expansion during the intervening glacial, which allowed the modern shoreline to return to a similar position as the MIS 5e shoreline

At the northern end of Tallifer Isthmus, an evaporite basin connects L'Haridon Bight and Freycinet Harbour and may have been breached during the early Holocene. This was the site for a seaway between L'Haridon Bight and Freycinet Harbour during the last interglacial (Donald, 2003) and is potentially analogous to present day South Passage or Herald Loop (**Fig. 4**). This narrow seaway would not have facilitated through-flow, as seawater exchange between the two marine basins would have been dominated by the flood- and ebb-tides as is evident in

the present South Passage and Herald Loop. It would appear that the general coastal configuration of Shark Bay during MIS 5e is comparable to the modern shoreline and as such did not contribute to enhanced marine circulation during MIS 5e.

C.8 PLEISTOCENE CORALS VERSES HOLOCENE STROMATOLITES

C.8.1 Holocene sea levels and the marine development of Shark Bay

A series of Holocene coquina beach ridges composed exclusively of the halotolerent mollusc species, *Fragum erugatum* are found along the southern margin of Hamlin Pool (Playford, 1990), with the oldest ridge returning an age of 5500 YBP (Nott, 2006). This would suggest Hamlin Pool reached meta/hypersaline levels not long after the initial +2 m early-Holocene sea-level highstand event, which in Western Australia occurred around 7 ka (Collins *et al.*, 2006) (**Fig. 5**). For such a rapid transition from oceanic to hypersaline conditions, it is likely a relict Pleistocene high (proto-Faure Sill), with its surface projections manifest in Faure and Pelican Islands, presented an initial barrier for seawater exchange between Hamlin Pool and Hopeless Reach (**Fig. 4**). Tidal flow across this barrier facilitated ooid precipitation, with vertical bank accretion reducing sill depth to its current 2 m, while the basin itself has an average depth of 4 m. This bathymetric configuration combined with a gradual late Holocene sea-level regression (Collins *et al.*, 2006) further restricted oceanic circulation where by 1250 YBP stromatolites had become firmly established (Chivas *et al.*, 1990) and contemporary salinities now reach 60-70‰ (**Fig. 5**).

Reduced marine circulation may also be aided by the lack or carbonate transport onshore, a consequence of shallow sand banks, extensive seagrass habitats and limited fetch, all of which reduce the ability of waves and currents to mobilise sediments. As a result carbonate deposition has been confined exclusively to the bays and reaches, filling available

accommodation space, reducing oceanic circulation and raising salinities. Given the present extent of the bank and shoal features and the fact that sea-level has only reached its present position within the last 7 ka (Collins *et al.*, 2006), continual filling and further oceanic restriction within Shark Bay is expected.

Whilst Hamlin Pool might be considered the near end product of carbonate infilling Freycinet Harbour might be considered as an intermediate stage. Its northern Fork Flat Sill has an average depth of 5 m, the bay itself has an average depth of 10 m. This bathymetric configuration has resulted in a metahaline (46-48‰) environment. While Freycinet still supports extensive seagrass habitats and other carbonate producing communities, both coral and stromatolite communities are absent. We therefore observe that with a more porous sill and deeper basin, as in Freycinet Harbour, circulation is increased and the potential for hypersalinity is diminished. The question then arises, if carbonate production was and is such an active process during the most recent sea level highstand, and assuming similar processes operated during previous interglacial highstands, why then are habitats once occupied by a diverse coral fauna now the exclusive domain of stomatolites?

C.8.2 MIS 5e sea levels and the marine development of Shark Bay

The rapid onset of hypersaline conditions in Hamlin Pool during the Holocene is in marked contrast to the MIS 5e marine environment, which shows periods of coral growth between 129 and 124 ka and another around 122 ka (**Fig. 3**). The primary difference between these two highstand events is in their respective sea level histories. Sea levels during the early stages of MIS 5e were at least 3 m higher than they are today, as is evidenced from emergent fossil reef terraces in Shark Bay and other MIS 5e sites (Hearty and Neumann 2001, McCulloch and Esat, 2000). This would mean, assuming an average embayment depth of 10 m, that there was 30% more accommodation space available during MIS 5e, allowing for enhanced marine

circulation (such as we observe in modern day Freycinet Harbour), also increasing the time required to infill the embayment and hence ultimately restrict oceanic circulation (**Fig. 4**).

Coral growth increased during the early and middle stages of MIS 5e and up to about 125 ka, before apparently abruptly halting at around 124 ka (**Fig 3**). The cause of this reduction in coral reef development could be twofold. By 124 ka, carbonate sedimentation within the bays and reaches may have been sufficient to restricted marine circulation thereby increasing salinities, as is the current situation in Hamlin Pool. However, coral development along the oceanic sections of the bay also seems to show a similar pattern, suggesting that it is not controlled by local features and does not appear to be an artefact from a sampling bias. The other possibility is a regression in sea level caused by a brief but complete halt to coral development within the bay. Several sea-level curves for the last interglacial including, Hearty and Neumann (2001) and Sherman *et al.* (1993), point to a brief regression in sea-level during mid 5e (**Fig. 5**), this could be correlated with the apparent age gap with the number of dated corals at 125 ka decreasing from six to nil at 124 ka.

Sea level is believed to have recovered from the mid-MIS 5e regression by 123 ka to an elevation of +3 to +4 m above current MSL (Hearty *et al.*, in review). This event saw a reestablishment of coral grow at sites deep within Shark Bay's embayments, including Pelican Island and Baba Head. The termination of MIS 5e was marked by a brief but rapid excursion to +6 to +9 m with an apparent rapid decent to MIS 5d at around 118 ka. The youngest Shark Bay coral is dated to 119 ka.

It would appear that the marine environments of Shark Bay have been strongly influenced by even relatively small changes in sea level. We observe that minor shifts in sea-level elevation can strongly affecting the hydrodynamics of the bay, more so where embayments are deep and water depths shallow. Fluctuations in highstand sea levels can have a major affect on

salinity gradients, which in turn control the distribution type and extent of carbonate producing habitats.

C.9 CONCLUSIONS

1. U-series dating of emergent fossil reefs point to an extended period of coral reef development within Shark Bay during the peak of the last interglacial - MIS 5e. There is little evidence of fossil reef development during the Middle/Upper Pleistocene (MIS 9 to 11). This then places most of the fossil reefs previously assigned to the Dampier Formation (Middle Pleistocene) such as those at Tetrodon Loop and Monkey Mia into the Bibra Formation - MIS 5e. Therefore the occurrence of an emergent coral reef within Shark Bay can be positively correlated to MIS 5e and be used as a chronostratigraphic benchmark. The extensively calcretized beach and dune ridges exposed along the coastal parts of Shark Bay also support evidence for Middle Pleistocene sea-level transgressions into Shark Bay.

2. Most of the major morphological features currently observed in Shark Bay were also prominent features during MIS 5e. This is based on the older ages of both the Peron sand complex and eolianites which form the major geomorphic features of Shark Bay, as well as the proximity of MIS 5e shorelines to those of present Holocene shorelines. The most recent features in Shark Bay have been bathymetric, and include the formation of Faure and Fork Flat sills, the latter being due to extensive carbonate sedimentation during the Holocene.

3. Coral reef development was widespread in MIS 5e Shark Bay compared to Modern Shark Bay. This can be attributed to higher sea levels and absence of major sill and bank structures that increase water depth, thereby enhancing marine circulation within the reaches and basins. Stromatolites are absent from the earlier geological record within Shark Bay; suggesting that the marine sedimentary processes that have operated over the precent Holocene sea-level highstand were unique in filling available accommodation space and thus reducing oceanic circulation and causing hypersaline conditions within upper embayments of Shark Bay, whereas during MIS 5e the persistence of higher sea levels resulted in the embayments having more open marine conditions.

C.9 REFERENCES

Andersen, M.B., Stirling, C.H., Potter, E.K., Halliday, A.N., 2004, Toward epsilon levels of measurement precision on 234U/238U by using MC-ICPMS: International Journal of Mass Spectrometry v. 237 (2-3), p. 107-118.

Bard, E., Fairbanks, R.G., Hamelin, B., Zindler, A., Huong, C.T., 1991, ^{234}U anomalies in corals older than 150,000 years, Geochimica et Cosmochimica Acta v. 55, 2385-2390.

Bernal, J.P., McCulloch, M.T., Mortimer, G.E., Esat, T., 2002, Strategies for the determination of the isotopic composition of natural Uranium, Geochemica et Cosmochemica Acta v. 66 (15A), p. A72-A72.

Bricker, O.P., 1971, Introduction: beachrock and intertidal cement, *in* Bricker, O.P. (Ed.), Carbonate Cements: John Hopkins Press, Baltimore, MD, p. 1-3.

Burling, M.C., Ivey, G.N., Pattiaratchi, C.B., 1999, Convectively driven exchange in a shallow coastal embayment: Continental Shelf Research 19, p. 1599-1616.

Chen, J.H., Curran, H.A., White, B., Wasserburg, G.J., 1991, Precise chronology of the Last Interglacial period: $^{234}U^{230}Th$ data from fossil coral reefs in the Bahamas, Geological Society of America Bulletin v. 103, p. 82-97.

Chivas, A.R., Torgersen, T., Polach, H.A., 1990, Growth rates and Holocene development of stromatolites from Shark Bay, Western Australia: Australian Journal of Earth Science v. 37, p. 113-121.

Donald, A., 2003, Marine and continental sediment flux in Shark Bay, Western Australia: Thesis (B.Sc. Hons) - James Cook University.

Hamelin, B., Bard, E., Zindler, A., Fairbanks, R.G., 1991, $^{234}U/^{238}U$ mass spectrometry of corals: How accurate is the U-Th age of the last interglacial period? Earth and Planetary Science Letters v. 106, p. 169-181.

Hatcher, B.G., 1991, Coral reefs in the Leeuwin Current – an ecological perspective: Journal of the Royal Society of Western Australia, v. 74, p. 115-127.

Hearty, P.J., Kaufman, D.S., 2000, Whole-rock aminostratigraphy and Quaternary sea-level history of the Bahamas: Quaternary Research, v 54, p. 163-173.

Hearty, P.J., Neumann, A.C., 2001, Rapid sea level and climate change at the close of the Last Interglaciation (MIS 5e): evidence from The Bahama Islands: Quaternary Science Reviews, v. 20, p. 1881-1895.

Hearty, P.J., Neumann, A.C., Hollin, J.T., O'Leary M.J., McCulloch M.T., in review, Sea level oscillations during the last interglaciation (sensu stricto MIS 5e): Quaternary Science Reviews.

Henderson, G.M., 2002, Seawater $^{234}U/^{238}U$ during the last 800 thousand years, Earth and Planetary Science Letters v. 199, p. 97-11.

Hocking, R.M., Moors, H.T., Van De Graff, W.J.E., 1987, Geology of the Carnarvon Basin of Western Australia: Geological Survey of Western Australia Bulletin, v. 133.

Kendrick, G.A., Huisman, J.M., Walker, D.I., 1990, Benthic Macroalgae of Shark Bay, Western Australia: Botanica Marina v. 33, p. 47-54.

Logan, B.W., Cebulski, D.E., 1970, Sedimentary environments of Shark Bay, Western Australia: The American Association of Petroleum Geologists, Memoir No. 13, p. 1-37.

Logan, B.W., Read, J.R., Davies, G.R., 1970, History of carbonate sedimentation, Quaternary Epoch, Shark Bay, Western Australia: American Association of Petroleum Geologists Memoir No. 13, p. 38-85.

Marsh, L.M., 1990, Hermatypic corals of Shark Bay, Western Australia, in: Berry, P.F., Bradshaw, S.D. & Wilson, B.R. (Eds.), Research in Shark Bay. Report of the France-Australe Bicentenary Expedition Committee: Western Australian Museum, Perth, p. 107-114.

McCulloch, M.T., Esat T., 2000, The coral record of last interglacial sea levels and sea surface temperatures, Chemical Geology v. 169, p. 107-129.

Nott, J., 2006, Tropical cyclones and the evolution of the sedimentary coast of northern Australia, Journal of Coastal research, v. 22 (1) p, 49-62.

Playford, P.E., Cockbain, A.E., Low, G.H., 1976, Geology of the Perth Basin, Western Australia: Bulletin Geological Survey of Western Australia, v. 124, p. 298.

Playford, P.E., 1990. Geology of the Shark Bay area, Western Australia, in: Berry, P.F., Bradshaw, S.D. & Wilson, B.R. (Eds.), Research in Shark Bay, Report of the France-Australe Bicentenary Expedition Committee: Western Australian Museum, Perth, p. 13-31.

Potter, E.K., Stirling, C.H., Andersen, M.B., Halliday, A.N., 2005, High precision Faraday collector MC-ICPMS thorium isotope ratio determination: International Journal of Mass Spectrometry v. 247 (1-3), p. 10-17.

Read, J.F., 1974, Calcrete deposits and Quaternary sediments, Edel Province, Shark Bay, Western Australia: American Association of Petroleum Geologists Memoirs No. 22, p. 250-282.

Robinson, L.F., Belshaw, N. S., Henderson G.M., 2004, U and Th concentrations and isotope ratios in modern carbonates and waters from the Bahamas, Geochimica et Cosmochimica Acta v. 68, p. 1777–1789.

Stirling, C.H., Esat, T.M., McCulloch, M.T., Lambeck, K., 1995, High-precision U-series dating of corals from Western Australia and implications for the timing and duration of the Last Interglacial: Earth and Planetary Science Letters 135, 115-130.

Stirling, C.H., 1996. High-precision U-series dating of corals from Western Australia: implications for Last Interglacial sea levels: Thesis (Ph.D.) – Australian National University.

Stirling, C.H., Esat, T.M., Lambeck, K., McCulloch, M.T., 1998, Timing and duration of the Last Interglacial: evidence for a restricted interval of widespread coral reef growth, Earth and Planetary Science Letters v. 160, p. 745-762.

Stirling, C.H., Esat, T.M., Lambeck, K., McCulloch, M.T., Blake, S.G., Lee D.C., Halliday, A.N., 2001, Orbital forcing of the marine isotope stage 9 interglacial, Science v. 291 (5502), p. 290-293.

Stirling, C.H., Halliday A.N., Porcell, D., 2005, In search of live Cm-247 in the early solar system: Geochimica et Cosmochimica Acta v. 69 (4), p. 1059-1071.

Thompson, W.G., Spiegelmann M.W., Goldstein S.L., Speed R.C., 2003, An open-system model for U-series age determinations of fossil corals, Earth Planetary Science Letters, v. 210, p. 365-38.

Walker, D.I., 1991, The effect of sea temperature on seagrasses and algae on the Western Australian coastline: Journal of the Royal Society of Western Australia v. 74, p. 71-77.

Walker, D.I., Woelkerling, Wm.J., 1988, Quantitative study of sediment contribution by epiphytic coralline red algae in seagrass meadows in Shark Bay, Western Australia: Marine Ecology-Progress Series v. 43, p. 71-77.

C.10 FIGURES 1-5

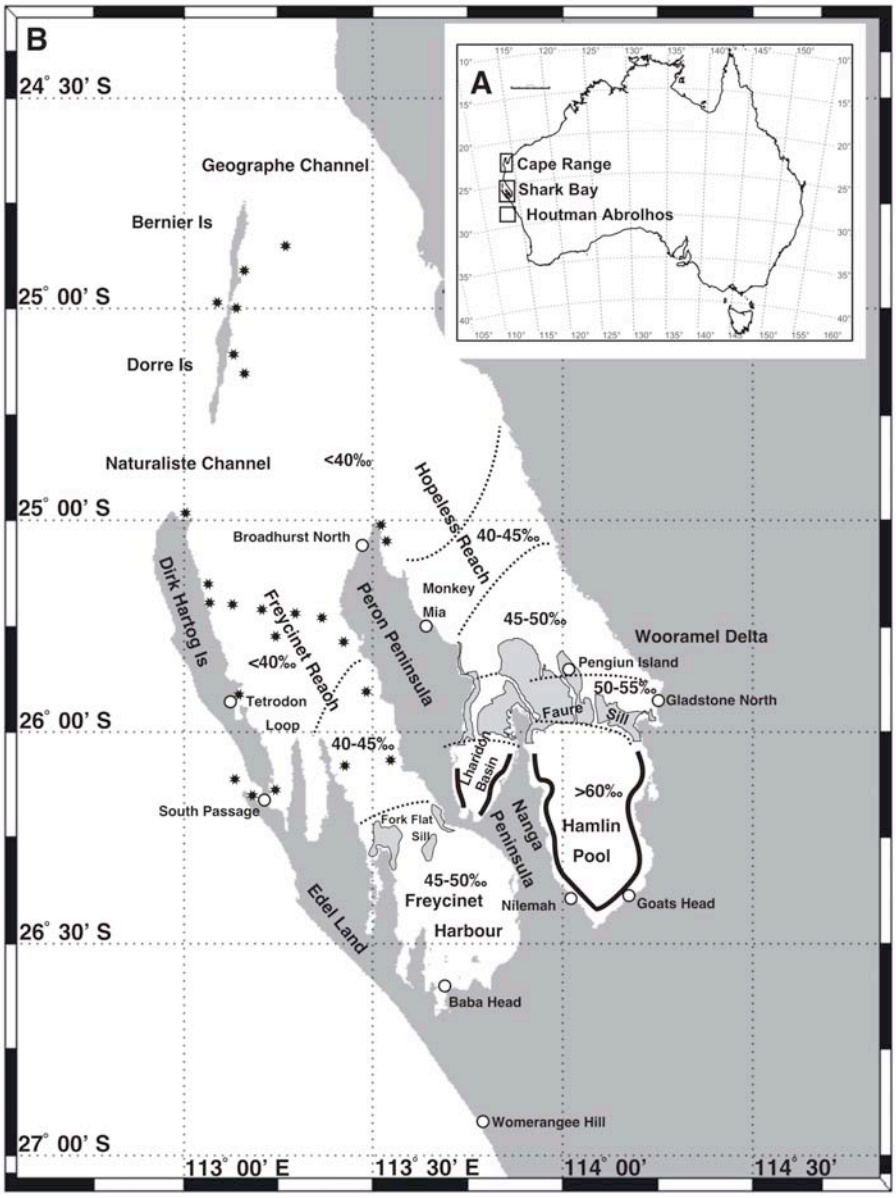

Figure 1: A) Map of Australia showing location of three principal reef growing regions along the West Australian coast including; Ningaloo Reef (Cape Range) 21˚- 23˚ S, Shark Bay (study location), 25.5 - 26.5˚ S and the Houtman Abrolhos (island group) 28˚ S. B) Location Map of Shark Bay. Salinity contours for in parts per thousand (ppt). Thick black lines represent areas of extensive stromatolite growth and black stars indicate presence of living corals (modified from Marsh 1990)

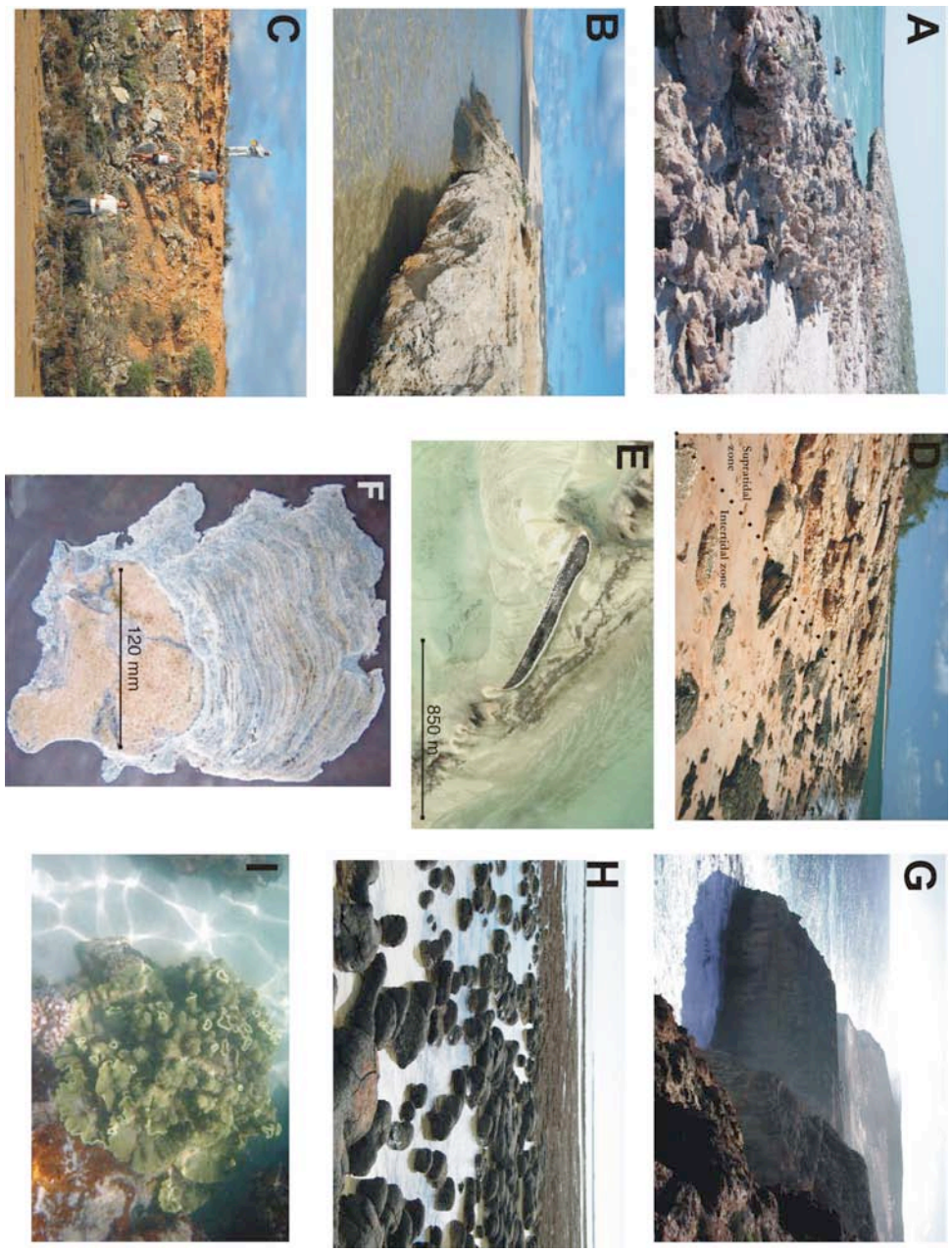

Figure 2: A) Baba Head, B) Tetrodon Loop, C) Monkey Mia, D) Gladstone North E) Satellite image of the 850 m long Pelican Island, F) Photo of sample SHP1, a living stromatolite from Nilemah, Hamlin Pool, impregnated with resin before sectioning, coral is approximately 15 cm wide, G) Zuytdorp sea cliffs looking north H) stromatolite community at Goat Point. H) Coral community at Broadhurst Bay.

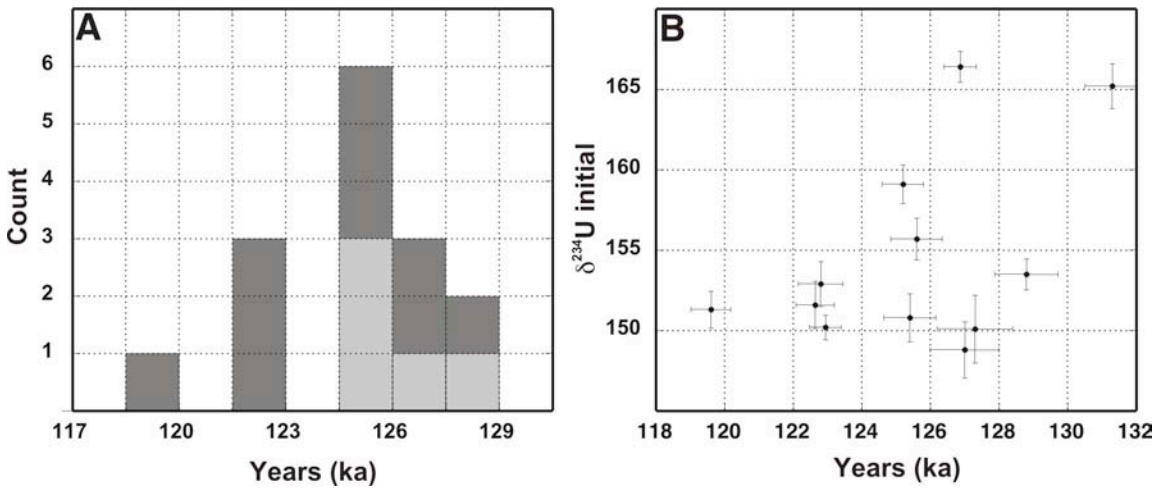

Figure 3: A) U-series coral ages for Shark Bay. The additional coral ages for Shark Bay (in grey) were excerpted from Stirling *et al.* (1995) figure 4a. B) Initial ^{234}U values verses ^{230}Th age, reliable U-series ages should fall within the 146.6 ± 10‰ initial $\delta^{234}U$ range, acceptable for reliable U-series age measurements.

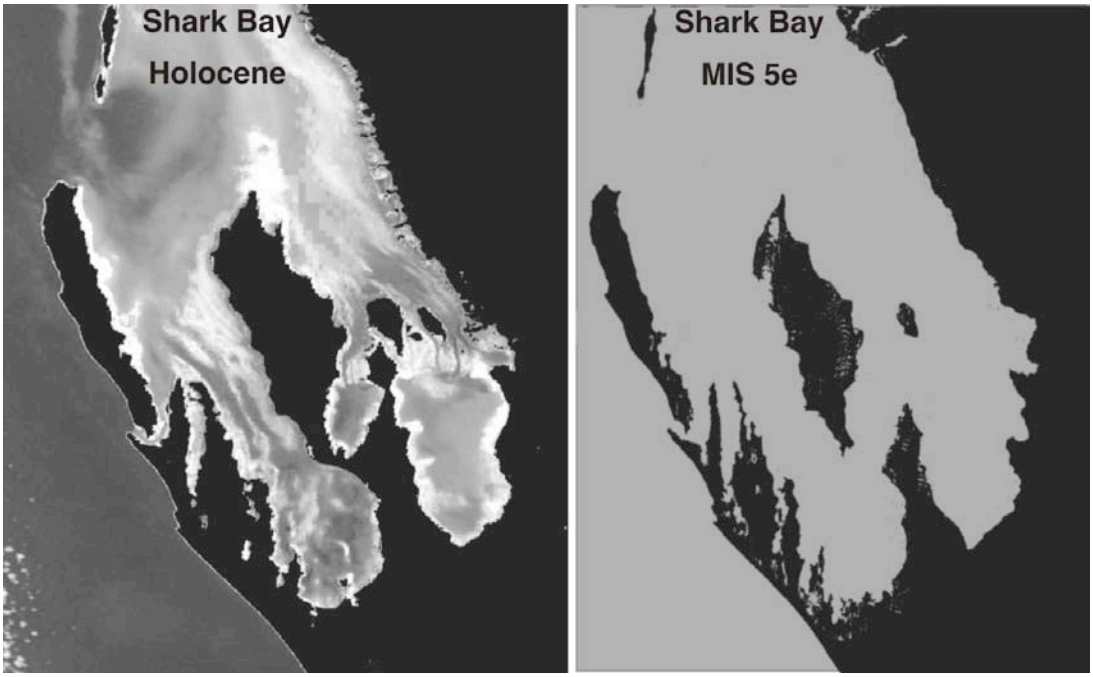

Figure 4: A) Present Shark Bay shoreline, lighter areas represent shallow bank or sill structures. B) A representation of Shark Bay shoreline during early MIS 5e. The position of the MIS 5e shoreline is based on the location of MIS 5e marine outcrops and current low-lying areas below +2 m MSL, basin depth is unknown.

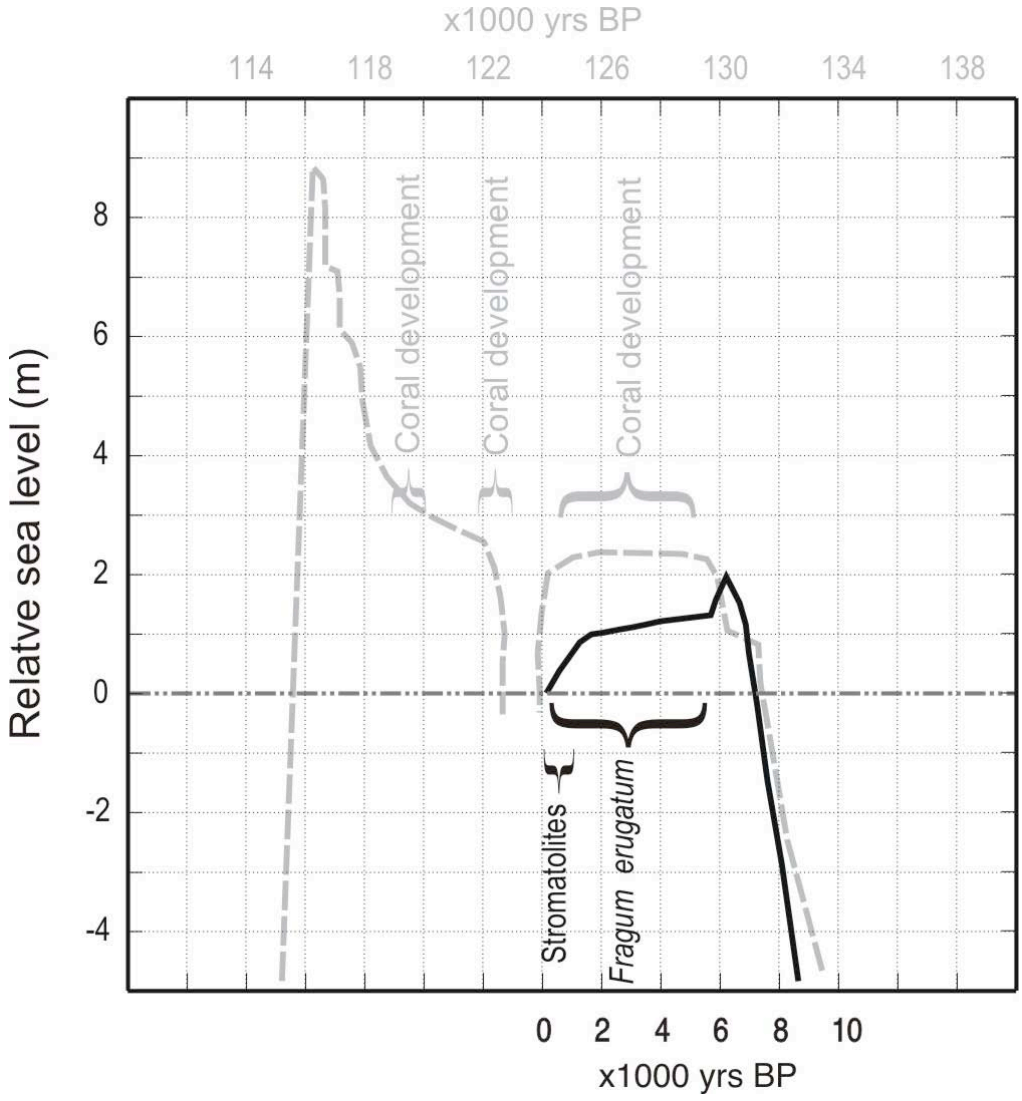

Figure 5: Sea level curves for Shark Bay and respective timing of both coral and stromatolite development. MIS 5e curve was excerpted from Hearty *et al.* (in review) and the Holocene sea level curve was excerpted from Collins *et al.* (2006) figure 5.

Table 1: Stratigraphic nomenclature for Shark Bay.

Period/Epoch	Teichert 1950	Playford 1990	Logan *et al.*, 1970	MIS
Holocene	Coastal Limestone	Tamala Limestone	Holocene-Recent	MIS 1
Last Glacial Cycle			Nilmah Sands Depuch Formation	MIS 2-4
Upper Pleistocene			Bibra formation Marine deposits	MIS 5a-5e
Middle Pleistocene			Dampier formation Carbla oolite	MIS 11
Lower Pleistocene			Tamala Eolianite	MIS 11 > 37
Upper Pliocene			Peron Sandstone	
		Trealla Calcarenite		

Table 2: U-series data

Sample[1]	U ppm[2]	^{230}Th ppt[3]	^{232}Th ppb[4]	δ ^{234}U[5]	^{234}U error	^{230}Th/ ^{238}U[6]	error	[^{230}Th/ ^{232}Th]	Age (ka)[7]	Age error	Initial δ ^{234}U[8]	δ ^{234}U error	Location
SBA1_c	2.81	34.79	x	107.07	1.10	0.76	0.002	3427.4	122.64	0.56	151.59	1.47	Baba Head
STG5_c	2.88	35.94	0.46	103.81	1.30	0.77	0.003	14766.3	127.00	1.00	148.80	1.75	Tetrodon L
STG1_c	2.46	31.09	0.08	106.57	0.66	0.78	0.003	72614.3	128.80	0.92	153.50	0.96	Tetrodon L
STG4_c	1.99	24.70	0.12	105.73	1.14	0.77	0.002	39536.2	125.40	0.76	150.80	1.50	Tetrodon L
SPI4_a	7.64	16.33	390.42	149.16	1.10	0.13	0.001	7.9	13.23	0.09	154.90	1.10	Pelican Is
SPI4_c	2.92	35.93	0.28	107.96	1.05	0.76	0.002	23948.4	122.80	0.65	152.90	1.40	Pelican Is
SPI5_c	2.36	28.64	0.59	107.80	0.88	0.75	0.002	9176.7	119.60	0.58	151.30	1.15	Pelican Is
SWO1_c	2.76	35.47	0.07	113.75	1.05	0.79	0.002	90677.5	131.30	0.79	165.20	1.40	Gladstone N
SWR1_c	4.56	77.11	145.30	80.99	0.61	1.05	0.003	99.5	313.00	5.60	196.80	3.05	Gladstone N
SGN1_c	2.22	47.64	261.43	197.30	2.10	1.32	0.008	34.2	127.30	1.10	150.10	2.10	Gladstone N
SGN3_c	3.25	41.08	0.41	116.18	0.72	0.78	0.001	18740.2	126.87	0.47	166.40	0.96	Gladstone N
SMM2_c	2.28	28.43	1.00	109.06	0.97	0.77	0.002	5347.0	125.60	0.75	155.70	1.30	Monkey Mia
SMM1_c	2.77	34.65	0.23	111.61	0.90	0.77	0.002	27790.8	125.20	0.60	159.10	1.20	Monkey Mia
SMM4_c	3.79	46.69	144.53	106.04	0.57	0.76	0.002	60.6	122.94	0.46	150.20	0.76	Monkey Mia
SWG1_f	0.37	3.86	1.67	64.61	1.83	0.65	0.003	432.6	100.80	0.76	86.00	2.30	Womerangee
SHP1_c	3.20	53.36	0.38	85.23	1.61	1.02	0.004	26013.2	283.00	5.35	190	3.5	Nilemah
SHP1_s	2.63	2.66	257.64	146.87	1.45	0.06	0.001	1.9	6.09	0.071	149.4	1.4	Nilemah

Notes to Table 2.

[1] Uranium concentrations are measured in parts per million (ppm).

[2] ^{230}Th concentrations measured in parts per trillion (ppt).

[3] ^{232}Th concentrations measured in parts per billion (ppb).

[4] $\delta^{234}U = \{[(^{234}U/^{238}U)/(^{234}U/^{238}U)_{eq}]-1\} \times 10^3$. $(^{234}U/^{238}U)_{eq}$ is the atomic ratio at secular equilibrium and is equal to $\lambda_{238}/\lambda_{234} = 5.4891 \times 10^{-5}$, , where λ_{238} and λ_{234} are the decay constants for ^{238}U and ^{234}U, respectively, adopting half-lives of Cheng *et al*., (1998)

[5] $[^{230}Th/^{238}U]_{act} = (^{230}Th/^{238}U)/(\lambda_{238}/\lambda_{230})$.

[6] U-series ages are calculated iteratively using:

1- $[^{230}Th/^{238}U]_{act} = \exp^{-\lambda_{230}T} - (\delta^{234}U(0)/1000)(\lambda_{230}/(\lambda_{230}-\lambda_{234}))(1-\exp(^{\lambda_{234}-\lambda_{230}T})$ where T is the age in years and λ_{230} is the decay constant for ^{230}Th. $\lambda_{238} = 1.551 \times 10^{-10}$ y^{-1}; $\lambda_{234} = 2.826 \times 10^{-6}$ y^{-1}; $\lambda_{230} = 9.158 \times 10^{-6}$ y^{-1}. Strictly reliable ages will have $^{234}U_{initial}$ 146.6 ± 5‰

[7] The initial value is given by $\delta^{234}U_i = \delta^{234}U(0)\exp(\lambda_{234}T)$, where T is the age in years.

SECTION D

Uranium-series dating of crustose coralline algae (Corallinaceae)

D.1 ABSTRACT

To investigate the geochemical evolution of CCA, 24 samples were analysed from a suite of coral reefs encompassing modern to marine isotope stage (MIS) 11 interglacials. Age control was provided by 21 U-series coral ages collected from the same fossil reefs.We find that living CCA record a $\delta^{234}U$ value of 147.02 ± 1.5‰, which is consistent with modern seawater values. Therefore it is possible to examine the isotope systematics of uranium and thorium over geological timescales and assess their potential utility for U-series dating. CCA underwent a three-fold increase in uranium concentration from 0.2 ± 0.07 ppm in living samples to 0.72 ± 0.15 ppm in MIS 5e samples. This additional uranium increases the $^{234}U/^{238}U$ atomic ratio, and reduces the $^{230}Th/^{238}U$ atomic ratio, resulting in higher initial $\delta^{234}U$ ratios, and younger overall ages when compared to similar age corals. Additionally, a several order-of-magnitude increase in detrital ^{232}Th in fossil CCA suggests that $^{230}Th_{nr}$ (non-radiogenic) may also be incorporated along with uranium. Due to the low initial concentrations of uranium in living CCA even a small addition of $^{230}Th_{nr}$ can result in large age errors. Uptake of ^{234}U-enriched uranium is responsible for the majority of observed age errors in CCA, and preludes it from accurate U-series dating. Although the source of excess ^{234}U has yet to be accurately determined, diagenetically altered Middle Pleistocene corals, were found to be depleted in ^{234}U and may contribute excess ^{234}U to the system.

D.2 INTRODUCTION

A reliable chronology, combined with accurate geological interpretation, is vital to both understand and reconstruct paleoclimate events. The ^{238}U-^{234}U-^{230}Th decay series (U-series) is the principal method for absolute dating of carbonate material beyond the range of ^{14}C (>50 ka) and up to 500 ka. The U-series dating method has been applied to corals due to their relatively high uranium concentrations, negligible initial thorium concentrations, and the incorporation of isotopic ratios in equilibrium with the seawater in which they grew. Coral ages are calculated from the radioactive decay and in-growth relationships among ^{238}U, ^{234}U and ^{230}Th. Assuming that the coral has remained closed to chemical exchange, it is possible to produce reliable and accurate absolute ages. However, fossil corals >20 ka are susceptible to calcite diagenesis or secondary aragonite precipitation, and it is now accepted that corals do not always operate as a closed system (Bard *et al.*, 1991; Hamilin *et al.*, 1991; Thompson *et al.*, 2003). Coral is additionally disadvantaged due to its geographic restriction to shallow-water, pan-tropical regions, and a growth interval limited to relatively short and warm interglacial periods. Also, lowstand subaerial exposure of the corals will cause significant diagenetic alteration.

In an effort to fill the temporal and spatial limitations, several attempts have been made to date other carbonate materials including; deep-sea corals (Slowey *et al.*, 1996), slope sediments (Henderson *et al.*, 2001), mollusks (Kaufman, 1971 and Kaufman *et al.*, 1996), and planktonic foraminifera (Henderson and O'Nions, 1995). Each of these dating materials is subject to a particular set of limitations. Deep-sea corals and slope sediments often contain high values of non-radiogenic $^{230}Th_{nr}$ (i.e. ^{230}Th not generated by in situ uranium decay), resulting from thorium adsorption from seawater or the surrounding sediments (Edwards *et al.*, 2003). Mollusks and planktonic foraminifera have uranium concentrations an order of magnitude lower than corals making them more difficult to date, they are also susceptible to post mortality uptake of uranium (Kaufman

et al., 1971). Until now, the potential use of crustose coralline algae (CCA) in U-series dating had not been investigated in any detail.

CCA are potentially excellent biomarkers as they provide relatively accurate information on paleo-sea level and paleoenvironmental change (Cabioch *et al.*, 1999). They are one of the dominant autotrophs in tropical and subtropical reef environments (Payri, 1997; Payri *et al.*, 2004) and like corals, the growth form and framework structure of CCA are directly related to the local hydrodynamic setting in which they grew (Gherardi and Bocense, 2001). Certain coralline associations (e.g., thick crusts of *Hyrolithon onkoides* or *Neogoniolithon*) can provide very precise sea-level information in shallow <5 m waters (Cabioch et al., 1999). CCA also inhabit a greater latitudinal range compared to that of corals (Kennedy and Woodroffe 2002).

Unlike aragonitic corals, CCA precipitate a high-magnesium calcite (HMC) skeleton (Goldsmith *et al.*, 1955, Millman *et al.*, 1971 and Kolesar, 1978). HMC is metastable and more susceptible to post mortality leaching and dissolution compared to aragonite (Bathurst, 1975). This potentially makes CCA more prone to chemical exchange and thus less suitable for U-series dating compared to corals.

This study has three distinct goals: 1). Establish the U-series systematics for modern CCA;2). Examine the geochemical evolution of CCA over successive interglacial periods and3). Determine the reliability and accuracy of CCA U-series age dates.

D.3 MATERIAL AND METHODS

D.3.1 Sample collection

Samples were collected from modern and succeeding emergent interglacial reefs across the Indo-Pacific (**Fig. 1**). Care was taken to collect in situ fossil samples from reef

crest biozones to insure that the samples grew in shallow water, high-energy paleoenvironments and at least originate from the taxonomic family, Corallinaceae.

The Australian Institute of Marine Science (AIMS) collected living CCA from windward reef crests of Myrmidon Reef (MYR), John Brewer Reef (JBR) and Yange Reef (NYR), central Great Barrier Reef, in water depths < 5 metres. Sub-modern CCA, encrusting branching coral rubble, was collected from storm ridge deposits at Point Quobba, Western Australia and North Beach, Henderson Island.

MIS 5e corals and CCA were collected from an emergent fossil reef complex at Cape Cuvier (LCC), Western Australia. Samples were collected stratigraphically from a 3 m high modern sea-cliff cut into a lower emergent fossil reef using a rock drill. Samples from an upper incipient coralgal reef were collected using a cold chisel and hammer.

A coral of the genus *Galaxia* exposed within a shallow wave cut notch at +21 m above sea level on "North Beach" Henderson Island, has a thick encrustation of CCA and was drilled to sample both the coral and the CCA. This outcrop was previously sampled by Pandolfi (1995) and dated to MIS 9 by Stirling *et al.* (2001).

Coral and CCA was collected from an emergent +7 to +9 m Middle Pleistocene reef (Jurabi Terrace), exposed along the seaward flank of Cape Range, Western Australia. CCA samples were collected from an emergent predominantly algal reef at Pilgonaman Gorge, Cape Range. An additional six corals were drilled across a section of reef at Tantabiddi Creek.

D.3.2 Sample preparation and analytical techniques

D.3.2.1 Mechanical cleaning

CCA >10 mm thick and showing no visual signs of detrital contamination were selected for pre-cleaning. The encrusting CCA was easily separated from the coral

fragment. Using a diamond drill, the outermost surfaces of the CCA were removed and samples were sliced into smaller fragments. Due to its low uranium concentration, a larger bulk sample of 500 mg was required for CCA, compared to 200 mg for corals. Samples were sonicated for several hours to remove foreign material adhering to the surface.

D.3.2.2 Column chemistry

Samples were progressively dissolved in distilled water by step addition of 10M HNO_3; any remaining solid organic material was removed dried and weighed. The dissolved samples were then spiked with a 50 mg 'U-2' $^{233}Th/^{235}U$ isotope solution and evaporated to a minimum solution. A few drops of H_2O_2 were added to oxidise any remaining organic material. Samples were redissolved in 3 ml of 2M HNO_3, then transferred to bio-spin ®Tru.spec columns for separation of uranium and thorium isotopes. A 0.1 normal solution of HF/HCl was then passed though the columns to collect and concentrate uranium and thorium. The solution was evaporated to dryness then redissolved with 2 ml 2% HNO_3 prior to injection.

D.3.2.3 $^{234}U/^{238}U$ and $^{230}Th/^{238}U$ measurements

U-series measurements were performed using a Neptune MC-ICPMS at the Research School of Earth Sciences, Australian National University. Measurements were conducted using a combination of simultaneous multiple-Faraday cup and ion counter protocols based on those previously described for TIMS (Stirling et al., 1998 and McCulloch and Esat 2000). The main difference being that ion counting/faraday gains where determined by reference to an external standard (SRM 960) for determination of $^{234}U/^{235}U$ ratios where ^{234}U is measured using ion counting. For the low abundance isotopes ^{230}Th and ^{229}Th (spike) these where both measured using the central ion counter,

but simultaneously with ^{235}U and ^{238}U and ^{232}Th on faraday cups allowing corrections for both beam instability as well as mass bias. For detailed protocols see McCulloch and Mortimer (in prep). This multiple-Faraday approach yield higher precision in conjunction with a significantly reduced sample size requirement, lowering age uncertainties by up to a factor of five (Stirling et al., 2001) compared to single cup procedures.

D.4 RESULTS

Twenty-four U-series measurements of CCA from recent to MIS 11 reefs are presented in **Table 1**; a further twenty-one coral dates provided additional age control.

D.4.1 Living CCA (< 10 years)

Living CCA collected from the Great Barrier Reef (**Table 1**) returned an average $\delta^{234}U$ activity ratio of 147.02 ± 1.5‰ (n=6) (**Fig. 2**), which is slightly higher, but within the error for Bahamian seawater, which average 146.6 ± 2.5‰ (Robinson *et al.*, 2004). A living coral from the Great Barrier Reef MYR1_C returned an equivalent $\delta^{234}U$ activity ratio of 147.11‰. These values are consistent with CCA incorporating ambient seawater $\delta^{234}U$ activities.

Living CCA has an order of magnitude lower uranium concentration, averaging 0.2 ± 0.07 ppm, compared to that of living coral, (**Fig. 2**; **Fig. 3**). Sample NYR2a_A has a lower uranium concentration of 0.042 ppm, however this sample was analysed along with the organic fraction, potentially diluting the overall concentration. ^{232}Th concentrations in living CCA range between 11.4 and 115.9 ppt (parts per trillion) (**Table 1**). Living corals are also found to have similar detrital ^{232}Th concentrations (Edwards *et al.*, 1987a; 1988; Cobb *et al.*, 2003).

Living CCA returned U-series ages of 0.53 ± 0.03 ka and up to 1.83 ± 0.03 ka, which is inconsistent with their exceptionally young age (< 10 yrs) (**Fig. 4**). These elevated ages coincide with the inclusion of $^{230}Th_{nr}$, which ranges between 0.013 and 0.065 ppt. Contrary to expectations increasing ^{230}Th concentrations coincided with a decrease in U-series age, while decreasing uranium concentrations correspond to an increase in U-series age.

D.4.2 MIS 5e (116-130 ka)

CCA collected from emergent MIS 5e reefs have an average uranium concentration of 0.72 ± 0.15 ppm, 3 times higher than their modern counterparts (**Fig. 3**). Highly variable ^{232}Th concentrations ranging from 0.02 up to 66.86 ppb were also measured (**Table 1**). Extremely high ^{232}Th values were often associated with visual red staining along micro fractures within the sample or where fine sediment was observed following carbonate dissolution.

CCA collected from an emergent MIS 5e reef at Cape Cuvier return highly variable U-series ages and $\delta^{234}U_{initial}$ values compared to corals from the same reef (**Fig. 5e**). CCA U-series age range from 81.5 ± 0.45 ka to 197.9 ± 2.4 ka, while coral age ranged from 109 ± 0.8 to 149 ± 1.7 ka (**Fig. 5d**). $\delta^{234}U_{initial}$ values averaged 206 ± 43‰ for the CCA compared to 180 ± 7‰ for the corals.

Plot of measured $\delta^{234}U$ versus $^{230}Th/^{238}U$ activity clearly reveals that CCA and coral did not behave as a closed system, because data points do not plot on the seawater evolution curve (**Fig. 6**), which describes the development of activity ratios with an initial value $\delta^{234}U$ of 146.6‰ under closed system conditions. CCA open-system exchange processes resulted in a broadly linear array of isotopic anomalies that intersect the closed system evolution curve at around 90 ka. A linear array is generated when different parts

of a coral (or reef system) gained varying amounts of uranium with a fixed $\delta^{234}U$ value at the same time (Scholz et al., 2004). This isotopic trend is not repeated in the coral samples (**Fig. 6**), and is evidence of a CCA isotopic uptake history in that is distinct from that of coral.

Coral mortality events generally result in rapid colonization of CCA at the coral surface (Harrington *et al.*, 2005), consequently the age of the coral and the encrusting CCA should be roughly coeval in age. This growth relationship allowed a direct comparison of U-series age from a coral and its encrusting CCA. CCA exhibited an average overall U-series age, 18.9 ± 2.1 ka (n=3) younger than the coral that they grew. One outlier, LCCq, displayed reverse stratigraphy with an untenable CCA age, 31 ka older than the coral in which it grew. However, in all cases, CCA have higher measured $^{234}U/^{238}U$ activity ratios compared to corals (**Fig. 5e**).

D.4.3 MIS 9

MIS 9 corals and CCA were collected from Henderson Island, an emergent coral atoll in the central South Pacific. Stirling *et al.* (2001) dated corals from the northern coast of the island at 292.8 ± 5.3 ka and 333.8 ± 3.9 ka, conforming to MIS 9. U-series measurements made on a single MIS 9 coral HEN1a_C, and its surface encrusting CCA HEN1a_A, returned ages and $\delta^{234}U_{initial}$ values of 313.8 ± 8.2 and 158.9 ± 3.85‰, and 305.9 ± 4.2 ka and 178.4 ± 2.2‰ respectively (**Table 1**). Both these ages fall within the known duration of MIS 9. Again we measure a younger (8.1 ka) age and higher measured $\delta^{234}U$ values for CCA compared to the coral.

D.4.4 Middle Pleistocene (MIS 11?)

The age of the Jurabi terrace is yet to be reliably dated, however, its elevation and state of diagenesis and position (landward of a MIS 5e reef) suggest a Middle Pleistocene MIS 11 age. CCA samples were collected from an emergent predominantly algal reef at

Pilgromana Gorge, Cape Range. Of the two MIS 11 CCA samples, RMS1_A returned a U-series age of 329 ± 6.5 ka with a $\delta^{234}U_{initial}$ of 561 ± 6.1‰, while RMS2_A returned an incalculable age. A total of 6 corals were also dated from the same reef but all returned incalculable ages (**Table 1**). These incalculable ages may result from advanced diagenesis, the fact that the corals have reached a secular equilibrium age, or both. The measured age of RMS1_A is too young to correlate with a possible Middle Pleistocene MIS 11 development, but with an extremely high $\delta^{234}U_{initial}$ of 561 ± 6.1‰, its age cannot be considered reliable. The advanced state of diagenesis in these corals and CCA is not conducive to reliable or accurate U-series ages.

D.4.5 U-series stratigraphy

A total of 9 CCA and 15 coral samples were collected and dated from a 3 m high reef section at Cape Cuvier (**Fig. 5**) This provides a stratigraphic context with which to compare CCA and coral age. Corals displayed approximate coeval ages of 130.5 ± 3.0 ka (n = 10) up section despite having elevated $\delta^{234}U$ values of 181.6 to 195.1‰. The CCA age trend up section was more erratic compared to the corals with ages ranging from 81.5 ka to 140.0 ka. However, if we discard the 91.8 and 81.5 ka samples, which, despite having reliable $\delta^{234}U_{initial}$ values of 145.4‰ and 141.1‰ are much younger than the known duration of MIS 5e, the remaining samples do display some stratigraphic integrity. CCA show an increase in $^{234}U/^{238}U$ activity and a decrease in $^{230}Th/^{238}U$ activity up section (**Fig. 5b,c**). This is manifest as an age decrease of 125 ka to 110 ka up section, but does not correspond to the U-series age model defined by the corals.

D.5 DISCUSSION

D.5.1 Geochemical evolution of CCA

D.5.1.1 Initial chemistries

The $\delta^{234}U_{initial}$ isotope ratio is used to screen carbonates and test whether diagenesis has occurred since formation (Edwards *et al.*, 1987b). This approach requires that marine carbonates incorporate the same $\delta^{234}U$ value as seawater, and that seawater has a known $\delta^{234}U$ history. The latter issue has been discussed in the literature and ^{234}U has not changed significantly over the last few hundred thousand years (Gallup *et al.*, 1994; Henderson, 2002). This study shows that living CCA record a $\delta^{234}U$ value of 147.02 ± 1.5 ‰, which is slightly higher but within error of modern Bahamian seawater values of 146.6 ± 2.5 ‰. Robinson *et al.* (2004) analysed two living Bahamian red algal samples and found they also capture slightly higher seawater value of approximately 148.0‰. Because living CCA incorporate modern seawater $^{234}U/^{238}U$ activities the examination of uranium and thorium evolution over geological timescales and an assessment of their utility in U-series dating is possible.

D.5.1.2 Uranium uptake and loss

Results from this study demonstrate that CCA experience post mortality uranium uptake (**Fig 3**); living CCA have uranium concentrations of 0.2 ± 0.07 ppm, while those from MIS 5e show a three fold increase with concentrations averaging 0.72 ± 0.15 ppm. Knowledge of the timing of any uranium migration is important. If uranium uptake occurs soon after death then reliable U-series age determinations are possible, whereas if late uptake occurs, it effectively dilutes the $^{238}U/^{230}Th$ atomic ratio giving younger apparent ages and higher $\delta^{234}U_{initial}$ ratios (Thompson *et al.*, 2003). In this study, whether this uptake is early, late, linear, or specific to particular environmental conditions remains

uncertain. The principal cause of uranium uptake may be post mortality decay of the organic matrix within the CCA, creating microporosity, which in turn provides a pathway for fluid movement. These micropores potentially allow for the transport and redistribution of thorium or uranium isotopes within CCA and provide nucleation sites for secondary mineral precipitation.

The oldest dated CCA in this study, RMS1_A and RMS2_A, from the Middle Pleistocene Jurabi Terrace, Cape Range, returned an average uranium concentration 0.3 ppm lower than those observed in MIS 5e CCA. Middle Pleistocene corals from the Jurabi Terrace also exhibit a uranium loss of at least 1 ppm compared to modern corals. Both coral and CCA from the Jurabi Terrace show evidence to suggest advanced calcite alteration, including loss of microstructural definition and crystal cleavage. With a net gain of uranium in MIS 5e reef systems and with highly altered Middle Pleistocene showing a net loss, it appears that these older reef systems may be a source of excess uranium observed in MIS 5e reef systems.

D.5.2 Reliability and accuracy of CCA U-series ages

The accuracy of U/Th dating depends on carbonates incorporating seawater $^{234}U/^{238}U$ activities and subsequently being closed to uranium and thorium gain or loss (Broecker, 1963). The standard quantitative approach of testing whether carbonates have acted as an open or closed system is to compare their back-calculated $\delta^{234}U_{initial}$ with modern seawater $\delta^{234}U_{initial}$. If the two values do not correspond then the sample is likely to have undergone some chemical exchange. Several empirical approaches such as petrologic and XRD evidence of diagenetic alteration, changes in uranium concentrations or addition of detrital ^{232}Th also confirm open system behavior within carbonates. A combination of these criteria was used to test for open system behavior in CCA.

D.5.2.1 Living CCA and U-series age anomalies

In general the incorporation of $^{230}Th_{nr}$ will increase the age of very young carbonates samples because radiogenic ^{230}Th ingrowth is an isotopically minor component. This age error can be corrected by measuring the ^{232}Th concentration against an initial $^{232}Th/^{230}Th$ background activity (Cobb *et al.*, 2003). However, in living CCA, where uranium concentrations are an order of magnitude lower than corals, this age error is amplified. The incorporation of $^{230}Th_{nr}$ into living CCA results in elevated measured ages of between 0.59 and 1.83 ka, this error is much greater than that observed in corals (see Cobb *et al.* 2003 for a comparison).

It is expected that higher concentrations of $^{230}Th_{nr}$ should lead to older measured ages, but for living CCA the opposite it true. It appears that the youngest ages correspond with the highest uranium concentrations. The concentration of uranium is a major controlling factor in age determination of very young CCA (**Fig. 4**). When uranium concentrations are low (> 0.2 ppm) as they are in living CCA, even a small (> 0.1 ppm) gain or loss of uranium can effectively half or double the concentration. This will have a dramatic effect on the $^{230}Th/^{238}U$ atomic ratio and the overall age measurement. This demonstrates the inherent difficulties in determining age for very young carbonate material, particularly where uranium concentrations are below 0.5 ppm

D.5.2.2 Affect of uranium and thorium uptake on a MIS 5e reef system

The addition of ^{234}U-enriched uranium will increase $^{234}U/^{238}U$ activity and decrease $^{230}Th/^{238}U$ activity, resulting in younger apparent U-series ages and elevated $\delta^{234}U_{initial}$ values. This isotopic trend is observed in CCA collected from a MIS 5e reef, which undergoes a three-fold increase in uranium concentration compared to modern counterparts. Uranium enrichment results in measured $\delta^{234}U_{initial}$, being significantly higher than that of corals of 206 ± 43‰ compared to 180 ± 7‰, and more variable but

generally younger U-series ages of 113.8 ± 17 ka compared to 131.5 ± 8 for corals. (**Fig. 5c,d**).

Despite the apparent variability in age and $\delta^{234}U_{initial}$, when $^{234}U/^{238}U$ and $^{230}Th/^{238}U$ activities are plotted on an activity ratio diagram, a linear array of isotopic anomalies appears to intersect the closed-system seawater evolution curve at around 90 ka (**Fig 6**). This linear array suggests that CCA may have gained different amounts of uranium with a fixed $\delta^{234}U$ value at around the same time (Scholz *et al.*, 2004). Those CCA that do not lie on the linear array may have been subjected to late uranium uptake or $^{234}U/^{238}U$ of different activities.

Corals from the same section of reef are likely to have been subject to the same groundwater chemistry and hydrology yet they did not display a similar linear array to CCA. This suggests that isotopic exchange processes that operate on CCA differ to those of corals. Simply put, CCA absorbs a higher proportion or uranium into their total fraction compared to corals, resulting in higher measured $\delta^{234}U$ values and younger ages. This was further illustrated when coeval coral/CCA couplets were analysed; CCA that grew on the surface of corals have younger average U-series of 18.9 ± 2.1 ka (**Fig. 5**) and had 20 to 30‰ higher $\delta^{234}U$ values.

D.5.2.3 Age reliability beyond the last interglacial

A single CCA sample (HEN1_A), collected from a known MIS 9 emergent reef (Stirling *et al.*, 2001), returned U-series age of 305.9 ± 4.2 ka. Thus despite the geochemical anomalies associated with dating CCA, as a sample material it was successfully able to identify the reef as belonging to MIS 9. The coral in which the CCA was encrusting returned an older U-series age of 313.8 ± 8.2 ka, again illustrating how uranium uptake can lead to younger apparent ages. A uranium concentration of 0.81 ppm is similar to levels recorded in MIS 5e CCA. This suggests that peak uranium

concentration may be reached by MIS 5e (**Fig. 3**) after which concentrations remain fairly stable. As datable material CCA, despite the geochemical anomolies can at least identify the MIS in which they grew.

D.5.2.4 Advanced calcite alteration, uranium loss, and U-series age reliability

It is known that the magnitude of isotopic anomalies recorded in aragonitic corals increase systematically with age to at least 550 ka (Bard *et al.*, 1991), but because CCA is composed of more unstable HMC, they are even less likely to maintain their chemical integrity over longer timescales. Advanced calcite alteration in Middle Pleistocene age CCA has resulted in the loss of uranium (**Fig. 3**). Uranium loss has the potential to alter uranium and thorium isotopic ratios and lead to inaccurate U-series age calculations. Whereas the uptake of uranium has results in younger ages by decreasing $^{230}Th/^{238}U$ activity ratio, the loss of uranium should increase the $^{230}Th/^{238}U$ activity ratio thereby return older ages. This is true for RMS2_A; with a $^{230}Th/^{238}U$ activity of 1.259 the sample returned an infinite (equilibrium) age. RMS1_A also had a near secular $^{230}Th/^{238}U$ activity, but returned a measured age of 329 ± 6.5 ka. This anomalously young age is due largely to ^{234}U enrichment, which resulted in an extremely high $^{234}U/^{238}U$ activity of 1.231 and an extremely high $\delta^{234}U_{initial}$ of 561 ± 9.9‰. The shift from HMC to low magnesium calcite and the subsequent loss of uranium makes it very difficult to obtain reliable U-series age data in older Middle Pleistocene age CCA.

D.5.2.5 Stratigraphic integrity of CCA U-series ages

A three metre high, stacked sequence of in situ reef framework provide a stratigraphic context for evaluating coral and CCA U-series age relationships (**Fig. 5**). Behaving as isotopically closed systems U-series coral and CCA age should decrease up-section. However, $\delta^{234}U_{inital}$ values of coral and CCA are incompatible with closed-system

decay from modern seawater, thus, all measured ages are considered unreliable (**Fig. 5e**). Despite this, measured $^{230}Th/^{238}U$ and $^{234}U/^{238}U$ activities for both coral and CCA do show the expected isotopic trends for decreasing age up section (**Fig. 5b,c**). The problem is that despite coral and CCA showing stratigraphic age conformity, they do not show age equivalence between each other (**Fig.5d**). This suggests that isotopic exchange systematics within coral and CCA is not the same.

D.6 CONCLUSIONS

1) Like corals, this study shows that living CCA inherit a $\delta^{234}U$ value of 147.02 ± 1.5‰, well within the range of modern seawater. The fact that living CCA captures modern seawater $^{234}U/^{238}U$ isotopic ratios prompts the examination of uranium and thorium evolution over geological timescales and an assessment of their potential use in U-series dating.

2) Living CCA has uranium concentrations of 0.2 ± 0.07 ppm, similar to mollusks and planktonic foraminifera, but an order of magnitude lower than corals. A threefold post mortality increase in uranium peaks at 0.72 ± 0.15 ppm in MIS 5e samples. A several order of magnitude ^{232}Th increase in fossil CCA suggests addition of $^{230}Th_{nr}$ may accompany uranium enrichment. Uranium loss occurs with advanced carbonate diagenesis. This can advance secular equilibrium ages as well as introduce ^{234}U-enriched uranium into a mobile phase.

3) Back-calculated CCA $^{234}U_{initial}$ is higher than modern seawater values. This limits the ability of CCA to provide accurate U-series ages. The geochemical anomalies observed are greater than those observed in corals and are directly related to the degree of uranium enrichment. Young CCA has sufficiently low uranium

concentrations that even minor inclusion of $^{230}Th_{nr}$ can result in older apparent ages. In contrast, MIS 5e and MIS 9 CCA undergo ^{234}U-enrichment, increasing $^{234}U/^{238}U$ activities. This enrichment results in higher $\delta^{234}U_{initial}$ values, lowering $^{238}Th/^{238}U$ activities and decreasing the overall calculated ages in a systematic manner.

D.7 REFERENCES

Andersen, M.B., Stirling, C.H., Potter, E.K., Halliday, A.N., 2004. Toward epsilon levels of measurement precision on U-234/U-238 by using MC-ICPMS, International Journal of Mass Spectrometry 237 (2-3), 107-118.

Bard, E., Fairbanks, R.G., Hamelin, B., Zindler, A., Huang, C.T., 1991. Uranium-234 anomalies in corals older than 150,000 years. Geochimica et Cosmochimica Acta 55, 2385–2390.

Bathurst, R.G.C., 1971. Carbonate sediments and their diagenesis: Developments in Sedimentology: Amsterdam, Elsevier, v. 12, 620 p.

Bosence ,D.W.J., 1983. Coralline algal reef frameworks. Journal of the Geological Society of London 140, 365-367.

Broecker, W.S., 1963. A preliminary evaluation of uranium series inequilibrium as a tool for absolute age measurement on marine carbonates. Journal of Geophysical Research 68, 2817-2834.

Cabioch, G., Montaggioni, L.F., Faure, G., Ribaud-Laurenti A., 1999. Reef coralgal assemblages as recorders of paleobathymetry and sea level changes in the Indo–Pacific province. Quaternary Science Reviews 18, 1681–1695

Cobb, M.M., Charles, D.D., Cheng, H., Kastner, M., Edwards, R.L., 2003. U/Th-dating living and young corals from the central tropical Pacific. Earth and Planetary Science Letters 210, 91-103.

Edwards, R.L., Chen, J.H., Wasserburg, G.J., 1987a. ^{238}U, ^{234}U, ^{230}Th, ^{232}Th systematics and the precise measurement of time over the past 500,000 years. Earth and Planetary Science Letters 81, 175-192.

Edwards, R.L., Chen, J.H., Ku, T.L., Wasserburg, G.J., 1987b. Precise timing of the last interglacial period from mass spectrometric determination of ^{230}Th in corals. Science 236, 1547-1553.

Edwards, R.L., Taylor, F.W., Wasserburg, G.J., 1988. Dating earthquakes with high-precision ^{230}Th ages of very young corals. Earth and Planetary Science Letters 90, 371-381.

Edwards, R.L., Cutler, K.B., Cheng, H., Gallup, C.D., 2003. Geochemical evidence for Quaternary sea-level change. in H., Elderfield: The Oceans and Marine Geochemistry Treatise on Geochemistry, Elviser 6 (13), 343-364.

Gallup, C.D., Edwards, R.L., Johnson, R.G., 1994. The Timing of High Sea Levels over the Past 200,000 Years, Science 263, 796-800.

Gherardi, D.F.M., Bosence, D.W.J., 2001. Composition and community structure of the coralline algal reefs from Atol das Rocas, South Atlantic, Brazil. Coral Reefs19, 205-19.

Goldsmith, J.R., 1955. The occurrence of magnesian calcites in Nature. Geochemica et Cosmochemica Acta 7, 212

Hamelin, B., Bard, E., Zindler, A., Fairbanks, R.G., 1991. $^{234}U/^{238}U$ mass spectrometry of corals: How accurate is the U-Th age of the last interglacial period? Earth and Planetary Science Letters 106, 169-180.

Harrington L., Fabricius K., Eaglesham G., Negri A., 2005. Synergistic effects of diuron and sedimentation on photosynthesis and survival of crustose coralline algae. Marine Pollution Bulletin 51 (1-4): 415-427

Henderson, G.M., Slowey, N.C., Fleisher, M.Q., 2001. U-Th dating of carbonate platform and slope sediments. Geochemica et Cosmochemica Acta 65, 2757-2770.

Henderson, G.M., O'Nions R.,K., 1995. U-234/U-238 ratios in Quaternary planktonic foraminifera. Geochemica et Cosmochemica Acta 59 (22), 4685-4694.

Henderson, G.M., 2002. Seawater (234U/238U) during the last 800 thousand years. Earth and Planetary Science Letters 199, 97–11

Kaufman, A., Broecker, W.S., Ku, T.-L., Thurber D.L., 1971. The status of U-series methods of mollusc dating. Geochimica et Cosmochimica Acta 35 (11), 1155-1183.

Kaufman, A., Ghaleb, B., Wehmiller, J.F., Hillaire-Marcel, C., 1996. Uranium concentration and isotope ratio profiles within *Mercenariu* shells: Geochronological implications. Geochimica et Cosmochimica Acta 60 (19), 3735-3746.

Kaufman, A., Ghaleb, B., Wehmiller, J.F., Hillaire-Marcel, C., 1996. Uranium concentration and isotope ratio profiles within *Mercenariu* shells: Geochronological implications. Geochimica et Cosmochimica Acta 60 (19), 3735-3746.

Kennedy, D.M., Woodroffe, C.D., 2002. Carbonate sediments of Elizabeth and Middleton Reefs close to the southern limits of reef growth in the southwest Pacific. Australian Journal of Earth Sciences 51, 847–857.

Kolesar, P.T., 1978. Magnesium in Calcite from a coralline algae. Journal of Sedimentary Petrology 48 (3), 815-819.

McCulloch, M.T., Esat T., 2000. The coral record of last interglacial sea levels and sea surface temperatures. Chemical Geology v. 169, p. 107-129.

Milliman, J.D., 1971. Utilization of magnesium in coralline algae. Geological Society of America Bulletin 82, 573.

Morse, J.W., 2004. Formation and diagenesis of carbonate sediments. In F.T. Mackenzie, ed., Sediments, Diagenesis, and Sedimentary Rocks: Treatise on Geochemistry, Elsevier, v. 7, 67-85. 768.

Pandolfi J.M., 1995. Geomorphology of the uplifted Pleistocene atoll at Henderson Island, Pitcairn Group. Biological Journal of the Linnean Society 56, 63-77.

Payri, C.E, Cabioch, G., 2004. The systematics and significance of coralline red algae in the rhodolith sequence of the Amedee 4 drill core (Southwest New Caledonia). Palaeogeography Palaeoclimatology Palaeoecology 204, 187–208.

Payri, C.E., 1997. Hydrolithon reinboldii rhodolith distribution, growth and carbon production of a French polynesian reef. Proceedings of the 8th Internaitonal Coral Reef Symposium. 1:755–60.

Potter, E.K., Stirling, C.H., Andersen, M.B., Halliday, A.N., 2005. High precision Faraday collector MC-ICPMS thorium isotope ratio determination, International Journal of Mass Spectrometry 247 (1-3), 10-17.

Robinson, L.F., Belshaw, N. S., Henderson, G.M., 2004. U and Th concentrations and isotope ratios in modern carbonates and waters from the Bahamas. Geochimica et Cosmochimica Acta 68, 1777-1789.

Scholz, D., Mangini, A., Felis, T., 2004. U-series dating of diagenetically altered fossil reef corals. Earth and Planetary Science Letters 218 (1-2), 163-178

Slowey, N.C., Henderson, G.M., Curry, W.B., 1996. Direct U – Th dating of marine sediments from the two most recent interglacial periods. Nature 383, 242-244.

Stirling, C.H., Halliday A.N., Porcell, D., 2005. In search of live Cm-247 in the early solar system, Geochimica Et Cosmochimica Acta 69(4), 1059-1071.

Stirling, C.H., Esat, T.M., Lambeck, K., McCulloch, M.T., Blake, S.G., Lee, D.C., Halliday, A.N., 2001. Orbital forcing of the marine isotope stage 9 interglacial, Science 291, 290-293.

Thompson, W.G., Spiegelmann, M.W., Goldstein, S.L., Speed, R.C., 2003. An open-system model for U-series age determinations of fossil corals. Earth and Planetary Science Letters 210, 36-380.

Veizer, R,J., Mackenzie, F.T., 2004. Evolution of sedimentary rocks, in F. T. Mackenzie, ed., Sediments, Diagenesis, and Sedimentary Rocks: Treatise on Geochemistry: Amsterdam, Elsevier, v. 7, p. 369-407.

Veron, J.E.N., 2000. Corals of the world. Australian Institute Marine Science, vol. 3, 463 pp.+429 pp.+490 pp.

D.8 FIGURES 1-6

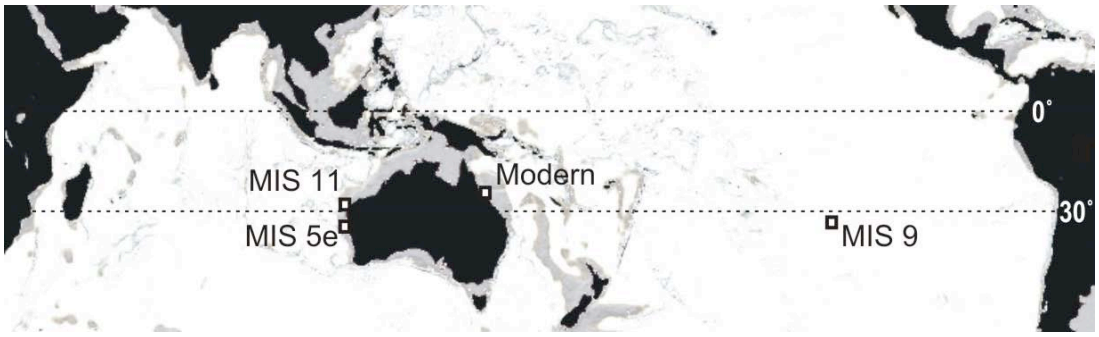

Figure 1: Map of the Indo-pacific showing sample locations; fossil reef ages have already been previously established (see body text).

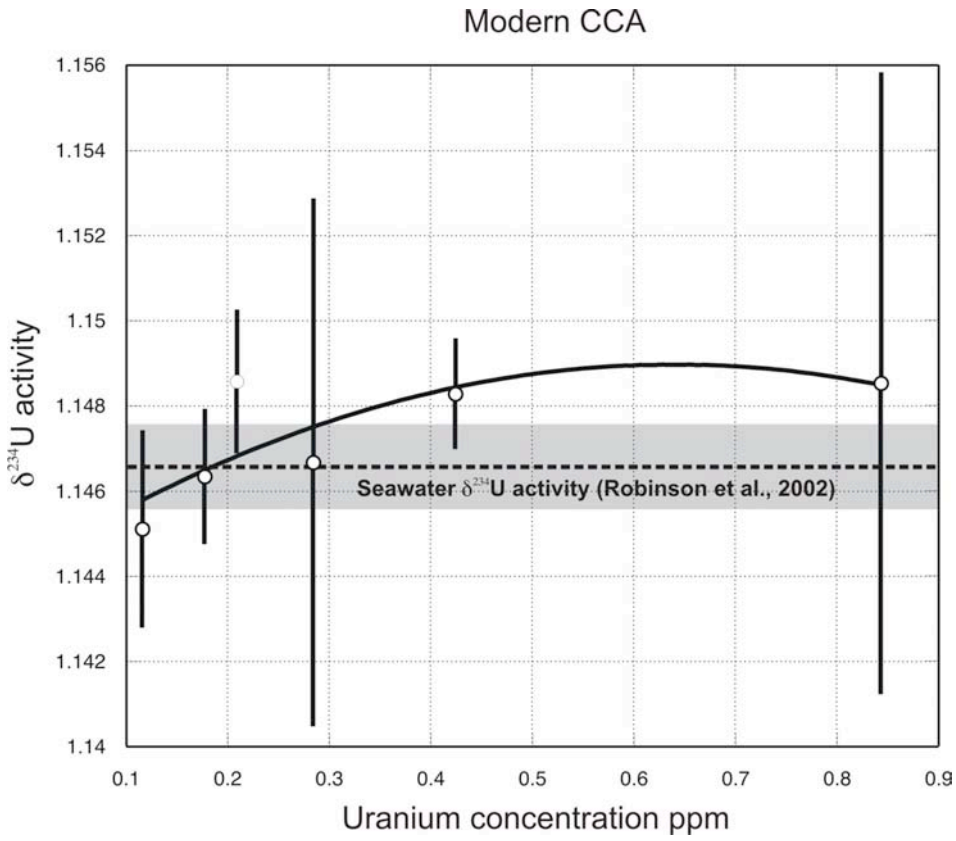

Figure 2: Measured $\delta^{234}U$ activities for living and modern CCA. The black dotted line represents modern seawater $\delta^{234}U$ activities (Robinson *et al.*, 2004); the shaded area represents 2 s.e. error. Higher measured $\delta^{234}U$ activities in living CCA corresponds to higher concentrations or uptake of ^{234}U enriched uranium.

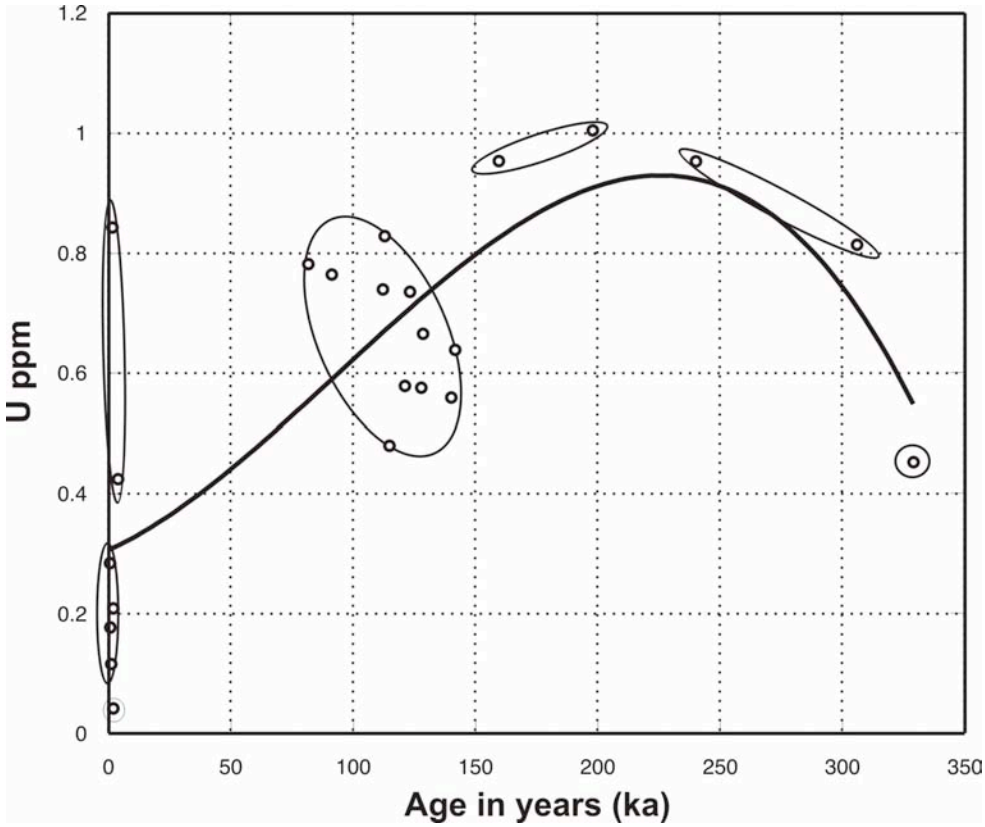

Figure 3: Uranium concentrations versus age for all CCA. There is an initial uptake of uranium in CCA with is then leached out of older samples.

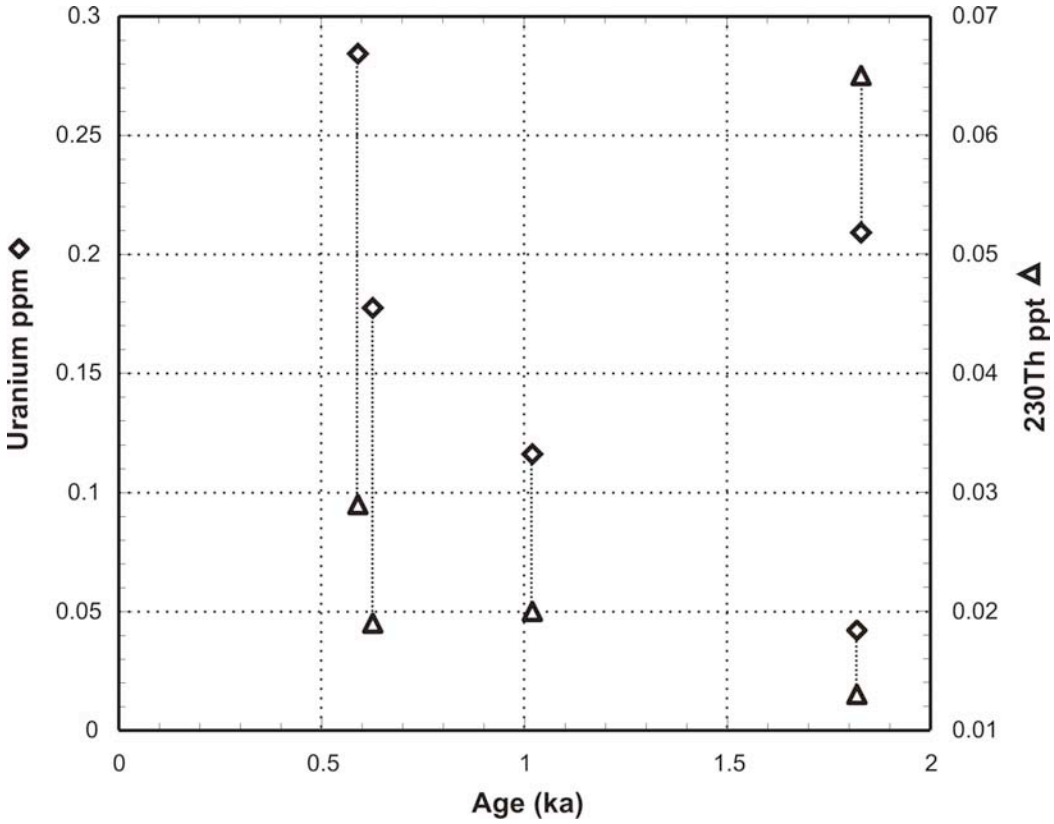

Figure 4: U and ^{230}Th concentrations in living (actual age <10 yearsß) CCA versus measured age. The lower the U concentration the higher the age error encountered.

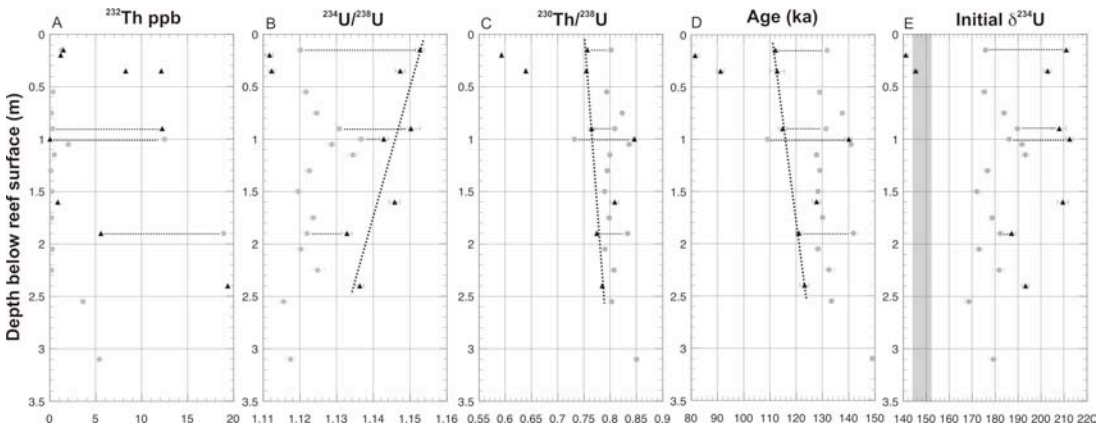

Figure 5: Isotopic ratios and age for CCA (black triangle) and coral (grey circle) collected down a 3 m measured section at Cape Cuvier. 5a – ^{232}Th concentrations in parts per billion. 5b – $^{234}U/^{238}U$ isotopic ratios. 5c – $^{230}Th/^{238}U$ isotopic ratios. 5d – U-series age in thousands of years (ka). 5e - $\delta^{234}U_{initial}$ back calculated for CCA and coral, closed system evolution should plot within the shaded area.

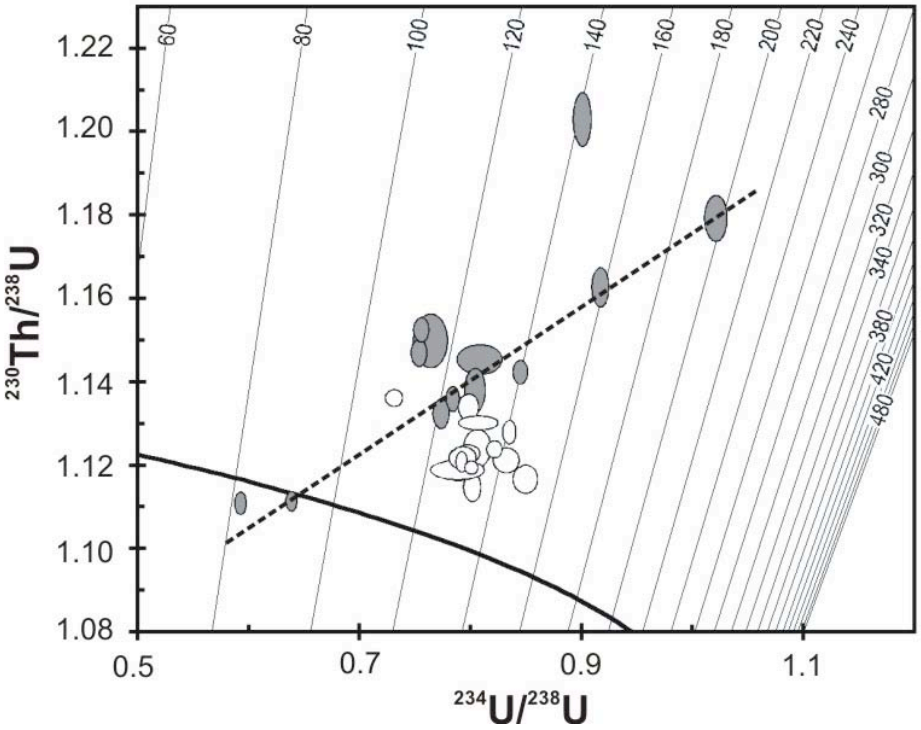

Figure 6 Compilation of the U-series data for CCA (grey) and corals (open circles) on a $^{234}U/^{238}U$ activity ratio diagram. The solid black line represents closed system evolution with and initial modern seawater $^{234}U/^{230}U$ activity of 1.1466. The dashed line indicates a linear compositional array representative of those observed for CCA.

Table 1: U-series

Sample Code	U ppm[1]	^{230}Th ppt[2]	^{232}Th ppb[3]	^{234}U/ ^{238}U[4]	Error	δ ^{234}U	Error	^{230}Th/ ^{238}U[5]	Error	^{230}Th/ ^{232}Th	Age (yrs)[6]	Age Error	Initial δ^{234}U[7]	δ^{234}U Error
Crustose Coralline Algal samples (CCA)														
JBR1_A	0.21	0.06	0.12	1.1486	0.0017	148.6	1.7	0.019	0.001	106	1830	95	149.30	1.70
JBR2_A	0.18	0.02	0.04	1.1463	0.0016	146.3	1.6	0.007	0.000	102	627	28	146.60	1.55
MYR1_A	0.28	0.03	0.02	1.1467	0.0062	146.7	1.1	0.006	0.000	228	590	28	146.90	0.99
NYR1_A	0.12	0.02	0.03	1.1451	0.0023	145.1	2.3	0.011	0.001	145	1020	76	145.50	2.30
NYR2_A	0.04	0.01	0.01	1.1484	0.0025	148.4	2.5	0.019	0.001	226	1820	135	149.20	2.50
HEN2_A	0.84	0.22	0.05	1.1485	0.0073	148.5	0.7	0.016	0.000	778	1559	25	149.20	0.72
LQC_A	0.42	0.27	2.94	1.1483	0.0013	148.3	4.6	0.039	0.001	17	3730	130	149.90	4.65
LCCd_A	0.74	9.35	19.37	1.1363	0.0012	136.3	1.2	0.785	0.002	90	123200	710	193.30	1.60
LCCj_A	0.58	7.26	5.56	1.1328	0.0014	132.8	1.4	0.774	0.003	245	121000	835	187.20	1.85
LCCl_A	0.58	7.54	0.88	1.1458	0.0015	145.8	1.5	0.808	0.008	1607	127800	2350	209.50	2.30
LCCq_A	0.56	7.65	0.02	1.1428	0.0012	142.8	1.2	0.846	0.003	76847	140000	1050	212.40	1.65
LCCr_A	0.48	5.94	12.24	1.1502	0.0026	150.2	2.6	0.765	0.006	91	114800	1700	207.90	3.20
LCCu1_A	0.76	7.91	12.13	1.1123	0.0009	112.3	0.9	0.639	0.002	122	91180	450	145.40	1.15
LCCu2_A	0.83	10.12	8.26	1.1473	0.0013	147.3	1.3	0.755	0.003	230	112800	770	202.80	1.65
LCCv_A	0.78	7.50	1.19	1.1117	0.0011	111.7	1.1	0.593	0.002	1177	81520	450	141.10	1.30
LCCw_A	0.74	9.06	1.49	1.1527	0.0012	152.7	1.2	0.756	0.003	1142	112100	745	210.90	1.50
LCV2e_A	0.95	14.25	66.86	1.1627	0.0019	162.7	1.9	0.919	0.003	40	159456	1327	255.73	2.58
LCV3e_A	1.01	16.72	11.47	1.1791	0.0022	179.1	2.2	1.023	0.004	273	197872	2418	313.82	3.26
LCV7t_A	0.67	8.72	57.27	1.1385	0.0022	138.5	2.2	0.805	0.004	29	128514	1180	199.31	2.83
LCV7e_A	0.64	9.37	2.60	1.2025	0.0026	202.5	2.6	0.902	0.003	674	141671	1153	201.40	3.38
HEN1_A	0.81	13.62	0.05	1.0750	0.0073	75.0	0.7	1.033	0.003	46970	305900	4200	178.40	2.20
RMS1_A	0.45	9.02	0.95	1.2211	0.0099	221.1	1.0	1.231	0.004	1777	329000	6500	561.00	9.90
RMS2_A	0.39	8.03	7.60	1.1708	0.0200	170.8	2.0	1.259	0.006	198	Equilibrium age			
Coral Samples														
MYR1_C	2.37	0.32	0.16	1.1471	0.0091	147.1	0.9	0.008	0.000	386	802	19	147.40	0.87
HEN2_C	2.75	1.61	0.04	1.1452	0.0081	145.2	0.8	0.036	0.001	7238	3496	51	146.64	0.82
LCCa_C	3.05	42.01	5.39	1.1174	0.0013	117.4	1.3	0.850	0.005	1462	149000	1700	179.20	2.00
LCCb_C	2.90	37.65	3.59	1.1155	0.0013	115.5	1.3	0.802	0.003	1966	133400	1100	168.50	1.80
LCCg_C	3.01	39.30	0.16	1.1248	0.0018	124.8	1.8	0.807	0.005	46520	132400	1550	181.60	2.50
LCCi_C	3.38	43.25	0.25	1.1202	0.0013	120.2	1.3	0.790	0.004	32419	128300	1350	172.90	1.85
LCCj_C	2.86	38.52	18.92	1.1219	0.0012	121.9	1.2	0.833	0.005	382	141700	1600	182.10	1.80
LCCk_C	3.16	40.76	0.16	1.1236	0.0009	123.6	0.9	0.798	0.005	48364	130000	1450	178.60	1.30
LCCm_C	3.04	38.83	0.18	1.1195	0.0010	119.5	1.0	0.789	0.010	40107	128300	2850	172.00	1.80
LCCn_C	3.11	40.02	0.07	1.1225	0.0011	122.5	1.1	0.794	0.005	113410	129000	1500	176.60	1.60
LCCo_C	3.18	41.08	0.47	1.1344	0.0013	134.4	1.3	0.799	0.004	16419	127700	1100	193.10	1.70
LCCp_C	3.47	46.98	2.01	1.1286	0.0011	128.6	1.1	0.836	0.003	4378	140800	890	191.60	1.55
LCCq_C	3.68	43.63	12.48	1.1366	0.0009	136.6	0.9	0.732	0.003	655	109000	790	186.00	1.10
LCCr_C	3.28	42.88	0.32	1.1307	0.0006	130.7	0.6	0.808	0.007	25336	131300	2250	189.70	1.45
LCCs_C	3.26	43.33	0.17	1.1245	0.0008	124.5	0.8	0.822	0.003	46762	137500	965	183.80	1.20
LCCt_C	3.21	41.22	0.34	1.1216	0.0010	121.6	1.0	0.793	0.002	22684	128900	685	175.20	1.30
LCCw_C	3.39	44.03	1.27	1.1201	0.0006	120.1	0.6	0.801	0.002	6511	131700	725	175.70	0.91
NJB3_1	1.76	30.02	0.06	1.0228	0.0011	22.8	1.1	1.048	0.002	94943	Equilibrium age			
NJB3_3	0.88	15.54	0.23	1.0317	0.0013	31.7	1.3	1.092	0.004	12655	Equilibrium age			
NPG_3	0.71	12.55	1.81	1.0323	0.0021	32.3	2.1	1.092	0.004	1301	Equilibrium age			
NJB4_1	1.05	18.26	0.34	1.0374	0.0015	37.4	1.5	1.072	0.003	10094	Equilibrium age			
NJB4_2	1.09	19.32	0.21	1.0350	0.0018	35.0	1.8	1.087	0.003	17602	Equilibrium age			
NJB4_3	0.79	13.95	0.09	1.0354	0.0016	35.4	1.6	1.080	0.003	30402	Equilibrium age			

Notes to Table 1.

[1] Uranium concentrations are measured in part per million (ppm) equivalent to ng/g.

[2] ^{230}Th concentrations measured in parts per trillion (ppt) equivalent to fg/g

[3] ^{232}Th concentrations measured in parts per billion (ppb) equivalent to pg/g

[4] $\delta^{234}U = \{[(^{234}U/^{238}U)/(^{234}U/^{238}U)_{eq}]-1\} \times 10^3$. $(^{234}U/^{238}U)_{eq}$ is the atomic ratio at secular equilibrium and is equal to $\lambda_{238}/\lambda_{234} = 5.4891 \times 10^{-5}$, , where λ_{238} and λ_{234} are the decay constants for ^{238}U and ^{234}U, respectively, adopting half-lives of Cheng *et al.*, (1998)

[5] $[^{230}Th/^{238}U]_{act} = (^{230}Th/^{238}U)/(\lambda^{238}/\lambda^{230})$.

[6] U-series ages are calculated iteratively using

$$1 - \left[\frac{^{230}Th}{^{238}U}\right]_{act} = e^{-l_{230}T} - \left(\frac{d^{234}U(0)}{1000}\right)\left(\frac{l_{230}}{l_{230}-l_{234}}\right)\left(1 - e^{(l_{234} - l_{230})T}\right)$$

where T is the age in years and λ_{230} is the decay constant for ^{230}Th. $\lambda_{238} = 1.551 \times 10^{-10}$ y^{-1}; $\lambda_{234} = 2.826 \times 10^{-6}$ y^{-1}; $\lambda_{230} = 9.158 \times 10^{-6}$ y^{-1}. Ages in bold type are strictly reliable

[7] The initial value is given by $\delta^{234}U_i = \delta^{234}Ue^{l_{234}T}$, where T is the age in years.

SECTION E

CONCLUSIONS

The aim of this thesis was to improve our understanding of abrupt sea level change during MIS 5e though detailed stratigraphic and geomorphic mapping of emergent marine deposits and advanced high-precision U-series dating techniques. This involved a regional survey of West Australian Pleistocene fossil reef sites, some of which were logged and sampled, in best cases along reef growth axes. U-series dating was conducted on 101 coral and 25 CCA samples utilizing MC ICPMS techniques.

The improvement in analytical precision has shown corals to be more susceptible to chemical and isotopic exchange than previously thought. Therefore prior to any geochronological interpretations all uncorrected and open-system corrected coral ages were subject to a rigorous geochemical screening procedures and independent age tests, including stratigraphic superposition and multiple dates from single coral colonies. Two areas, Cape Cuvier and Shark Bay provided the largest amount of stratigraphic and geochronological data for interpreting nature of sea level during MIS 5e as well as provide a geologic case study for assessing the reliability of U-series age dates. This study also afforded the opportunity to test the potential benefits of crustal coralline algae in U-series dating.

While geomorphological investigations of emergent marine deposits along the West Australian coast reveal evidence supporting unstable MIS 5e sea levels, geochronological data was not able to offer corroborating evidence. This is solely due to the inability to obtain reliable U-series age data, resulting from open-system exchange processes. The application of independent age controls to both uncorrected and corrected U-series coral ages: 1) reveal the false credence given to analytical precision where multiple ages from a single coral often exceed analytical error; and 2) call into question the validity of open-system corrections which fail to agree with any of the age tests.

While this multi-method approach was originally applied to improve our understanding of high frequency sea level oscillations the ability to identify measured U-series that come closest to representing the corals true age, this study reveals just how unreliable U-series dating of corals can be. It also revealed how open-system 'systematics' does not operate in a systematic way and questions the utility of open-system corrections.

REFERENCES

Andersen, M.B., Stirling, C.H., Potter, E.K., Halliday, A.N., 2004. Toward epsilon levels of measurement precision on $^{234}U/^{238}U$ by using MC-ICPMS. International Journal of Mass Spectrometry 237 (2-3), 107-118.

Andersen M.B., Stirling C.H., Potter E-K., Halliday, A.N., Blake, S.G., McCulloch M.T., Ayling B.F., O'Leary M.J., *in review*. Direct chronology of the Marine Isotope Stage 15 (~600 ka) estimated from high-precision U-series ages from Henderson Island, south Pacific.

Bard, E., Fairbanks, R.G., Hamelin, B., Zindler, A., Huong, C.T., 1991. ^{234}U anomalies in corals older than 150,000 years. Geochimica et Cosmochimica Acta 55, 2385-2390.

Bard, E., Hamelin, B., Fairbanks, R.G., 1990. U/Th ages obtained by mass-spectrometry in corals from Barbados: sea level during the past 130,000 years. Nature 346 (6283), 456-458.

Bard, E., Fairbanks, R.G., Hamelin, B., 1992. How accurate are the U/Th ages obtained by mass spectrometry on coral terraces, in: G.J. Kukla, E. Went (Eds.), Start of a Glacial, NATO ASI Series 13, Springer, Berlin, pp. 15-21.

Bar-Matthews, M., Wasserburg, G. J., Chen, J.H., 1993. Diagenesis of fossil coral skeletons: correlation between trace-elements, textures, and $^{234}U/^{238}U$. Geochimica et Cosmochimica Acta 57, 257-276.

Bathurst, R.G.C., 1971. Carbonate sediments and their diagenesis: Developments in Sedimentology: Amsterdam, Elsevier, v. 12, 620 p.

Bender, M.L., Fairbanks, R.G., Taylor, F.W., Matthews, R.K., Goddard, J.G., Broecker, W.S., 1979. Uranium-series dating of Pleistocene reef tracts of Barbados, West Indies. Geological Society of America Bulletin 90, 577-594.

Bosence ,D.W.J., 1983. Coralline algal reef frameworks. Journal of the Geological Society of London 140, 365-367.

Broecker, W.S., 1963. A preliminary evaluation of uranium series in equilibrium as a tool for absolute age measurement on marine carbonates. Journal of Geophysical Research 68, 2817-2834.

Burling, M.C., Ivey, G.N., Pattiaratchi, C.B., 1999. Convectively driven exchange in a shallow coastal embayment. Continental Shelf Research 19, 1599-1616.

Cabioch, G., Montaggioni, L.F., Faure, G., Ribaud-Laurenti, A., 1999. Reef coralgal assemblages as recorders of paleobathymetry and sea level changes in the Indo-Pacific province. Quaternary Science Reviews 18, 1681-1695.

Chen, J.H., Edwards, R.L., Wasserburg, G.J., 1986. ^{238}U, ^{234}U and ^{232}Th in seawater, Earth and Planetary Science Letters 80 (3-4), 241-251.

Chen, J.H., Curran, H.A., White, B., Wasserburg, G.J., 1991. Precise chronology of the Last Interglacial period: $^{234}U^{230}Th$ data from fossil coral reefs in the Bahamas. Geological Society of America Bulletin 103, 82-97.

Cheng, H., 2003. Uranium-series dating of marine and lacustrine carbonates (*in* Uranium-series geochemistry). Reviews in Mineralogy and Geochemistry 52, 363-405

Cherniak, D.J., 1997. An experimental study of strontium and lead diffusion in calcite, and implications for the carbonate diagenesis and metamorphism. Geochimica et Cosmochimica Acta 61, 4173-4179.

Chivas A.R., Torgersen T., Polach H.A., 1990. Growth rates and Holocene development of stromatolites from Shark Bay, Western Australia. Australian Journal of Earth Science 37, 113-121.

Coles, S.L., Jokiel, P., 1992. Effects of salinity on coral reefs. In D. W. Connell and D. W. Hawker (eds.), Pollution in tropical aquatic systems, Chapter 6, 147-166. CRC Press, Boca Raton.

Coles, S.L., 1988. Limitations on coral reef development in the Arabian Gulf: Temperature or algal competition? Proc. 6th Int. Coral Reef Symposium, 3, 211.

Collins, L.B., Zhu, Z.R., Wyrwoll, K.H., Hatcher, B.G., Playford, P.E., Chen, J.H., Eisenhauer, A., Wasserburg, G.J., 1993a. Late Quaternary evolution of coral reefs on a cool-water carbonate margin: the Abrolhos carbonate platforms, Southwest Australia. Marine Geology 110, 203-212.

Collins, L.B., Zhu, Z.R., Wyrwoll, K.H., Hatcher, B.G., Playford, P.E., Eisenhauer, A., Chen, J.H., Wasserburg, G.J., Bonani, G., 1993b. Holocene growth history of a reef complex on a cool-water carbonate margin: Easter Group of the Houtman Abrolhos, eastern Indian Ocean. Marine Geology 115, 29-46.

Collins, L.B., Zhu, Z.R., Wyrwoll, K.-H., 1996. The structure of the Easter Platform, Houtman Abrolhos Reefs: Pleistocene foundations and Holocene reef growth. Marine Geology 135, 1-13.

Collins, L.B., Zhu, Z.R., Wyrwoll, K-H., Eisenhauer, A., 2003. Late Quaternary structure and development of the northern Ningaloo Reef, Australia. Sedimentary Geology 159, 81-94.

Denman, P.D., Van de Graaff, W.J.E., 1976. Emergent Quaternary marine deposits in the Lake MacLeod area, Western Australia. Western Australia Geological Survey Annual Report 1977, 32-36.

Eisenhauer, A., Zhu, Z.R., Collins, L.B., Wyrwoll, K.H., Eichstatter, R., 1996. The Last Interglacial sea-level change: new evidence from the Abrolhos Islands. West Australia. Geol Rundsch 85, 606-614.

Edwards, R.L., Chen, J.H., Wasserburg, G.J., 1987a. ^{238}U, ^{234}U, ^{230}Th, ^{232}Th systematics and the precise measurement of time over the past 500,000 years. Earth and Planetary Science Letters 81, 175-192.

Edwards, R.L., Chen, J.H., Ku T.-L., Wasserburg, G.J., 1987b. Precise timing of the last inter-glacial period from mass spectrometric analysis of ^{230}Th in corals. Science 236, 1547-1553.

Edwards, R.L., Taylor, F.W., Wasserburg, G.J., 1988. Dating earthquakes with high-precision ^{230}Th ages of very young corals. Earth and Planetary Science Letters 90, 371-381.

Edwards, R.L., Cutler, K.B., Cheng, H., Gallup, C.D., 2003. Geochemical evidence for Quaternary sea-level change. in H., Elderfield: The Oceans and Marine Geochemistry Treatise on Geochemistry, Elviser 6:13, 343-364.

Fabricius, K., De'ath G., 2001. Environmental factors associated with the spatial distribution of crustose coralline algae on the Great Barrier Reef. Coral Reefs 19 (4), 303-309

Fairbridge, R.W., 1950. The geology and geomorphology of Point Peron, Western Australia. Royal Society of Western Australia Journal 34, 35-72.

Fruijtier, C., Elliot, T., Schlager, W., 2000. Mass-spectrometric ^{234}U/^{230}Th ages from the Key Largo Formation, Florida Keys, United States: Constraints on diagenetic age disturbance. Geological Society of America Bulletin 112, 267-277.

Gallup, C.D., Edwards, R.L., Johnson, R.G., 1994. The Timing of high sea levels over the past 200,000 years. Science 263, 796-800.

Gallup, C. D., Cheng, H., Taylor, F. W., Edwards, R.L., 2002. Direct determination of the timing of sea-level change during Termination II. Science 295, 310-313.

Gherardi, D.F.M., Bosence, D.W.J., 2001. Composition and community structure of the coralline algal reefs from Atol das Rocas, South Atlantic, Brazil. Coral Reefs19, 205-19.

Goldsmith, J.R., 1955. The occurrence of magnesian calcites in Nature. Geochemica et Cosmochemica Acta 7, 212

Hamelin, B., Bard, E., Zindler, A., Fairbanks, R.G., 1991. ^{234}U/^{238}U mass spectrometry of corals: How accurate is the U-Th age of the last interglacial period? Earth and Planetary Science Letters 106, 169-181.

Harrington L., Fabricius K., Eaglesham G., Negri A., 2005. Synergistic effects of diuron and sedimentation on photosynthesis and survival of crustose coralline algae. Marine Pollution Bulletin 51 (1-4): 415-427

Hatcher, B.G., 1991. Coral reefs in the Leeuwin Current – an ecological perspective. Journal of the Royal Society of Western Australia 74, 115-127.

Hagan, G.M., Logan, B.W., 1974. Development of carbonate banks and hypersaline basins, Shark Bay, Western Australia. American Association of Petroleum Geologists Memoir 22: 61-139.

Helfrich, P., 1973. The feasibility of brine shrimp production on Christmas Island, Sea Grant Tech. Rep. UNIHI-SEAGRANT-TR-73-02, University of Hawaii, Honolulu.

Hearty, P.J., 1987. New data on the Pleistocene of Mallorca. Quaternary Science Reviews 6, 245-257.

Hearty, P.J., Neumann, A.C., 2001. Rapid sea level and climate change at the close of the Last Interglaciation (MIS 5e): evidence from The Bahama Islands. Quaternary Science Reviews 20 (18), 1881-1895.

Henderson, G.M., O'Nions R.,K., 1995. U-234/U-238 ratios in Quaternary planktonic foraminifera. Geochemica et Cosmochemica Acta 59 (22), 4685-4694.

Henderson, G.M., Slowey, N.C., 2000. Evidence from U-Th dating against Northern Hemisphere forcing of the penultimate deglaciation. Nature 404 (6773), 61-66

Henderson, G. M., Slowey, N. C.,Fleisher, M.Q., 2001. U/Th dating of carbonate platform and slope sediments. Geochemica et Cosmochemica Acta 65, 2757-2770.

Henderson, G.M., 2002. Seawater $^{234}U/^{238}U$ during the last 800 thousand years. Earth and Planetary Science Letters 199, 97-11.

Hocking, R.M., Moors, H.T., Van De Graff, W.J.E., 1987. Geology of the Carnarvon Basin of Western Australia. Geological Survey of Western Australia Bulletin 133.

Kaufman, A., Broecker, W.S., Ku, T.-L., Thurber D.L., 1971. The status of U-series methods of mollusc dating. Geochimica et Cosmochimica Acta 35 (11), 1155-1183.

Kaufman, A., Ghaleb, B., Wehmiller, J.F., Hillaire-Marcel, C., 1996. Uranium concentration and isotope ratio profiles within *Mercenariu* shells: Geochronological implications. Geochimica et Cosmochimica Acta 60 (19), 3735-3746.

Kingsman D.J.J., 1964. Reef tolerance of high temperatures and salinities. Nature 202, 1280.

Kendrick G.A., Huisman J.M., Walker D.I., 1990. Benthic Macroalgae of Shark Bay, Western Australia. Botanica Marina 33, 47-54.

Kendrick, G.W., Wyrwoll, K.H., Szabo, B.J., 1991. Pliocene-Pleistocene coastal events and history along the western margin of Australia. Quaternary Science Reviews 10, 419-439.

Kennedy, D.M., Woodroffe, C.D., 2002. Fringing reef growth and morphology: a review Earth-Science Reviews 57 255-277.

Kigoshi, K., 1971. Alpha-recoil thorium-234: dissolution into water and the uranium-234/ uranium-238 disequilibrium in nature. Science 173 (3991), 47-48.

Kolesar, P.T., 1978. Magnesium in Calcite from a coralline algae. Journal of Sedimentary Petrology 48 (3), 815-819.

Ku, T.-L., Ivanovich, M., Luo, S., 1990. U-series dating of Last Interglacial high sea stands: Barbados revisited. Quaternary Research 33, 129-147.

Lazar, B., Enmar, R., Schossberger, M., Bar-Matthews, M., Halicz, L., Stein, M., 2004. Diagenetic effects on the distribution of uranium in live and Holocene corals from the Gulf of Aqaba. Geochimica et Cosmochimica Acta 68 (22), 4583-4593.

Logan, B.W., Read, J.R., Davies, G.R., 1970. History of carbonate sedimentation, Quaternary Epoch, Shark Bay, Western Australia. American Association of Petroleum Geologists Memoir 13: 38-85.

Marsh, L.M. 1990. Hermatypic corals of Shark Bay, Western Australia. In: Berry, P.F., Bradshaw, S.D. & Wilson, B.R. (Eds.). Research in Shark Bay. Report of the France-Australe Bicentenary Expedition Committee. Western Australian Museum, Perth, 107-114.

McCulloch, M.T., Esat T., 2000. The coral record of last interglacial sea levels and sea surface temperatures. Chemical Geology 169, 107-129.

Milliman, J.D., 1971. Utilization of magnesium in coralline algae. Geological Society of America Bulletin 82, 573.

Morse, J.W., 2004. Formation and diagenesis of carbonate sediments, in F. T. Mackenzie, ed., Sediments, Diagenesis, and Sedimentary Rocks: Treatise on Geochemistry, Elsevier, v. 7, 67-85. 768.

Muhs, D.R., Simmons, K.R., Steinke, B., 2002. Timing and warmth of the Last Interglacial period: new U-series evidence from Hawaii and Bermuda and a new fossil compilation for North America. Quaternary Science Reviews 21 (12-13), 1355-1383.

Murray-Wallace, C. V. 2002. Pleistocene coastal stratigraphy, sea-level highstands and neotectonism of the southern Australian passive continental margin - a review. Journal of Quaternary Science17, 469 - 489.

Neumann, A.C., Hearty, P.J., 1996. Rapid sea-level changes at the close of the last interglacial (substage 5e) recorded in Bahamian island geology Geology 24 (9), 775-778.

O'Leary, M.J., Hearty, P.J., McCulloch, M.T., 2004. Multiple sea-level highstands during marine isotope substage (MIS) 5e: Examples from Western Australia. 32nd International Geological Convention, Florence, Italy.

O'Leary, M.J., Hearty, P.J., McCulloch, M.T., 2003. ICPMS 234U anomalies of West Australian fossil coral reefs. 80th Australian Coral Reef Society convention, Townsville, Queensland.

Payri, C.E, Cabioch, G., 2004. The systematics and significance of coralline red algae in the rhodolith sequence of the Amedee 4 drill core (Southwest New Caledonia). Palaeogeography Palaeoclimatology Palaeoecology 204, 187–208.

Payri, C.E., 1997. Hydrolithon reinboldii rhodolith distribution, growth and carbon production of a French polynesian reef. Proceedings of the 8th Internaitonal Coral Reef Symposium

Playford PE. 1988. Guidebook to the Geology of Rottnest Island. Excursion Guidebook No. 2, Western Australia Division of the Geological Society of Australia: Perth; 67 pp.

Playford, P.E., 1990. Geology of the Shark Bay area, Western Australia. In: Berry, P.F., Bradshaw, S.D. & Wilson, B.R. (Eds.). Research in Shark Bay. Report of the France-Australe Bicentenary Expedition Committee. Western Australian Museum, Perth, 13-31.

Playford, P.E., 1997. Geology and hydrology of Rottnest Island, Western Australia, in: Vacher, H.L., T. Quinn, (Eds.), Geology and Hydrology of Carbonate Islands, Developments in Sedimentology 54, Elsevier, London, pp. 783–810.

Penrose, D.L., 1996a. Genus *Hydrolithon*. In: Womersley, H.B.S. (Ed.) The Marine Benthic Flora of Southern Australia - Part IIIB. *Gracilariales, Rhodymeniales, Corallinales* and *Bonnemaisoniales*. Canberra, Australian Biological Resources Study (effective publication date 29.vi.1996). pp.255-266.

Potter, E.K., Stirling, C.H., Andersen, M.B., Halliday, A.N., 2005. High precision Faraday collector MC-ICPMS thorium isotope ratio determination. International Journal of Mass Spectrometry 247 (1-3), 10-17.

Reid, R.P., Visscher, P.T., Decho, A.W., Stoltz, J.F., Bebout, B.M., Dupraz, C., Macintyre, I.G., Paerl, H.W., Pinckney, J.L., Prufert-Bebout, L., Steppe, T.F., DesMarais D.J., 2000. The role of microbes in the accretion, lamination and early lithification of modern stromatolites. Nature 406, 989-993.

Robinson, L.F., Belshaw, N. S., Henderson G.M., 2004. U and Th concentrations and isotope ratios in modern carbonates and waters from the Bahamas. Geochimica et Cosmochimica Acta 68, 1777–1789.

Robinson, L.F., Adkins, J.F., Fernandez, D.P., Burnett, D.S., Wang, S-L., Gagnon, A.C., Krakauer, N., 2006. Primary U-distribution in scleractinian corals and its implications for U-series dating. Geochemistry Geophysics Geosystems 7 (5), 1-20.

Read, J.F., 1974. Calcrete deposits and Quaternary sediments, Edel Province, Shark Bay, Western Australia. American Association of Petroleum Geologists Memoirs 22, 250 - 282.

Scholz, D., Mangini, A., Felis, T., 2004. U-series dating of diagenetically altered fossil reef corals. Earth and Planetary Science Letters 218 (1-2), 163-178.

Shen, G.T., Dunbar, R.B., 1995. Environmental Controls on Uranium in Reef Corals. Geochimica et Cosmochimica Acta 59 (10), 2009-2024.

Shepard, C.R.C., 1988. Similar trends, different causes: responses of corals to stressed environments in Arabian Seas. 6th Int. Coral Reef Symposium, 3, 297.

Sherman, C.E., Glenn, C.R., Jones, A.T., Burnett, W.C., Schwarcz, H.P., 1993. New evidence for 2 highstands of the sea during the last interglacial, oxygen-isotope substage-5e. Geology 21 (12), 1079-1082.

Slowey, N.C., Henderson, G.M., Curry, W.B., 1996. Direct U – Th dating of marine sediments from the two most recent interglacial periods. Nature 383, 242-244.

Steneck, R.S., 1997. Crustose corallines, other algal functional groups and sediments: complex interactions along reef productivity gradients. Proc. 8th Int. Coral Reef Sym. 1: 695-700.

Stirling, C.H., Esat, T.M., McCulloch, M.T., Lambeck, K., 1995. High-precision U-series dating of corals from Western Australia and implications for the timing and duration of the Last Interglacial. Earth and Planetary Science Letters 135, 115-130.

Stirling, C.H., Esat, T.M., Lambeck, K., McCulloch, M.T., 1998. Timing and duration of the Last Interglacial: evidence for a restricted interval of widespread coral reef growth. Earth and Planetary Science Letters 160, 745-762.

Stirling, C.H., Halliday A.N., Porcell, D., 2005. In search of live Cm-247 in the early solar system. Geochimica et Cosmochimica Acta 69 (4), 1059-1071.

Stirling, C.H., Esat, T.M., Lambeck, K., McCulloch, M.T., Blake, S.G., Lee D.C., Halliday, A.N., 2001. Orbital forcing of the marine isotope stage 9 interglacial. Science 291 (5502), 290-293.

Taylor, J.G., Pearce, A.F., 1999. Ningaloo Reef Current observations and implications for biological systems: Coral spawn dispersal, zooplankton and whale shark abundance. Journal of the Royal Society of Western Australia 82, 57-65.

Thompson, R.O.R.Y., 1984. Observations of the Leeuwin Current off Western Australia. Journal of Phyical Oceanography 14, 623-628.

Thompson, W.G., Spiegelmann M.W., Goldstein S.L., Speed R.C., 2003. An open-system model for U-series age determinations of fossil corals. Earth Planetary Science Letters 210, 365-38.

Thompson, W.G., Goldstein, S.L., 2005. Open-system coral ages reveal persistent suborbital sea-level cycles, Science 308 (5720), 401-404.

Trudgill, S.T., 1983. Preliminary estimates on intertidal limestone erosion, One Tree Island, Southern Great Barrier Reef, Australia. Earth Surface Processed and Landforms 8 (2), 189-193.

Van de Graaff, W.J.E., Denman, P.D., Hocking, R.M., 1976. Emerged Pleistocene marine terraces on Cape Range, Western Australia. Geological Survey of Western Australia Annual Report 1975, 62-69.

Veeh, H.H., Van de Graaff, W.J.E., Denman, P.D., 1979. Uranium-series ages of coralline terrace deposits in Western Australia. Journal of the Geological Society of Australia 26, 285-292.

Veizer, R,J., Mackenzie, F.T., 2004. Evolution of sedimentary rocks, in F. T. Mackenzie, ed., Sediments, Diagenesis, and Sedimentary Rocks: Treatise on Geochemistry: Amsterdam, Elsevier, v. 7, p. 369-407.

Villemant, B., Feuillet, N., 2003. Dating open systems by the 238U-234U-230Th method: application to Quaternary reef terraces. Earth and Planetary Science Letters 210, 105-118.

Walker, D.I., Woelkerling, Wm.J., 1988. Quantitative study of sediment contribution by epiphytic coralline red algae in seagrass meadows in Shark Bay, Western Australia, Marine Ecology-Progress Series 43, 71-77.

Walker, D.I., 1985. Correlations between salinity and growth of the seagrass Amphibolis[A1] Antarctica in Shark Bay, Western Australia, using a new method for measuring production rate. Aquatic Botany, 23, 13-26.

APPENDIX 1. U-SERIES DATA

Sample Code	U ppm	230Th ppt	232Th ppb	Delta 234U	234 error	230Th/ 238U	error	[230Th/ 232Th]	Age (ka)	Age error	Initial Delta 234U	Delta 234U error	Location
S8 S2a	3.057	38.32	5.70	116.34	0.49	0.7711	0.00	1260.00	123.75	0.35	165.23	0.65	Lake Mcleod
S8 S2b	2.617	32.89	12.52	115.92	0.71	0.7729	0.00	492.00	124.39	0.47	164.91	0.91	Lake Mcleod
S8 S2c	3.384	42.86	8.92	121.21	0.74	0.7790	0.00	900.00	124.92	0.36	172.72	0.97	Lake Mcleod
S8 S5a	3.110	38.99	1.57	117.63	0.86	0.7712	0.00	4666.00	123.47	0.48	166.93	1.15	Lake Mcleod
S8 S5b	3.160	39.56	1.59	117.99	0.72	0.7698	0.00	4693.00	122.99	0.46	167.21	0.95	Lake Mcleod
S8 S5c	2.696	34.14	0.33	117.58	0.58	0.7787	0.00	19112.00	125.69	0.48	167.91	0.81	Lake Mcleod
LDS D1	2.843	35.75	234.9872	109.25	1.03	0.7734	0.00	31.00	126.09	0.52	156.19	1.32	Lake Mcleod
LDS E1	3.076	40.63	532.53	113.49	0.99	0.8070	0.00	15.00	135.48	0.54	166.64	1.32	Lake Mcleod
LDS D2	2.993	37.63	1.99	114.69	0.75	0.7732	0.00	3964.00	124.75	0.46	163.34	1.00	Lake Mcleod
LDS E2	2.962	38.00	7.72	120.67	1.08	0.7892	0.00	993.00	128.05	0.59	173.62	1.42	Lake Mcleod
LCV 2e DA	0.954	14.25	66.86	162.73	1.90	0.9191	0.00	40.00	159.46	1.33	255.73	2.58	Cuvier upper marine unit
LCV 2e CA	1.005	16.72	11.47	179.08	2.20	1.0232	0.00	273.00	197.87	2.42	313.82	3.26	Cuvier upper marine unit
LCV_1e_2	2.203	28.28		111.69	0.63	0.7874	0.00	454.00	129.74	0.37	161.34	0.79	Cuvier upper marine unit
LCV_1e_2 rpt	2.201	28.33	11.63	110.59	0.98	0.7914	0.00	457.00	131.27	0.64	160.45	1.28	Cuvier upper marine unit
LCV_1e_3	3.350	44.07	0.15	114.10	0.84	0.8091	0.00	54759.00	135.98	0.68	167.76	1.17	Cuvier upper marine unit
LCV_2e_1	3.169	42.81	0.10	133.64	0.76	0.8309	0.00	78065.00	137.73	0.90	197.47	1.09	Cuvier upper marine unit
LCV_2e_3	3.877	50.91	1.481269	130.34	0.80	0.8076	0.00	6441.00	131.25	0.87	189.10	1.15	Cuvier upper marine unit
LCV_2e_4	4.365	55.70		128.44	0.65	0.7848	0.00	14451.00	124.95	0.45	183.04	0.87	Cuvier upper marine unit
LCV_2e_4 rpt	4.368	56.01	0.75	126.80	0.84	0.7887	0.00	13939.00	126.46	0.53	181.48	1.10	Cuvier upper marine unit
LCC1+10	1.243	15.671	0.595	108.678	0.703	0.7787	0.002	4938.383	127.804	0.693	156.134	0.934	Cuvier upper marine unit
LCC2+10	2.930	36.746	0.629	107.970	0.932	0.7748	0.004	10948.529	126.803	1.220	154.677	1.308	Cuvier upper marine unit
LCC3+10	1.431	18.404	0.319	107.440	0.537	0.7948	0.004	10813.573	133.154	1.249	156.714	0.845	Cuvier upper marine unit
LCC4+10	2.672	33.173	0.987	104.933	2.400	0.7672	0.008	6282.325	125.236	2.415	149.661	3.196	Cuvier upper marine unit
LCV 7T4 A	0.666	8.72	57.27	138.45	2.16	0.8050	0.00	29.00	128.51	1.18	199.31	2.83	Cuvier main Platform
LCV 7e A	0.639	9.37	2.60	202.54	2.57	0.9021	0.00	674.00	141.67	1.15	201.40	3.38	Cuvier main Platform
LCV 6.5	2.214	28.88		124.98	0.68	0.8021	0.00	89622.00	130.93	0.59	181.14	0.90	Cuvier main Platform

LCV7 T1	2.685	34.21		128.60	1.03	0.7837	0.00	39635.00	124.57	0.61	183.07	1.41	Cuvier main Platform
LCV7 T2	3.135	40.36		119.20	1.02	0.7917	0.00	56496.00	129.18	0.73	171.92	1.38	Cuvier main Platform
LCV7 T3	3.218	40.83		112.43	1.01	0.7803	0.00	10213.00	125.02	0.53	174.50	1.31	Cuvier main Platform
LCV7e_3c	3.439	42.37		124.62	1.04	0.7577	0.00	25669.00	118.13	0.66	174.19	1.33	Cuvier main Platform
LCV3e_2a	3.128	42.64		143.32	0.85	0.8384	0.00	94188.00	137.53	0.88	211.66	1.20	Cuvier main Platform
LVC3e_2b	3.160	42.17		139.27	1.21	0.8208	0.00	76512.00	133.06	0.86	203.08	1.68	Cuvier main Platform
LCCa_C	3.054	42.01	5.39	117.45	1.33	0.8500	0.00	1462.19	149.00	1.70	179.20	2.00	Cuvier wave cut Section
LCCb_C	2.901	37.65	3.59	115.49	1.34	0.8021	0.00	1965.55	133.40	1.10	168.50	1.80	Cuvier wave cut Section
LCCd_A	0.736	9.35	19.37	136.33	1.23	0.7849	0.00	90.48	123.20	0.71	193.30	1.60	Cuvier wave cut Section
LCCg_C	3.010	39.30	0.16	124.80	1.84	0.8067	0.00	46520.48	132.40	1.55	181.60	2.50	Cuvier wave cut Section
LCC1i_C	3.384	43.25	0.25	120.18	1.34	0.7897	0.00	32419.32	128.30	1.35	172.90	1.85	Cuvier wave cut Section
LCC1j_A	0.579	7.26	5.56	132.83	1.42	0.7744	0.00	244.77	121.00	0.84	187.20	1.85	Cuvier wave cut Section
LCC1j_C	2.857	38.52	18.92	121.89	1.21	0.8330	0.00	381.71	141.70	1.60	182.10	1.80	Cuvier wave cut Section
LCCk_C	3.156	40.76	0.16	123.60	0.87	0.7978	0.00	48364.31	130.00	1.45	178.60	1.30	Cuvier wave cut Section
LCC1l_A	0.576	7.54	0.88	145.82	1.45	0.8085	0.01	1607.34	127.80	2.35	209.50	2.30	Cuvier wave cut Section
LCC1m_C	3.040	38.83	0.18	119.54	0.97	0.7891	0.01	40107.35	128.30	2.85	172.00	1.80	Cuvier wave cut Section
LCC1n_C	3.113	40.02	0.07	122.49	1.13	0.7942	0.01	113409.87	129.00	1.50	176.60	1.60	Cuvier wave cut Section
LCC1o_C	3.176	41.08	0.47	134.44	1.26	0.7991	0.00	16419.23	127.70	1.10	193.10	1.70	Cuvier wave cut Section
LCCp_C	3.473	46.98	2.01	128.56	1.14	0.8359	0.00	4377.79	140.80	0.89	191.60	1.55	Cuvier wave cut Section
LCCq_A	0.559	7.65	0.02	142.80	1.18	0.8458	0.00	76846.53	140.00	1.05	212.40	1.65	Cuvier wave cut Section
LCCq_C	3.684	43.63	12.48	136.55	0.85	0.7317	0.00	655.49	109.00	0.79	186.00	1.10	Cuvier wave cut Section
LCC1r_A	0.480	5.94	12.24	150.17	2.56	0.7646	0.01	91.00	114.80	1.70	207.90	3.20	Cuvier wave cut Section
LCC1r_C	3.279	42.88	0.32	130.74	0.64	0.8080	0.01	25335.62	131.30	2.25	189.70	1.45	Cuvier wave cut Section
LCCs_C	3.256	43.33	0.17	124.52	0.82	0.8224	0.00	46761.62	137.50	0.97	183.80	1.20	Cuvier wave cut Section
LCCt_C	3.213	41.22	0.34	121.59	1.00	0.7928	0.00	22683.90	128.90	0.69	175.20	1.30	Cuvier wave cut Section
LCCu_Aa	0.765	7.91	12.13	112.29	0.94	0.6390	0.00	122.25	91.18	0.45	145.40	1.15	Cuvier wave cut Section
LCCu_Ab	0.829	10.12	8.26	147.30	1.28	0.7547	0.00	229.60	112.80	0.77	202.80	1.65	Cuvier wave cut Section
LCCv_A	0.782	7.50	1.19	111.69	1.09	0.5930	0.00	1177.20	81.52	0.45	141.10	1.30	Cuvier wave cut Section
LCCw_A	0.740	9.06	1.49	152.67	1.17	0.7564	0.00	1141.79	112.10	0.75	210.90	1.50	Cuvier wave cut Section
LCCw_C	3.395	44.03	1.27	120.14	0.64	0.8013	0.00	6511.32	131.70	0.73	175.70	0.91	Cuvier wave cut Section
SBA1 2	2.815	34.79		107.07	1.10	0.7601	0.00	3427.40	122.64	0.56	151.59	1.47	Baba Head Shark Bay

STG5 c	2.876	35.94	0.46	103.81	1.30	0.7720	0.00	14766.30	127.00	1.00	148.80	1.75	Tetragon loop Shark Bay
STG1c	2.462	31.09	0.08	106.57	0.66	0.7801	0.00	72614.26	128.80	0.92	153.50	0.96	Tetragon loop Shark Bay
STG4	1.987	24.70	0.12	105.73	1.14	0.7683	0.00	39536.21	125.40	0.76	150.80	1.50	Tetragon loop Shark Bay
SPI4 A	7.642	16.33	390.42	149.16	1.10	0.1320	0.00	7.87	13.23	0.09	154.90	1.10	Penguin Island Shark Bay
SPI4_C	2.916	35.93	0.28	107.96	1.05	0.7612	0.00	23948.40	122.80	0.65	152.90	1.40	Penguin Island Shark Bay
SPI5_C	2.359	28.64	0.59	107.80	0.88	0.7500	0.00	9176.74	119.60	0.58	151.30	1.15	Penguin Island Shark Bay
SWO1	2.759	35.47	0.07	113.75	1.05	0.7942	0.00	90677.52	131.30	0.79	165.20	1.40	Gladstone North Shark Bay
SWR1	4.559	77.11	145.30	80.99	0.61	1.0451	0.00	99.48	313.00	5.60	196.80	3.05	Gladstone North Shark Bay
SGN1b Spk 01	2.223	47.64	261.43	197.30	2.10	1.3239	0.01	34.17	127.30	1.10	150.10	2.10	Gladstone North Shark Bay
SGN3	3.247	41.08	0.41	116.18	0.72	0.7816	0.00	18740.21	126.87	0.47	166.40	0.96	Gladstone North Shark Bay
SMM3_2	2.276	28.43	1.00	109.06	0.97	0.7717	0.00	5346.95	125.60	0.75	155.70	1.30	Monkey Mia Shark Bay
SMM3_1	2.772	34.65	0.23	111.61	0.90	0.7723	0.00	27790.82	125.20	0.60	159.10	1.20	Monkey Mia Shark Bay
SMM4	3.794	46.69	144.53	106.04	0.57	0.7603	0.00	60.56	122.94	0.46	150.20	0.76	Monkey Mia Shark Bay
SWG1	0.368	3.86	1.67	64.61	1.83	0.6484	0.00	432.57	100.80	0.76	86.00	2.30	Womerangee Hill Edel peninsular
JBR1_A	0.209	0.06	0.12	148.57	1.69	0.0191	0.00	106.18	1.83	0.10	149.30	1.70	John Brewer reef GBR
JBR2_A	0.177	0.02	0.04	146.34	1.59	0.0066	0.00	102.06	0.63	0.03	146.60	1.55	John Brewer reef GBR
MYR1_A	0.284	0.03	0.02	146.67	1.05	0.0062	0.00	227.80	0.59	0.03	146.90	0.99	Myrmidon reef GBR
MYR1_C	2.368	0.32	0.16	147.11	0.91	0.0084	0.00	386.48	0.80	0.02	147.40	0.87	Myrmidon reef GBR
NYR1_A	0.116	0.02	0.03	145.11	2.32	0.0107	0.00	144.88	1.02	0.08	145.50	2.30	Yange reef GBR
NYR2_A	0.042	0.01	0.01	148.40	2.51	0.0191	0.00	226.44	1.82	0.14	149.20	2.50	Yange reef GBR
RMS1a	0.452	9.02	0.95	221.10	0.99	1.2314	0.00	1776.71	329.00	6.50	561.00	9.90	Pilgromana Cape Range
RMS2a	0.394	8.03	7.60	170.82	2.00	1.2594	0.01	198.07					Pilgromana Cape Range
NJB3b 1	1.763	30.02		22.82	1.07	1.0475	0.00	94943.00					Tantabidi Cape Range
NJB3b 3	0.876	15.54		31.67	1.30	1.0915	0.00	12655.00					Tantabidi Cape Range
NPG 2_3	0.706	12.55		32.30	2.13	1.0923	0.00	1301.00					Tantabidi Cape Range
NJB4 1	1.048	18.26		37.44	1.54	1.0721	0.00	10093.57					Tantabidi Cape Range
NJB4 2	1.093	19.32		34.98	1.79	1.0872	0.00	17602.03					Tantabidi Cape Range
NJB4 3	0.794	13.95		35.39	1.62	1.0802	0.00	30401.76					Tantabidi Cape Range
NJZ1d 1	2.024	25.26		108.60	1.22	0.7675	0.00	929.00	124.47	0.70	154.55	1.58	Jacobz quarry Cape Range
NJZ1d 2	2.137	26.58		108.52	0.81	0.7653	0.00	6291.00	123.84	0.61	154.16	1.04	Jacobz quarry Cape Range
NYC A2	2.318	28.94		103.67	1.55	0.7678	0.0021	8483	125.741	0.762	148.07	2.02	Yardie Creek

NYC A3	2.450	33.59		111.65	1.19	0.8433	0.002	22	148.48	0.838	170.09	1.64	Yardie Creek
MFU 1a A	0.522	6.52		131.29	2.80	0.7680	0.00	32.00	119.55	1.02	184.26	3.49	Foul Bay Margaret River
MFU1a 3	3.191	36.96		118.58	0.83	0.7124	0.00	3212.00	107.42	0.42	160.79	1.05	Foul Bay Margaret River
HFB1 1	2.606	32.79		104.22	1.06	0.7736	0.00	63382.00	127.37	0.68	149.55	1.36	Margaret River
HFB1 2	2.928	36.90		105.64	0.92	0.7751	0.00	76807.00	127.46	0.47	151.61	1.17	Margaret River
HFB2	3.633	42.96		122.70	0.79	0.7272	0.00	1048.00	110.43	0.49	167.80	0.99	Margaret River
HFB1_2	3.010	39.30		105.49	0.85	0.8022	0.00	13627.00	136.10	1.42	155.16	1.27	Margaret River
USD_03 3	2.650	32.50		105.16	0.75	0.7540	0.00	33540.00	121.32	0.43	148.33	0.96	Margaret River
USD_03 1	2.640	32.60		109.32	2.11	0.7585	0.00	30011.00	121.68	0.74	154.35	2.75	Margaret River
USD 03 A	0.536	7.32		117.81	2.51	0.8403	0.00	13.00	145.47	1.73	177.95	3.44	Margaret River
USD_03	2.520	31.00		104.91	3.37	0.7568	0.00	34249.00	122.18	1.54	148.33	4.31	Margaret River
USD 03	2.829	36.58		105.44	0.76	0.7780	0.00	25486.00	128.40	0.52	151.74	1.05	Margaret River
MMFB2	3.065	38.63		103.61	0.92	0.7752	0.00	62265.00	127.98	0.57	148.93	1.21	Margaret River
MMFB2	2.960	38.00		106.19	0.59	0.7898	0.00	48270.00	131.88	0.83	154.33	0.85	Margaret River
MMFB2	3.065	38.63		103.61	0.92	0.7752	0.00	62265.00	127.98	0.57	148.93	1.21	Margaret River
FB04_2a	2.795	35.056	0.121	104.477	0.792	0.7748	0.005	54395.232	127.662	1.491	150.039	1.223	Foul Bay Margaret River
FB04_3a	1.891	23.623	0.052	103.935	0.564	0.7718	0.003	85830.197	126.870	0.916	148.925	0.801	Foul Bay Margaret River
FB04_4a	5.323	65.962	0.155	105.625	0.674	0.7656	0.005	80212.184	125.000	1.500	150.400	1.100	
FB04_6d	2.661	33.077	0.104	106.697	1.701	0.7680	0.004	59629.524	125.100	1.300	152.100	2.200	
CMP1b_1	3.100	38.30		108.38	0.47	0.7591	0.00	4380.00	122.05	0.97	153.19	0.74	Cowaramup Margaret River
OHE 1c	2.506	30.74		114.85	0.71	0.7547	0.00	20917.00	119.37	0.57	161.11	0.93	Kahe Oahu
OHE 2a 1	2.275	27.38		115.21	1.55	0.7403	0.00	38643.00	115.35	1.15	159.77	2.01	Kahe Oahu
OHE 2a 2	2.204	26.82		111.94	1.23	0.7487	0.00	135934.00	118.31	0.89	156.56	1.59	Kahe Oahu
OKP 2a	2.216	28.78		119.63	0.87	0.7987	0.00	53242.00	131.24	0.41	173.56	1.16	Mokapu Oahu
OKP 2c	2.449	32.13		111.50	0.81	0.7910	0.00	273.00	130.90	0.46	161.59	1.07	Mokapu Oahu
OKP 3c	2.482	31.83		108.39	0.79	0.7887	0.00	18865.00	130.97	0.49	157.13	1.05	Mokapu Oahu
UKP_A	0.953	14.22	753.84	28.21	2.14	0.9218	0.02	3.54	240.00	15.00	55.70	4.40	Ulapau
AHW2d 1	3.126	37.76		111.82	0.76	0.7431	0.02	38458.76	116.79	6.83	155.71	3.08	Bahamas
AHW2d 2	2.988	37.32		115.73	0.91	0.7681	0.00	9304.43	123.01	1.14	164.02	1.28	Bahamas
AHW2d 3	2.047	25.03		105.66	1.16	0.7518	0.00	58416.44	120.58	0.52	148.72	1.51	Bahamas
AHW2d 6	1.829	26.42		109.80	1.08	0.8885	0.00	34362.39	167.01	0.94	176.29	1.54	Bahamas

HEN1_A	0.814	13.62	0.05	74.99	0.73	1.0329	0.00	46969.85	305.90	4.20	178.40	2.20	Henderson Island
HEN1_C	1.735	28.79	0.03	65.53	0.81	1.0253	0.01	167452.62	313.80	8.20	158.90	3.85	Henderson Island
HEN2_A	0.843	0.22	0.05	148.53	0.73	0.0164	0.00	777.89	1.56	0.03	149.20	0.72	Henderson Island
HEN1_LC1	1.858	30.905	0.043	28.995	0.741	1.0279	0.007	135092.834	480.431	60.466	113.198	20.349	Henderson Island
HEN2_C	2.749	1.613	0.043	145.196	0.815	0.0363	0.001	7237.600	3.496	0.051	146.642	0.822	Henderson Island
BKE1e 1	2.425	32.10		114.56	1.12	0.8141	0.00	68127.09	137.49	0.72	169.16	1.44	Cape Keradran
LQC_A	0.424	0.27	2.94	148.28	4.64	0.0387	0.00	17.06	3.73	0.13	149.90	4.65	Quabba station
LQC_C	2.698	0.58	15.20	144.79	1.04	0.0132	0.00	7.15	1.26	0.04	145.30	1.00	Quabba station
Ber_F	0.051	0.84	0.49	24.34	5.36	1.0159	0.01	323.54	442.00	123.00	85.00	29.50	Bermuda
Ber_S	0.084	0.06	0.19	33.13	3.31	0.0422	0.00	57.90	4.53	0.16	33.60	3.30	Bermuda
GCB1a_A	0.787	10.14	24.12	138.59	1.28	0.7954	0.00	78.78	125.70	1.20	197.90	1.75	Cape Burney
GCB_2a	2.757	34.52	0.12	104.63	1.60	0.7738	0.00	52810.07	127.30	1.10	150.10	2.10	Cape Burney
GCBx_A	0.715	8.41	120.08	128.44	3.26	0.7268	0.01	13.12	109.20	1.70	175.00	4.15	Cape Burney
BSM1c	1.756	1.74	188.83	138.76	1.84	0.0614	0.00	1.74	6.02	0.09	141.10	1.85	Port Smith
AWH2d_2	1.83	23.09	0.30	112.97	1.97	0.7787	0.012	14885.0	127.00	3.5	161.8	3	
CRB1a	3.16	38.70	0.19	105.88	1.64	0.7568	0.005	39589.5	122.00	1.5	149.6	2.2	Red Bluff CC
CRB1b	2.57	31.60	0.18	104.12	2.12	0.7583	0.004	33400.0	122.80	1.25	147.5	2.8	Red Bluff CC
CRB2a	2.30	28.44	0.06	107.73	1.25	0.7633	0.005	83980.6	123.40	1.35	152.9	1.7	Red Bluff CC
EC2	3.48	4.16	94.58	145.98	1.24	0.0737	0.001	8.2	7.22	0.12	149	1.2	Elim beach coral (For Dave)
LCC1f_C	2.32	35.88	13.83	123.24	1.19	0.9540	0.006	486.4	191.70	3.2	212.2	2.4	Cape Cuvier North Coral
LCC1f_E	0.08	0.88	7.30	74.06	6.59	0.6565	0.012	22.5	101.20	3.05	99	8.15	Cape Cuvier North Echinoder
OKP_4nb	1.01	13.52	681.00	115.44	3.54	0.8254	0.010	3.7	141.00	3.3	172.2	4.9	
OMUb_C	2.18	27.04	0.09	109.03	2.32	0.7654	0.004	58442.5	123.80	1.3	154.8	2.95	
ORS1(3)	2.44	2.75	5.28	144.99	2.33	0.0697	0.001	97.6	6.82	0.0975	147.8	2.3	Orpheus Is coral
SHP1_C	3.20	53.36	0.38	85.23	1.61	1.0287	0.004	26013.2	283.00	5.35	190	3.5	Hamlin Pool coral
SHP1_M	2.63	2.66	257.64	146.87	1.45	0.0626	0.001	1.9	6.09	0.071	149.4	1.4	Hamlin Pool strom
UWQ7c	0.04	0.60	0.07	24.19	8.63	1.0237	0.014	1608.0	503.00	#VALUE!	101	#VALUE!	
UWQ8n(1)	0.06	0.44	2.43	68.36	6.83	0.4720	0.008	34.1	62.90	1.45	82	7.9	
UWQ8n(2)	0.06	0.43	1.43	69.91	8.69	0.4278	0.004	56.4	55.20	0.91	82	9.7	

APPENDIX 2 – XRD DATA

AAC Run No	Sample Code	Quartz SiO2	Aragonite CaCO3	Calcite CaCO3	HMC (Ca,Mg)CO3	Dolomite CaMg(CO3)2	Ankerite Ca(Mg,Fe)(CO3)2	Sodium Chloride NaCl
5547-02	LDS1i	4%	79%	2%	10%	5%		
5547-03	LDS1j							
5547-09	LDS1g	3%	61%	2%	2%		31%	
5547-19	LDS1h	1%	98%	1%				
5547-01	LCV7_1		99%			1%		
5547-15	LCV7_3	1%	99%					
5547-04	NYC1a	2%	71%	24%		3%		
5547-07	NYC1b	3%	86%	9%		3%		
5547-08	NYC1c		71%	26%		3%		
5547-11	NYC1d		84%	15%	1%			
5547-05	LCV1b		86%	9%	3%	2%		
5547-16	LCV1c		99%	1%				
5547-12	LCV2a		96%	1%	2%	1%		
5547-13	LCV2b	4%	14%	26%	54%			2%
5547-20	LCV2c	1%	99%	0%				
5547-18	LCV2d	1%	99%	1%				
5547-06	MFU1a			3%	97%			
5547-21	MFU1b		99%	1%				